



Groundwater investigation and modeling - western desert of Iraq

By the Faculty of Geosciences, Geo-Engineering and Mining
Technische Universität Bergakademie Freiberg
Chair of Hydrogeology institute

Approved

PhD. Thesis

To attain the academic degree of Doctor rerum naturalium
Dr. rer. Nat.

Submitted by

Sameh Wisam Al-Muqdadi

(MSc.)

Born on Dec.01.1976 in Baghdad

Reviewers:

Prof.Dr.Broder Merkel
Prof.Dr.Peter Udluft
Dr.Volkmar Dunger

TU.Bergakademie Freiberg
University of Würzburg
TU.Bergakademie Freiberg

Date of the award: May.04.2012 , Freiberg - Germany

Dedication

*To the memory of Haider Obaid Al-Sultan, Mahdi Mizil ... and all the Iraqi souls have
been lost during the war...*

The unknown soldiers that lit a candle to enlighten the long dark path...

Sameh

Acknowledgment

My deepest thanks to my supervisor Prof. Dr. habil Broder J. Merkel, Head of Geology Department and Chair of Hydrogeology for his, guidance, support, inspiration, fruitful suggestions and multiple efforts.

A special thank goes to Dr. Volkmar Dunger, for his continues help, valuable comments and discussions to enhance this work.

The author wishes to express his special thanks and gratitude to the German Academic Exchange Service (Deutscher Akademischer Austausch Dienst – DAAD) for the financial Support.

Many thanks for the scientific diving center team at TU.Freiberg for such innovative, unique moments and hard scientific work (Prof. Dr. Broder J. Merkel, Dr.Thomas Pohl , Gerald Barth, Dr.Elke Eckardt, Dr.Mandy Schipek, my diving buddy Christin Müller, Stephan schulz,Robert Sieland, Marco Ponepal ,Katja Winkler,Richard Stanulla,Franziska Vinzenz).

A special thanks to my office mate Mohammed Omer and for dear mate Iwona Woloszyn for all help and valuable discussion.

Thanks for all colleagues of hydrogeology team at the Geology faculty for the wonderful time and constructive discussions : Dr.Sascha Kummer, Hajo Peter, Rudy Abo, Sosina Shieleses, Shimelis Berhanu, Nadja Schmidt, Ramadan Abdel Aziz, Lotfallah Karimzadeh, Nair Sreejesh, Eyad Aboshindi, Raghid Sabri, Wondem Gezahegne, Andrea Berger, Samer Bachmaf, Karina Taupadel, Anne Kaulisky, Beanca Störr, Arsalan Othman, Eric pohl, Hussein Jassas, Omed Mustafa, Shwan Ismael, Wael Kanoua , Arab Alireza,Gisela Schmiedgen and Tino Beier.

The author expresses his gratitude to the university administration office especially Dagmer Heim, Dr.Corina Dunger - GraFA program and the International University Center (IUZ).

Thanks for all my special friends for continues support: Ahmed Al-Suraifi, Ahmed Khalil,Ahmed Riad, Ahmed Mashaalah ,Ali Salman, Aseel Anton, Bashar and Aygun Hanna,Basma Basheer, Fatin Fawzi, Gulirmo Bolonas, Haider Abbas, Hassanein Hoshi, Hussein Abdul Ameer, Khaldun Abualhin, Khalid Hoshi, Mohammed H. Al-Rashdee, May Al-Naimi, Mohammed Salih, Muntasar Mohammed, Nashwan Othman, Dr.Nicole Birkner, Sahel M. Al-Azzawi, Zaid T. Al-Ukaily, Zaid F. Zidan and Yasser Riyad.

Special thanks goes to my first teacher Sanaa Izzat and the best trainer ever Riham Faruk El-Sedfy.

Guides and friends who help me during the field work my brother Mustafa and his wife Dania, Atheer Nail Al-Hashimi, Mohammed M.Oaina,Ammar Falah, Yasser Kassim and Abu Duraid.

Special thanks to Baghdad university,Prof.Dr. Balsam Al-Tawash , Prof.Dr.Khalid Al-Muktar, Dr.Qusay Al-Suhail, Dr.Sawsan Al-Jaff, Basrah university Prof.Dr.Mohammed Al-Asadi, Geosurve - Iraq Prof. Dr. Khaldun Al-Bassam, Dr. Sadik Al-Jawad, Salahaddin University Dr.Mariwan Chnari, Tikrit University Dr.Omar Sabah, MOST Dr. Maitham Al-Sultan and Mr.Muslim Oaina.

My family, great mother, sister, brothers Mustafa and Haider,the soul of my father, last not least my lovely wife Farah Qassim and her family my father and mother in law.

List of Content		Page
	Dedication	2
	Acknowledgment	3
	List of contents	4
	List of Figures	8
	List of Tables	9
	List of abbreviations	10
	English Abstract	12
	German Abstract	14
1	Introduction	16
1-1	Preface	16
1-2	Region of interest	16
1-3	Previous Studies	17
1-3-1	Local studies	17
1-3-1-1	Hydrogeological Studies	17
1-3-1-2	Remote Sensing Studies	18
1-3-2	Global studies	18
1-3-2-1	Groundwater flow and fracture zone	19
1-3-2-2	Lineaments extraction	19
1-3-2-3	Watershed delineation	20
1-4	Importance of investigation area	24
1-5	Motivation	24
1-6	Deliverables	24
1-7	Problems	26
2	Methodology	27
2-1	Literature review	27
2-2	Personal contact	27
2-3	Field work	27
2-4	Evaluation of geological data	27
2-4-1	Geological cross section	27
2-4-2	Fault system by means of remote sensing techniques	28

2-5	Climate and Meteorology.....	28
2-5-1	Meteorological data	28
2-5-2	Aridity index	28
2-5-3	Groundwater recharge	29
2-5-4	Vegetation index	29
2-5-5	Actual evaporation	30
2-5-6	Soil moisture	32
2-5-7	Runoff	32
2-6	Hydrogeology	34
2-6-1	Pumping test	34
2-6-2	Groundwater flow	34
2-6-3	Wadi catchment delineation	34
2-6-3-1	Dataset	34
2-6-3-2	Approaches	34
2-6-3-3	Software packages	35
2-6-4	PC options	39
2-6-5	Groundwater Model	39
2-6-5-1	Conceptual model	40
2-6-5-2	Input	41
2-6-5-3	Properties	41
2-6-5-4	Boundary conditions	41
2-6-5-5	Observation wells	42
2-6-5-6	Solver	42
2-6-5-7	Calibration	42
3	Geological setting	44
3-1	Preface	44
3-2	Tectonic and structure	44
3-3	Stratigraphy	46
3-3-1	Tayarat formation	47
3-3-2	Umm Er Radhumma formation	47
3-3-3	Dammam formation	48
3-3-4	Euphrates formation.....	48

3-4	Topography and Ubaiydh Wadi	49
4	Climate and meteorology.....	51
4-1	Preface	51
4-2	Precipitation	51
4-3	Temperature	52
4-4	Potential evaporation	53
4-5	Relative humidity	54
4-6	Wind	55
4-7	Sunshine duration	56
5	Hydrogeology	57
5-1	Preface	57
5-2	Tayarat aquifer	57
5-2-1	Pressure conditions	57
5-2-2	Hydraulic characteristics	57
5-2-3	Water quality	58
5-3	Um Er Radumma aquifer	58
5-3-1	Pressure conditions	58
5-3-2	Hydraulic characteristics	58
5-3-3	Water quality	59
5-4	Dammam aquifer	59
5-4-1	Pressure conditions	59
5-4-2	Hydraulic characteristics	60
5-4-3	Water quality	60
6	Result and discussion	61
6-1	Topographic contour map	61
6-2	Geological cross section	62
6-3	Lineaments evaluation	65
6-4	Groundwater flow	66
6-5	Pumping test evaluation	70
6-6	Catchment calculation	72

6-7	Water balance and Recharge	76
6-8	Groundwater model	78
6.8.1	Model sensitivity	80
6.8.2	Groundwater management	83
7	Conclusion and recommendations	84
7.1	Conclusion	84
7.2	Recommendations	85
8	References	86
9	Appendixes	90
10	Field work Photos	115
11	Author CV.	116

List of Figures

Figure No.	Title	Page
Fig. 1-1	Local and regional investigation area – western desert of Iraq	17
Fig. 2-1	Groundwater recharge model	29
Fig. 2-2	Soil moisture curve (Noaa, 2009)	32
Fig. 2-3	SCS relation between storm runoff and rainfall (Maidment, 1993)	33
Fig. 2-4	Flow direction and watershed boundaries	35
Fig. 2-5	Flow direction	35
Fig. 2-6	Fill depression	36
Fig. 2-7	GIS software packages flowchart	36
Fig. 2-8	Groundwater flow model by Visual Modflow	40
Fig. 2-9	Polygon for main wadi drainages where recharge implemented	42
Fig. 3-1	Cross section showing Rutba subzone	45
Fig. 3-2	Faults in the local ROI	45
Fig. 3-3	Stratigraphy for the western desert of Iraq	46
Fig. 3-4	Outcrops of the local ROI	46
Fig. 3-5	Western desert wadis – Iraq	49
Fig. 3-6	previous catchment area calculation for Ubaiydh wadi	50
Fig. 4-1	Precipitation monthly means 1980 - 2008 Nukaib station	52
Fig. 4-2	Precipitation annual means 1980 - 2008 Nukaib station	52
Fig. 4-3	Temperature monthly means 1980 - 2008 Nukaib station	53
Fig. 4-4	Temperature annual means 1980 - 2008 Nukaib station	53
Fig. 4-5	Evaporation monthly means 1980 - 2008 Nukaib station	54
Fig. 4-6	Evaporation annual means 1980 - 2008 Nukaib station	54
Fig. 4-7	Relative Humidity monthly means 1980 - 2008 Nukaib station	55
Fig. 4-8	Relative Humidity annual means 1980 - 2008 Nukaib station	55
Fig. 4-9	Wind speed monthly means 1980 - 2008 Nukaib station	56
Fig. 4-10	Sunshine duration monthly means 1980 - 2008 Nukaib station	56
Fig. 6-1	Topographic counter map Regional and Local ROI	61
Fig. 6-2	Position of geological cross section in the local ROI	62
Fig. 6-3	Lithology of the 4 boreholes used to construct the cross sections	63
Fig. 6-4	Geological cross section's for local ROI	64
Fig. 6-5	Lineament extraction into different dataset and different algorithms	66
Fig. 6-6	Extension of Damman aquifer and structural elements. Map of GW contour lines and GW flow directions for Dammam aquifer	67
Fig. 6-7	Extension of Umm Er Radhumma aquifer and structural elements, ap of GW contour lines and GW flow directions for Umm Er Radhumma aquifer	68
Fig. 6-8	Extension of Tayarat aquifer and structural elements. Map of GW contour lines and GW flow directions for Tayarat aquifer	69
Fig. 6-9	Pumping test plot for well 9	71
Fig. 6-10	Pumping test plot for well 17	71
Fig. 6-11	Catchment delineation by three software for Ubaiydh Wadi – 90 m DTM	74
Fig. 6-12	Catchment delineation by three software for Ubaiydh Wadi – 30 m DTM	74
Fig. 6-13	Catchment delineation for Ubaiydh Wadi - TNT mips using NO seeding point	75
Fig. 6-14	Catchment delineation for Ubaiydh Wadi – Arc Hydro 30m ASTER	75
Fig. 6-15	Groundwater recharge fluctuation from 1980-2008	77
Fig. 6-16	The Model showing main layers, observation wells and dry area	78
Fig. 6-17	The Model showing Water table and active zone	79
Fig. 6-18	Groundwater flow within Fault zone	79
Fig. 6-19	Plots model 3 residuals before and after excluded wells	82

List of Tables

Table No.	Title	Page
Table 2-1	Aridity index	29
Table 2-2	Potential evaporation values based on temperature rates ≥ 26.5 C°	31
Table 2-3	Hydrologic soil groups based on infiltration rates (Maidment, 1993)	33
Table 2-4	Arc Hydro data structures	38
Table 5-1	Groundwater type for Tayarat aquifer	58
Table 5-2	Groundwater type for Um Er Radumma aquifer	59
Table 5-3	Groundwater type for Dammam aquifer	60
Table 6-1	Pumping test comparison of wells	70
Table 6-2	CPU comparison for watershed delineation into 3 software packages	73
Table 6-3	RASTER and ASTER dataset delineation results for the three software	76
Table 6-4	Groundwater recharge values for timeframe 1980-2008	77
Table 6-5	Results for implemented models by Visual Modflow V4.2	81
Table 6-6	Results for implemented models for K values by Visual Modflow V 4.2	82
Table 6-7	Groundwater inflow calculation	83

List of abbreviations

AE	Actual Evaporation
ASTER	Advanced Spaceborne Thermal Emission and Reflection Radiometer
C°	Degree centigrade (Celsius scale)
Ca ⁺²	calcium (ion)
Cl ⁻¹	Chloride (ion)
cm	Centimeter
CN	Curve Number
CPU	central processing unit
DEDNM	Digital Elevation Drainage Network Model
DEM	Digital Elevation Model
DTM	Digital Terrain Model
DRLN	Digital river and lake network
D8	eight directions for neighbor pixels
epm	Equivalents per million
D _∞	Infinity directions for neighbor pixels
E	East
E	Evaporation
EC	electrical conductivity
ETM	Enhanced Thematic Mapper
ET	Evapotranspiration
F	Fault
GAP	Southeastern Anatolia Project
GB	Gigabyte
GIS	Geological Information System
GW _i	Groundwater inflow
GW _r	Groundwater recharge
HCO ₃ ⁻	Bicarbonate (ion)
I	index of aridity
I	Annual heat index °C
i	Monthly heat index C°
K	constant correction factor
KH	Keyholes
Km	Kilometer
Km ²	Square kilometer
Lat	Latitude
Lon	Longitude
m	Meter
masl	meter above sea level
Max.	Maximum
Mg ²⁺	magnesium (ion)
Min.	Minimum
min	Minute
MSS	Multi Spectral Scanner
μS	Micro Siemens
N	North
Na ⁺	sodium (ion)
NE	Northeast

NDVI	Normalized Difference Vegetation Index
NO ₃ ⁻	Nitrate (ion)
NS	North – South
NW	Northwest
p	Monthly precipitation
P	Annual precipitation
PE	potential Evaporation
PEc	Potential evaporation corrected
PET	Potential Evapotranspiration
ppm	Parts per million
RAM	Random-access memory
RH	Relative Humidity
RO	Runoff
ROI	Region of investigation
S	South
SAR	sodium adsorption ratio
SCS	Soil Conservation Service
SM	soil moisture
SO ₄ ²⁻	Sulfate (ion)
SRTM	Shuttle Radar Topography Mission
START	segment tracing and rotation transformation
SW	Southwest
SYR	Sun, Yang and Ren algorithm
T	Temperature C°
TAS	Terrain Analysis System
TDS	total dissolved solids
TIN	Triangular Irregular Network
TM	Thematic mapper
tr	Tiny rain
USGS	United States Geological Survey
W	West
WS	Water Surplus
%	Percent
°	Degree
~	About
ΔS	Storage change (in soil or the bedrock)

ABSTRACT

The region of interest is part from Iraqi western desert covering an area about 100,000 km². Several of the large wadis such as Hauran, Amij, Ghadaf, Tubal and Ubaiydh traverse the entire region and discharge into the Euphrates River.

The present study included the following hydrogeological investigations:

Lineaments interpretation was done by using different data sets (SRTM 30 m and Landsat ETM 15m), within different algorithms. Some faults recognized by field survey match rather well with the automatically extracted lineaments with only a small difference between field data and remote sensed data.

The groundwater flow directions (west to east) for three aquifers were determined by using different spatial interpolation algorithms. Due to the faults impact, the flow direction gets a slightly other direction when reaching the fault's zone.

Two pumping test were performed close to fault 2 in the unconfined aquifer Dammam using well no. 9 and 17. Results of pumping test and recovery were evaluated with the analytical model MLU for Windows. Well 17 shows a slightly higher transmissivity (0.1048 m²/min) in comparison to well 9 (T= 0.0832 m²/min). This supports the assumption of a zone of unique elevated permeability between fault 1 and fault 2 because of the tectonic stress and the anticline structure.

The catchment and watershed delineation was performed by means of four GIS packages utilizing three DTM's: 90 m and 30 m SRTM (Shuttle Radar Topography Mission) and the ASTER 30 m. A thorough field survey and manual catchment delineation of the same area was available from Division 1944. Software used was Arc Hydrotools, TNTmips, River Tools and TecDEM.

Ten 90 m SRTM and twelve 30 m ASTER files were merged by means of ArcGIS. The 30 m SRTM dataset of Iraq was supplied by courtesy of the US Army and the region of interest (ROI) was clipped from this DTM using ArcGIS. No additional steps were performed with both DTM data sets before using the mentioned software products to perform the catchment analysis. As a result the catchment calculations were significantly different for both 30 m and 90 m data and the different software products.

The groundwater model implemented in Visual Modflow V.4.2 was built by 5 main layers representing Dammam aquifer, first aquiclude, UmEr Duhmma aquifer, second aquiclude and the Tayarat aquifer. Averaged readings of groundwater head from 102 observation wells were used to calibrate the model.

Calculated recharge average was 17.5 mm/year based on the water balance for ~30 years (1980-2008). A sensitivity analysis was performed by using different permeability and recharge values.

However, the model showed a rather low sensitivity because the values of the standard error of the estimation were between 2.27 m and 3.56 m. Models with recharge less than 11.85 mm/year or more than 60 mm/year did not converge and thus failed to produce a result. Models with K_f values from 1.1^{-3} to 1.1^{-4} m/s for aquifers and from 1.1^{-7} to 1.1^{-8} m/s for aquicludes converged. Water budget is about $2.17 \cdot 10^{10}$ m³/year; by irrigating the greenhouses this budget will cover only 1.75% of the total area. However, this value could be upgraded up to 8 – 9 % by utilizing the groundwater inflow from Saudi Arabia.

ZUSAMMENFASSUNG

Das Untersuchungsgebiet umfasst eine Fläche von etwa 100.000 km² und ist Teil der westlichen irakischen Wüste. Einige der großen Wadis wie Hauran, Amij, Ghadaf, Tubal und Ubaiydh durchqueren die gesamte Region und entwässern in den Euphrat.

Die vorliegende Arbeit umfasst folgende hydrogeologische Untersuchungen:

Die Interpretation der Lineamente wurde anhand verschiedener Datensätze (SRTM 30 m und Landsat ETM 15 m) und unter Nutzung unterschiedlicher Algorithmen durchgeführt.

Einige Störungen, welche während Feldmessungen identifiziert wurden, stimmen gut mit automatisch extrahierten Lineamenten überein, der Unterschied zwischen Feld- und Fernerkundungsdaten ist somit gering.

Die Ermittlung der Grundwasserfließrichtungen (von West nach Ost) der drei Aquifere erfolgte unter Nutzung verschiedener Algorithmen zur räumlichen Interpolation. Es zeigte sich, dass die Störungen zu einer leichten Veränderung der Fließrichtung mit zunehmender Nähe zur Störungszone führen.

Zwei Pumpversuche in den Brunnen 9 und 17 wurden nahe der Störung 2 im ungesättigten Aquifer Dammam durchgeführt. Die Auswertung der Ergebnisse der Pump- und Wiederanstiegsversuche erfolgte mittels des analytischen Modells MLU für Windows.

Es zeigte sich, dass Brunnen 17 eine leicht höhere Transmissivität aufweist ($T = 0,1048 \text{ m}^2/\text{min}$) im Vergleich zu Brunnen 9 ($T = 0,0832 \text{ m}^2/\text{min}$). Dies unterstützt die Annahme der Existenz einer Zone erhöhter Permeabilität zwischen den Störungen 1 und 2, verursacht durch tektonischen Stress und die Antiklinalstruktur.

Die Erfassung von Einzugsgebiet und Wasserscheiden erfolgte anhand von vier GIS-Paketen unter Nutzung von 3 DTM's: 90 m und 30 m SRTM (Shuttle Radar Topography Mission) sowie ASTER 30 m. Genaue Daten aus einer Feldkampagne und eine manuelle Abgrenzung des Einzugsgebietes derselben Region standen zur Verfügung (Division 1944). Als Software kamen Arc Hydrotools, TNTmips, River Tools und TecDEM zum Einsatz.

Zehn SRTM- (90 m) und zwölf ASTER-Files (30 m) wurden mittels ArcGIS vereinigt. Ein 30 m SRTM-Datensatz des Irak (bereitgestellt durch die US-Armee) diente als Grundlage für das Ausschneiden des Untersuchungsgebietes (ROI) mit Hilfe von ArcGIS. An beiden DTM Datensätzen wurden vor der Ermittlung des Einzugsgebietes mit den genannten Software-Produkten keine zusätzlichen Schritte durchgeführt. Als Resultat ergaben sich signifikante Unterschiede zwischen den 30 m und 90 m Datensätzen sowie der verschiedenen Software.

Das in Visual Modflow V.4.2 implementierte Grundwassermodell wurde aus fünf Hauptschichten bestehend aus Dammam Aquifer, erster Stauer, UmEr Duhmma Aquifer, zweiter Stauer und Tayarat Aquifer aufgebaut. Durchschnittliche Werte der Grundwasserstände aus 102 Observationsbrunnen dienten der Kalibrierung des Modells.

Die berechnete mittlere Grundwasserneubildung betrug 17,5 mm/a, basierend auf dem Wasserhaushalt der letzten 30 Jahre (1980-2008). Unter Einbeziehung verschiedener Werte für Permeabilität und Grundwasserneubildung wurde eine Sensitivitätsanalyse durchgeführt. Dabei ergab sich allerdings eine geringe Empfindlichkeit des Modells, resultierend aus einer Standardabweichung der Schätzung zwischen 2,27 m und 3,56 m. Modelle mit einer Grundwasserneubildung kleiner 11,85 mm/a und größer 60 mm/a zeigten keine Konvergenz und führten somit zu keinem Ergebnis. Modelle mit k_f Werten zwischen 1.1^{-3} und 1.1^{-4} m/s für Aquifere und zwischen 1.1^{-7} und 1.1^{-8} m/s für Grundwasserstauer konvergierten.

Die Grundwasserneubildung betrug etwa $2,17 \cdot 10^{10}$ m³/a, für Bewässerung von Gewächshäusern deckt diese Summe nur 1,75% des gesamten Gebietes ab. Allerdings könnte dieser Wert durch die Nutzung des Grundwasserzuflusses aus Saudi Arabien auf 8 – 9% gesteigert werden.

1. Introduction

1.1 Preface

The western Desert of Iraq (West of the Euphrates River) is an area covering nearly 32% of whole Iraq (437.072 km²) and habits a population of about 1.3 million (NIC, 2004). The region is classified as hyper-arid based on (Unep, 1992). Ground water exists in several horizons at different depths. The major part of the groundwater is assumed as not renewable in semi-confined aquifers. However, it is assumed that recharge happens only in limited flood areas in the desert.

Since more than two decades, Iraqi territories are suffering from insufficient water resources to meet future demands. Reasons beyond that can be summarised by external reasons such as GAP (Southeastern Anatolia Project – Turkey by constructing 22 dams on Tigris and Euphrates River) and on the other hand internal reasons due to the absence of optimal utilization of water resource by creating more sophisticated irrigation system. Therefore, water harvesting and implementation of modern irrigation systems is one of the most important national priorities.

Another idea is to investigate groundwater resources, which is considered as an effective substitute for surface water. The present study emphases to investigate the groundwater resource in one part of Iraq and creating a groundwater model to simulate the groundwater flow behaviour.

1.2 Region of interest

The region of interest is part from Iraqi western desert (44:00 – 39:00E and 33:00 – 31:00N) covering an area about 100,000 km². It extends to the state borders with Syria, Jordan and Saudi Arabia. Several of the large wadis such as Hauran ,Amij , Ghadaf ,Tubal and Ubaiydh traverse the entire region and discharge into the Euphrates river (Division, 1944).

Part of the area (41.14E – 32.59N and 42.78E – 31.86N) was of special interest covering an area of about 12400 km². It embeds a part from the main wadi (Ubaiydh). This local region was chosen because of two reasons: on the one hand it was classified by (Consortium-Yugoslavia, 1977) as a promising groundwater abstraction zone and on the other hand offering a sufficient number of wells for carrying out a thorough ground water study (Fig.1-1).

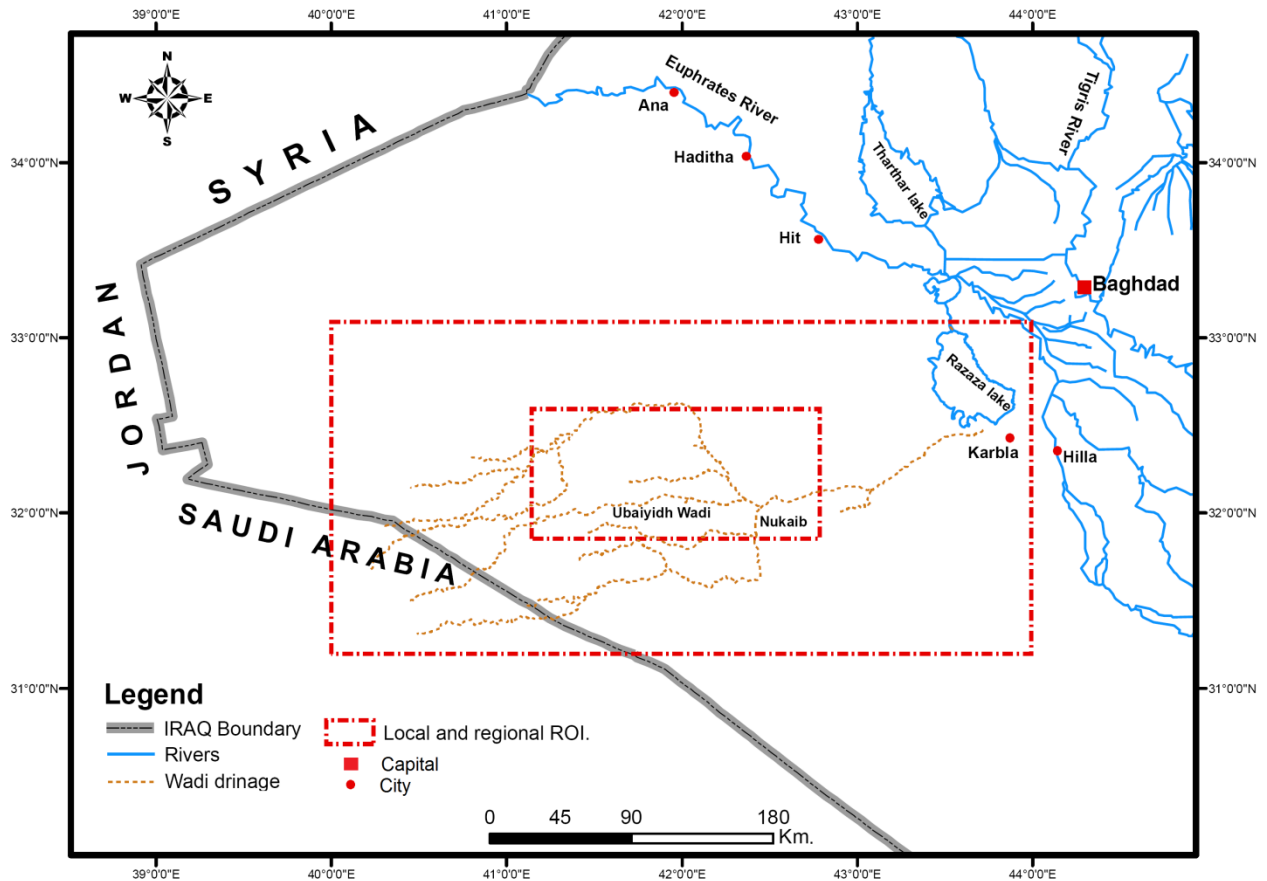


Fig.1-1: Local and regional investigation area – western desert of Iraq

1.3 Previous Studies

1.3.1 Local studies

Generally, only few studies have been performed with respect to the region of interest in terms of hydrogeology and remote sensing aspects. Unfortunately during the war and military operation in 2003 some internal reports have been either lost or suffer from data missing because many universities and governmental institutes have been burned and looted. No groundwater modelling study was conducted so far for the western desert in particular for the region of interest.

1.3.1.1 Hydrogeological Studies

(Parsons, 1957) made an investigation and estimation for groundwater resources in the northern and western Iraqi desert. They were drilling many wells, and recognized a sort of deep fractured aquifers.

Ingra Yugoslavian Company (1961-1967) investigated the groundwater resources by drilling 266 producing and explorative wells in the western desert; some of them have been evaluated by pumping test and chemical analysis.

(Consortium-Yugoslavia, 1977), studied the hydrogeological conditions for the area located between Latitude N 32°, Longitude W 41° 30. Exploration wells were drilled, water was analysed, and rate of leakage was estimated. They calculated the total recharge, appointed the location and extensions for confined and unconfined aquifers and divided the project area in mutable blocks. The region of interest is a part from block 7, which was determined as a promising zone. One of the main recommendations was to provide a groundwater model as an approach for future water harvesting development.

(AlFurat, 1989) prepared a regional geological and hydrogeological study for Iraq including geophysical and hydrogeological sections. They calculated the specific capacity for wells and evaluated chemical analysis.

(AlFurat, 1995) drilled numeral wells in the Dibdiba formation south of Razaza Lake, showing that the thickness of this formation is not more than 30 m. They found that the aquifer is recharged by rainfall.

1.3.1.2 Remote Sensing Studies

(Al-Amiri, 1978) was one of the earliest studies that used visual interpretation of Landsat images. He figured out the relation between lineaments found by Landsat images for the Western Iraqi Desert and the subsurface structures where some fault maps have been prepared.

(Al-Azawi, 1988) compared lineaments found by Landsat images in the scale 1:250,000 covering the Western Desert with hydrogeological and economical maps. He concluded conformability between the density for some of these lineaments with groundwater and the probability to find ore bodies.

(Al-Mankoshy, 2008) attempted to illustrate the groundwater potential zones in the western desert of Iraq using an integrated approach of remote sensing and GIS. He compiled a digital map for Ubaiydh wadi (a total catchment of only 5912 km²) focusing only on the main single drainage line of the wadi.

1.3.2 Global studies

1.3.2.1 Groundwater flow and fracture zone

Numerous studies have been performed in order to determine fractured zones in aquifers and its impact onto groundwater flow and heads.

(Braathen, 1999; Rojstaczer, 1987) examined the hydrogeology of regional flow system in carbonate terrain by large-scale pumping for irrigation. Water-level decline in corresponding wells was used as a proof to identify hydraulic connection between several wells. The study showed that the orientation of water bearing fractures or conduits inferred is consistent with the major orientation of local and regional structural features.

(Mayo and Koontz, 2000) implemented a conceptual model of groundwater flow for fractured zones associated with faulting in sedimentary rocks. The model is based on the results of field and laboratory investigations, groundwater and methane gas inflows from fault-fracture systems, showing that groundwater stored in fractured sandstone, is confined by clayey layers.

(Sharma and Baranwal, 2005) used electromagnetic surveys by VLF-WADI resistivity sounding to interpret the geological structures and groundwater movement through fractures rock.

(Qian et al., 2005) carried out laboratory experiments to study groundwater flow in a single fracture with different surface roughness and apertures. Results show that the gradient of the Reynolds number versus the average velocity in a single fracture was almost independent of the change of fracture surface roughness, and it decreased when the aperture decreased under the same surface roughness.

1.3.2.2 Lineament's extraction

Several techniques have been developed and applied to extract lineaments from air-photos, satellite images, and digital terrain models.

(Raghavan et al., 1995) created a comprehensive toolkit for extracting lineaments from digital images using segment tracing and rotation transformation (START). This algorithm was coded in FORTRAN 77 and implemented on a UNIX-based workstation and is executed in two stages: at first a binary line element image is generated using the segment tracing algorithm; then in a second step the rotation transformation algorithm is used to extract lineaments from the line element image. This algorithm may work with different data set such as LANDSAT MSS, LANDSAT thematic mapper (TM), DEM's as well as shaded aeromagnetic images.

(Kim et al., 2004) developed for ArcView SHP files Avenue scripts to extract lineaments and lineament density from satellite images. The scripts may facilitate together with borehole data the analysis of the relationship between groundwater characteristics and lineament distribution. Accuracy of extracted lineaments depends strongly on the spatial resolution of images: the higher the resolution the better will be the quality of a lineament map (Hung et al., 2005).

1.3.2.3 Watershed delineation

Watershed Delineation tools have been developed since the 1980's. A brief review is given in the following paragraphs:

(Palacios-Velez and Cuevas-Renaud, 1986) developed an algorithm for defining the path of steepest slope in downstream or upstream direction by using TIN (Triangular Irregular Network) data. This algorithm allows for the definition of basin and sub-basins to any point on a river course. However, most digital terrain data are not provided as TIN but as raster based digital terrains models (DTM).

(Jenson and Domingue, 1988) developed software tools to derive morphologic information from raster DEM that have proven to be useful in hydrologic applications. First part of the analysis is a conditioning phase that generates three data sets: a DEM with depressions filled, a data set indicating the flow direction for each cell, and a flow accumulation data set in which each cell receives a value equal to the number of cells that drain to it. The original DEM and these three derivative data sets can then be processed in a variety of ways to optionally delineate drainage networks, overland paths, watersheds for user-specified locations, sub-watersheds for the major tributaries of a drainage network, or pour point linkages between watersheds. The efficient derivation of watersheds for large numbers of stream sediment and hydrologic geochemical samples also presents an extremely useful potential application and a software development challenge.

(Band, 1989) generated a set of recursive algorithms performing the actual topographic feature extraction and synthesis into a full basin model. He improved a framework for automatically watershed extracted from a DEM. The method is based on algorithms that automatically extract drainage lines and divide the networks of watersheds from a DEM. The framework is conducted to support and serve hydrologic models parameters for any sort of landscape investigation when topography plays an important role by using a set of recursive algorithms, which describe a new implementation. This method supports the parameterization of distributed components for runoff models and various hydrological applications.

(Martz and Garbrecht, 1992) presented a set of ten algorithms to automate the determination of drainage network and sub-catchments from DEM's. Main purpose of the algorithms named DEDNM was to parameterize rapidly drainage network and sub-watershed properties from DEM's for subsequent use in hydrologic surface runoff models. The algorithms perform DEM aggregation, depression identification and treatment, relief incrimination of certain areas, flow vector determination, watershed boundary delineation, drainage network and sub-catchment definition and systematic indexing, tabulation of channel and sub-catchment properties and evaluation of drainage network. The algorithms were developed using raster DEM's with a spatial resolution of 30 x 30 m and 1 m in elevation, similar to those distributed by the USGS for the 7.5' x 7.5' topographic quadrangles. Even though the development of the algorithms focused on problems encountered at this DEM resolution, their application is not restricted to this resolution.

A major improvement with respect to single flow direction algorithms was introduced by (Quinn et al., 1991) presenting a multiple flow direction techniques through distributing the upslope area among all possible directions and thus producing a more realistic picture of surface water flow.

(Garbrecht and Martz, 1993) performed an automated extraction of channel network and sub-watershed characteristics from raster DEM by using DEDNM (Martz and Garbrecht, 1992). This model can process DEM data of limited vertical resolution representing low relief terrain. Such representations often include ill-defined drainage boundaries and flow paths. It is similar to other models that are based on flow routing concepts, but it includes enhancements for processing low relief landscapes where the rate of elevation change. This model should be applied to subareas that are homogeneous. In general, the close agreement between the various parameters describing the overall network and sub-watershed characteristics demonstrates the ability of DEDNM to over-come the problems associated with ill-defined drainage boundaries and indeterminate flow paths in low relief terrain.

(Tarboton, 1997) presented an algorithms (D-infinity or D_{∞}) based on representing flow direction as a single angle taken as the steepest downwards slope on the eight triangular facets centred at each grid point. The upslope area is then calculated by proportioning flow between two down slope pixels, according to how close this flow direction is to the direct angle to the down-slope pixel. This procedure offers improvements over prior procedures that have restricted flow to eight possible directions or proportioned flow according to slope. The new procedure is more robust than prior procedures based on fitting local planes while retaining a simple grid based structure.

(Martz and Garbrecht, 1998) presented two new algorithms based on a deductive, but qualitative assessment of the most probable nature of depressions and flat areas in raster DEM's. The algorithms have proved to be robust and able to handle all types of actual and hypothetical topographic configurations. The algorithms also provide results that are intuitively more satisfactory and more realistic than other methods. The method proposed to solve drainage over flat areas in a DEM is using information of the surrounding topography and allows for flow convergence within the flat area.

(Saunders, 1999) introduced the stream burning process by integrating vector hydrography into raster DEM. This process can be summarized in four general steps: (1) rasterization of a digitized (vector) stream network, (2) assignment of DEM elevation values to the grid cells of the raster stream network, (3) manipulation of the stream network raster cells to ensure that elevations progress in a descending manner toward the outlet point(s), and (4) introduction of a fixed elevation differential between the stream network raster cells and the land surface raster cells. Stream burning promotes the digital replication of known stream networks through the automated flow direction and flow accumulation functions. This is important to ensure stream network coincidence with point locational data.

(Turcotte et al., 2001) showed numerous limitations of the widely used D8 approach and highlighted that these limitations could be overcome by the proposed approach, where D8 leads to a rather coarse drainage structure when monitoring or gauging stations need to be accurately located within a watershed. The D8 algorithm it is also unable to differentiate lakes from plain areas. Therefore using a digital river and lake network (DRLN) as input in addition to the DEM an algorithm has been developed allowing for the definition of a drainage structure, which is in agreement with the DRLN. It also led to a better match between observed and modelled flow structure and results of the proposed approach clearly demonstrate an improvement over the conventionally modeled drainage structure.

(P.Venkatchalam, 2001) implemented a procedure as part of the raster analysis module of the windows based GRAM++GIS, developed by the centre of studies in resources engineering, (Indian Institute of Technology). Results are showing that this module can serve for applications in hydrological modelling, watershed studies, and land use management.

(Jones, 2002) presented a new "drainage enforcement" that insures drainage continuity through flat areas and out of depressions. This algorithm is based on the priority-first-search weighted-

graph algorithm. Relatively simple methods for defining internal basins and incorporating digitized stream data are also discussed.

(Arge et al., 2003) presented and implemented a new I/O-and CPU-efficient algorithm (Terraflow) for flow routing on massive terrain datasets. Terraflow is a comprehensive software package designed and optimized for large datasets, which provides consistent performance as data size increase and significant speedups.

(Kiss, 2004) outlines the most important methods of automated mapping of flow routing, highlighting their utilities and limitations as well as the complex procedure, which combines the favourable characteristics of different methods.

(Lindsay, 2005) designed the Terrain Analysis System (TAS) to meet the research needs and being simple enough to be used for student instructions. TAS is a stand-alone GIS that possesses much of the spatial analysis functionality typically found in GIS packages. It is also capable of advanced modelling catchment processes. This program matches the visualization and spatial analysis needs commonly found in raster GIS packages with an extensive list of sub-programs specially designed for research in hydrology and geomorphology.

(Wanchang Zhang, 2005) proposed a new delineation approach that is mainly based on D8 algorithm for determination of flow field over rugged terrain and in association with D_{∞} algorithm for the relative flat area to fully take the advantage of D8 and D_{∞} in watershed delineation. The D_{∞} algorithms is based on representing flow direction as a single angle taken as the steepest downwards slope on the eight triangular facets centred at each grid point.

(Osma-Ruiz et al., 2007) described a new algorithm to calculate the watershed transform through rain simulation of grayscales digital images by means of pixel narrowing. The efficiency of this method is based on limiting the necessary neighbouring operations, which is the most expensive computation and in the total number of scans performed over the whole image. Experiments demonstrate that the proposed algorithm is able to reduce CPU time (30%) significantly in comparison to the fastest known algorithm without involving any loss of efficiency.

(Danner et al., 2007) presented the TERRASTREAM software package and the experimental results on real elevation point sets show that the implemented algorithm handle large multi-gigabyte terrain data sets. A data set containing over 300 million points and over 20GB of raw data was processed in less than 26 hours on a system, where most of the time (76%) is spent in the initial CPU-intensive DEM construction stage. The author performed experiments on a Dell

Precision Server 370 (3.40 GHz Pentium 4 processor) running Linux 2.6.11. The machine had 1 GB of physical memory.

If all eight cells of DEM have higher elevation than a central cell, the water is trapped in that cell. The common fill sinks function modifies the elevation value to eliminate these problems and this is the common approach to handle the problem.

(Kenny et al., 2008; Thommeret et al., 2009) developed two separate routines (one for sinks and one for flats) to establish flow direction in an unfilled DEM environment. Each sink and flat is analysed in sequence and flow directions are resolved iteratively, utilizing the surrounding terrain, the morphology within an unfilled DEM and the recognized flow patterns translated from surface hydrology features. In comparative analysis with five commonly employed sink flow routing algorithms the proposed sink routing routine resulted in the least alteration to both the elevation and flow direction surfaces.

(Thommeret et al., 2009) proposed a method aiming at extracting tree-structured gully floors and corresponding continuous talweg networks. Whereas classical methods of extraction are based on an arbitrary threshold, the presented method extracts a talweg only where the DTM expresses a landform. Thus, this method allows a more robust computation of topological indices of talweg networks that can otherwise be highly disrupted in geometry and topology. Moreover, the main parameter used in the method is the spatial distribution of the altitude error of DTM data, giving an objective threshold for the delineation of significant flow convergence areas.

1.4 Importance of investigation area

Investigate and utilize the water resource is one of the major problems nowadays in Iraq especially after the GAP project (22 dams on Tigris and Euphrates rivers by Turkey). Syria also started to construct some dams. Both countries are claiming that Iraq offers no management for both rivers and waste fresh water to the gulf. The negative impact of the GAP project is briefly presented by surface water depleting: Syria will lose at the final stage of the project 40% from the Euphrates water share while Iraq will lose finally about 90%, which lead to increase the desertification and pollution issues. 65% from Iraqi water demand for agriculture depends on Tigris and Euphrates. In addition 80% from domestic use rely on both rivers. Statistically, during the last couple of years about 20% from Iraqi territories have been deserted. Moreover, 70% from cropping potential has been lost. (MOWR, 2010).

The Western Desert is one of those areas which will be badly influenced by the activities mentioned above because it will prevent any plans for the future use of sophisticated irrigation system by using water from the Euphrates river. The entire region lacks of surface water resources, except some flash floods that rarely occur each year immediately after rapid but short rushes of rainfall. Conversely this region is well known as a rich metalliferous area, such as iron ore (Al-Hussayniyat formation), phosphate (Akashat area), pure sand for glass manufactures, clay for ceramics industries, and many others, in addition to the presence of several oases where people are working in agriculture and cattle grazing. Therefore, the government is developing a scheme for desert inhabitation and has plans to expand the use of ground water for agriculture and industrial purposes. Because groundwater is the only source for water in the region of interest intensive and detailed studies are needed.

1.5 Motivation

The general objectives of this research are to:

- Investigate groundwater flow with respect to the geological conditions.
- Evaluate two lineaments classified as suspected faults by applying different techniques (remote sensing and pumping tests in the fractured rock aquifer).
- Determining the catchment area for Wadi Ubaiydh
- Evaluate GIS techniques for catchment's delineation in flat and arid region by means of DTM by using different GIS packages for watershed evaluation, with three DTM data set: the 90 m and 30 m SRTM (Shuttle Radar Topography Mission) in addition to the ASTER 30m (Advanced Spaceborne Thermal Emission and Reflection Radiometer).
- Create a groundwater flow model as tool to determine the impact of structural geology and as overall tool to evaluate the future groundwater utilization

1.6 Deliverables

The general deliverables of the present research is:

- Providing sound numbers about groundwater available in the ROI.
- Providing sound numbers about GW recharge and areas where GW recharge takes place.
- Proving sound information where artificial groundwater recharge could be established.
- Providing a numerical groundwater model as tool for further investigation and prognosis.

1.7 Problems

After 2008, the region of interest was considered as a conflict area and war zone. This made any field work difficult respectively impossible. Several additional obstacles had to be considered. It was very difficult to find an appropriate guide, data, the transport of scientific equipment was rather time consuming and a general lack of observation wells had to be considered for the pumping tests.

2. Methodology

2.1 Literature review

A vast literature review was done to collect all data within different aspects such as scientific papers, reports of state agencies, books, unpublished academic reports; data sets (DTM's) and maps. The review was focusing on both regional aspects and relevant work concept.

2.2 Personal contacts

The aim beyond the personal contacts was getting the appropriate data to achieve the research purposes. Contacts have been established with the following authorities:

- Ministry of Science & Technology /Hydrogeological department & Meteorological unit.
- Ministry of Water Resources / Al-Furat center for hydrogeological studies.
- Ministry of Industry / GEOSURV-IRAQ the State Company of Geo Survey & Mining.
- Baghdad University / College of science.
- TU Bergakademie Freiberg / Library.
- Local farmers and inhabitants to get additional information during the field work.

2.3 Field work

Two field surveys were planned at the beginning to investigate the region of interest. The first field survey was in March 2009; the aim was to check the water wells positions and state, water sampling, field tests (pH, EC, O₂, C°) and performing pumping tests. Due to the critical security situation, the first fieldwork covered only 20 % of the entire region in the southeast. 14 water samples were collected for analyzing major and minor elements and 14 water samples for stable isotopes, moreover two pumping tests were accomplished for two wells (9 and 17). Unfortunately, the second fieldwork was impossible because this region was and still rated as a conflict area.

2.4 Evaluation of geological data

The geological data has been evaluated by the following methods:

2.4.1 Geological cross section

The geological cross section and correlation was generated by FreeHand v.9 based on the data from (Consortium-Yugoslavia, 1977) and (Buday, 1984). The topographic map was compiled by the SRTM DTM with 30m resolution for both the local and the regional ROI.

The general average slope according to (Quinn et al., 1991) was 0.002 for both the regional ROI [(967-22)/ 543000 m] and the local ROI [(233 – 609) / 155000 m].

2.4.2 Fault system by means of remote sensing techniques

Sharpening tools were used for automatic merging a low-resolution color, multi-, or hyper-spectral image with a high-resolution grey scale image and resembling to the high-resolution pixel size. The Gram-Schmidt Spectral Sharpening algorithm (Laben and Brower, 2000) may sharpen multispectral data using high spatial resolution data and simulating a panchromatic image for the corresponding sensor ETM. Gram-Schmidt transformation was performed with the simulated panchromatic band and the spectral bands, using the simulated panchromatic band as the first band by swapping the high spatial resolution panchromatic band with the first Gram-Schmidt band.

A directional algorithm implemented by ENVI is a first derivative edge enhancement filter that selectively enhances image features having specific direction components (gradients). The sum of the directional filter kernel elements is zero. The result is that areas with uniform pixel values are zeroed in the output image, while those that are variable are presented as bright edges.

The lineament extraction algorithm implemented by Geomatica is based on three fundamental steps to extract linear features from an image: at first, an edge detection operator is used to produce a gradient image from the original image. Then a threshold value is applied on the gradient image to create a binary edge image and finally linear features are extracted from the binary edge image. The last step contains several sub steps such as edge thinning, curve pruning, recursive curve segmentation, and proximity curve linking.

2.5 Climate and Meteorology

The climate data has been interpreted as following:

2.5.1 Meteorological data

The meteorological data used for the present research was provided by (MOST, 2009). Data of Nukaib meteorological station located in the region of interest (796510N, 3547165E) were adopted for climate analysis. This data covers the period from 1980 to 2008 for rainfall, temperature, potential evaporation, relative humidity, wind speed, and sunshine duration.

2.5.2 Aridity index

(Unep, 1992) has adopted an index of aridity, defined as: $I = P / PET$ where:

PET = potential evapotranspiration

P = Average annual precipitation

Table 2-1: Aridity index by (Unep, 1992)

Climate Type	Aridity index range
Hyper-arid	< 0.05
arid	0.05 – 0.2
semi arid	0.2 – 0.5
Dry sub-humid	0.5 – 0.65

According to this definition, the ROI is a hyper-arid region

2.5.3 Groundwater recharge

The groundwater recharge for the ROI (Fig.2-1) was calculated based on four crucial parameters (vegetation index, actual evapotranspiration, soil moisture and runoff):

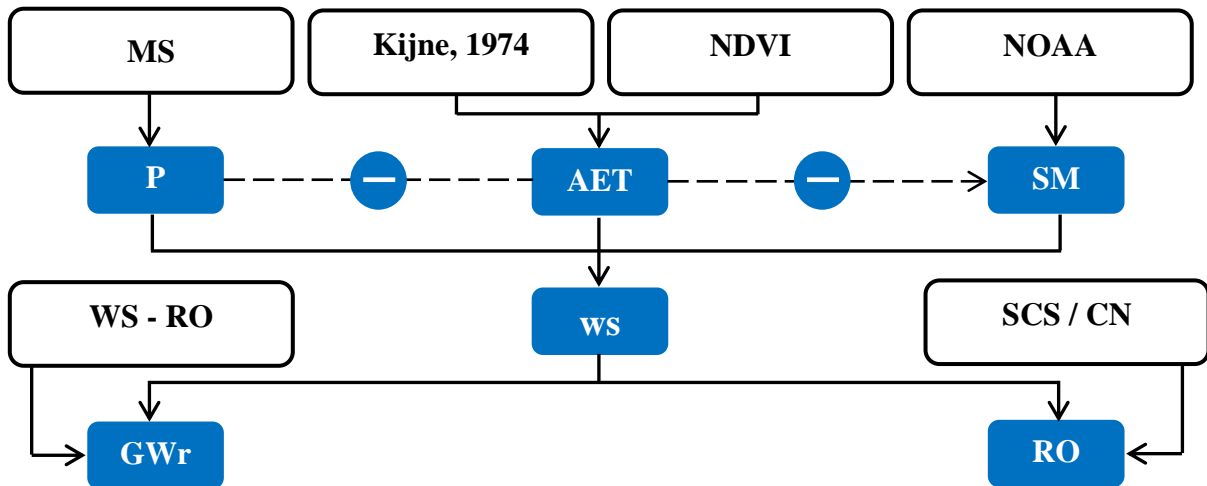


Fig.2-1: Groundwater recharge model

Where:

MS: Meteorological Station ,NDVI: Normalized Difference Vegetation Index, NOAA: National Oceanic and Atmospheric Administration, P: precipitation, RO: runoff, AET: Actual evapotranspiration, SM: Soil Moisture, WS: Water Surplus, SCS: Soil Conservation Service, CN: Curve Number, GWr: Groundwater recharge.

2.5.4 Vegetation index

To estimate the vegetation cover the NDVI was calculated by ENVI v 4.3 using Thematic Mapper (TM) data (Short, 2010) with band 3 (Red) and band 4 (Near infrared, NIR) as following:

$$NDVI = (NIR - Red) / (NIR + Red).$$

The minimum NDVI was -0.628 and the maximum was 0.572, while the mean was -0.087. Since values close to zero (-0.1 to 0.1) generally correspond to barren areas of rock, sand, or snow (Cohen and Shoshany, 2002). Therefore the region of interest shows that it lacks vegetation cover where no significant impact could occur with respect to evapotranspiration.

2.5.5 Actual evaporation

Different equations may be used to calculate the actual evaporation ((Penman, 1950), (Thornthwaite, 1948), and (Turc, 1954)) . In the present study the actual evaporation calculation is based on (Thornthwaite, 1948), because no field measurements were possible e.g. by using lysimeters. The equation’s parameters were fit to the available data and monthly temperature data were used instead of daily records. Moreover, the equation adopted for arid regions by (Kijne, 1974) :

$$PE = 16 \left[\frac{10T}{I} \right]^a \dots\dots\dots (2-1)$$

PE = potential evaporation mm, PEc = PE * K (2-2)

PEc = potential evaporation corrected

K = constant

The rates of PE were corrected for each month based on latitude due to the solar difference during the day for the geographic position in Appendix 2-1 (Kijne, 1974).

$$I = \sum_1^{12} i \dots\dots\dots (2-3)$$

I= Annual heat index °C

a = 0.016 I + 0.5..... (2-4)

a= constant

$$i = \left[\frac{T}{5} \right]^{1.514} \dots\dots\dots (2-5)$$

i = monthly heat index C°

T= average monthly temperature C°

The formula has a limitation when temperatures exceed 26.5 °C. In such cases PE was calculated directly from the following table (Kijne, 1974):

Table 2-2: PE values based on temperature rates ≥ 26.5 C° (Kijne, 1974)

T(C°)	PE (mm)
26.5	135.0
27.0	139.5
27.5	143.7
28.0	147.8
28.5	151.7
29.0	155.4
29.5	158.9
30.0	162.1
30.5	165.2
31.0	168.0
31.5	170.7
32.0	173.1
32.5	175.3
33.0	177.2
33.5	179.0
34.0	180.5
34.5	181.8
35.0	182.9
35.5	183.7
36.0	184.3
36.5	184.7
37.0	184.9
37.5	185.0
38.0	185.0

$$AE = PE - p \dots\dots\dots (2-6)$$

AE= Actual evaporation

p = Monthly rainfall mm

AE = PE_c when $p \geq PE_c$

AE = p when $p < PE_c$ the

$$WS = AE - SM \dots\dots\dots (2-7)$$

SM = soil moisture mm.

2.5.6 Soil moisture

The monthly data set consists of a file containing monthly averaged soil moisture water height equivalents from National Oceanic and Atmospheric Administration (Noaa, 2009) and the Climate Prediction Center (CPC). They provide temporal coverage of monthly means (from Jan.1948 to present), which are modelled data and not measured directly (Fig.2.2) (Appendix 2-2).

Data can be downloaded from: www.esrl.noaa.gov/psd/cgi-bin/db_search/SearchMenus.pl

Via soil moisture > make plot or subset > chose the coordinates > chose the dates.

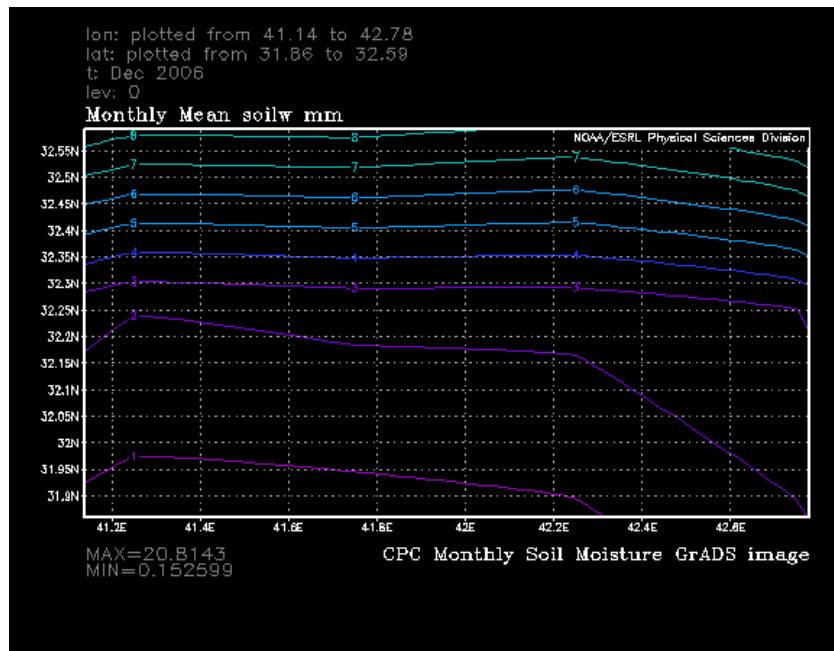


Fig.2-2: Soil moisture curve (Noaa, 2009)

2.5.7 Runoff

The water surplus (WS) will be divided into two parts: runoff (RO) and groundwater recharge (GWr). Since neither information was available or provided by hydrological data nor any empirical formula is applicable to be implemented for the ROI, runoff had to be calculated in a different way. Several runoff estimation models could be used such as: Overton, Holtan, Haggins - Monake, Kostikov, Green - Ampt, Horton and Philip Two - Term (Singh, 1992). However, these models need special parameters, which were not available. Thus, the simple SCS-approach (Soil Conservation Service Curve Number Approach) was implemented with four soil classes (hydrologic soil groups):

Table 2-3: Hydrologic soil groups based on infiltration rates (Maidment, 1993)

Group type	Infiltration rate cm/h	Runoff rate	Soil Description
A	≥ 0.76	Low	Sands or gravels
B	0.38 – 0.76	Moderate - Fine	Silt loam and loam
C	0.13 – 0.38	Fine - High	Sandy clay loam
D	0.0 – 0.13	High	Clay loam, silty clay loam, sandy clay, silty clay and clay

Since soils in the ROI belong to hydrologic soil group A and the curve number for a natural desert is 63 (Maidment, 1993), the SCS relation between storm RO and rainfall (see Fig.2-3) shows that the ROI has a cumulative rainfall of ~ 1.5 inch (38 mm.). This mean the RO will be considered as zero or very close to zero especially with the long distance travel for the expected RO through the region in addition to the low gradient (0.002).

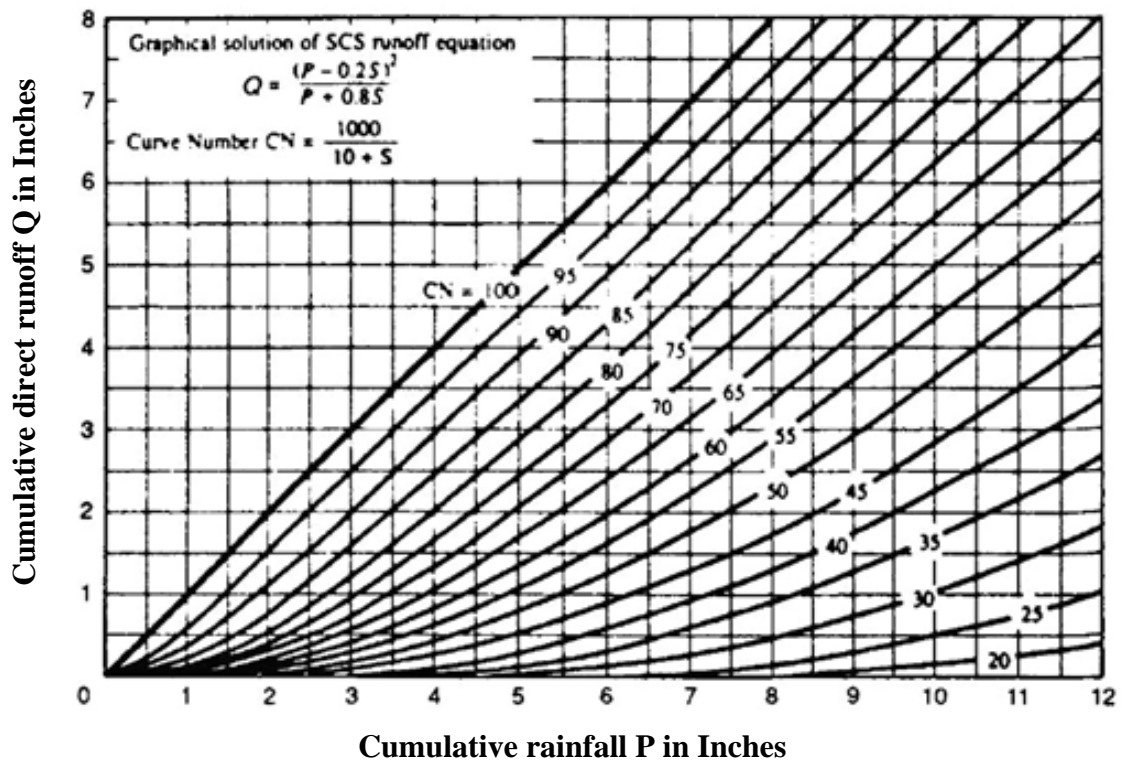


Fig.2-3: SCS relation between storm runoff and rainfall (Maidment, 1993)

2.6 Hydrogeology

2.6.1 Pumping tests

Pumping tests were performed in order to provide additional information. A great variety of equations and procedures are known for pumping tests with observations wells. However, if as in the case of this study no observation wells are available the evaluation of such pumping test data is awkward. Analytical and numerical models may offer a viable approach. In this study, the analytical model MLU was used for drawdown calculations and inverse modeling of transient well flow. MLU estimates selected aquifer parameters based on a best fit analytical solution to measured time-distance-drawdown data. The software includes an automatic curve-fitting algorithm computing optimized aquifer parameters and fitted drawdown results (Hemker, 1999).

2.6.2 Groundwater contour maps

Static water levels from 102 wells were used to determine the groundwater flow direction for the different aquifers by using different spatial interpolation algorithms. Minimum curvature algorithm (Smith and Wessel, 1990), Kriging (Cressie, 1990) and radial basis function (Carlson and Foley, 1992) did not result in significant different contour lines.

2.6.3 Wadi catchment delineation

Implemented by the following steps:

2.6.3.1 Data set

Ten 90 m SRTM and twelve 30 m ASTER files were merged by means of ArcGIS. A 30 m SRTM dataset of Iraq was supplied by courtesy of the US Army and the ROI was clipped from this DTM using ArcGIS. No additional steps were performed with both DTM data sets before using four software products to perform the catchment analysis. Three software have been implemented (TNTmips, ArcHydrotools and River tools); a fourth (TecDEM) was skipped because it was not applicable to deal with watershed delineation but rather to generate lineaments extractions, moreover TecDEM has no seeding point concept and has a limitation with respect of data capacity.

2.6.3.2 Approaches

The backbone of many GIS performing watershed delineation from a raster DEM is either the D8-algorithms (Fairfield and Leymarie, 1991) or the D^∞ (Tarboton, 1997), both extracting a po-

tential drainage network. While D8 only extract the drainage network at specific 8 neighbor cells, D_{∞} work along infinite directions. (Fig. 2-4). However, both D8 and D_{∞} face a problem, if more than one lowest neighboring cell is identified this problem can be either solved by a predefined direction or randomize single flow approach (Fig.2-5). On contrary to single flow direction algorithms multiple flow direction techniques (Quinn et al., 1991) produce more realistic water flow pattern. The second general problems are depressions within a digital terrain model, which can be solved to some, extend by depression filling algorithms (Fig.2-6)

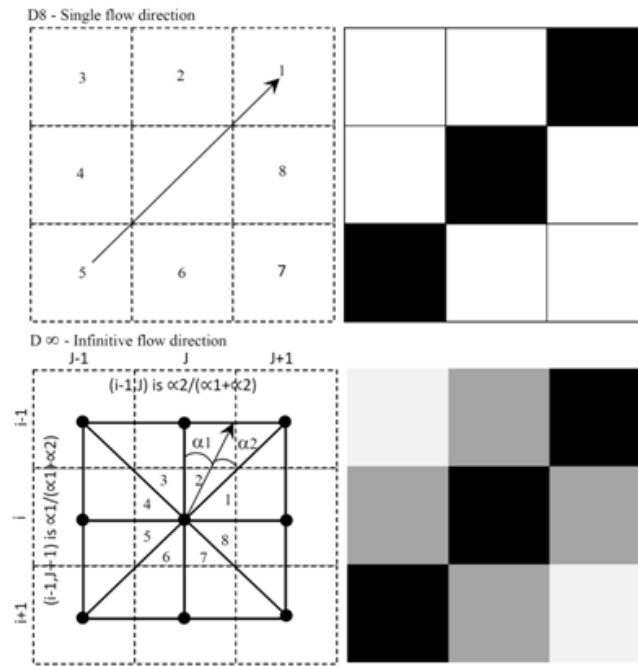


Fig.2-4: Flow direction and Watershed boundaries based on D8 & b- D_{∞} Fairfield and Leymarie, 1991, Tarboton, D.G., 1997)

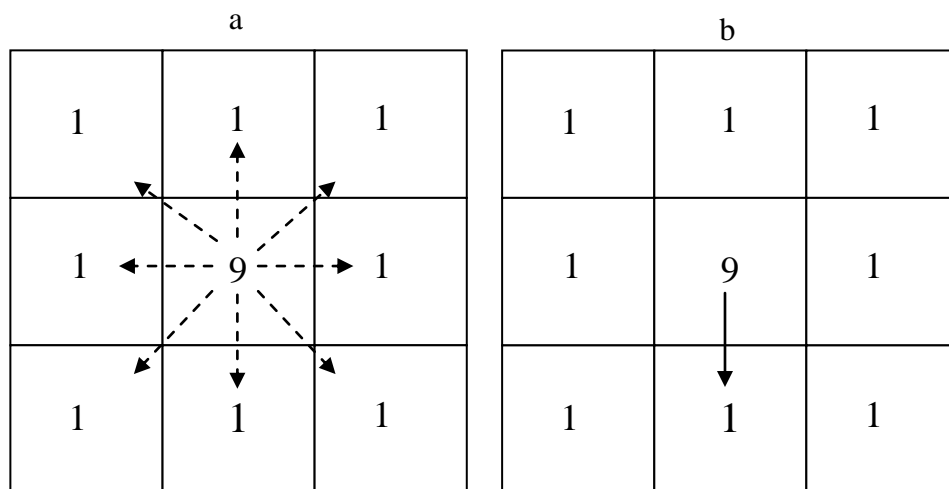


Fig.2-5: Flow direction a) Randomized. b) Non Randomized

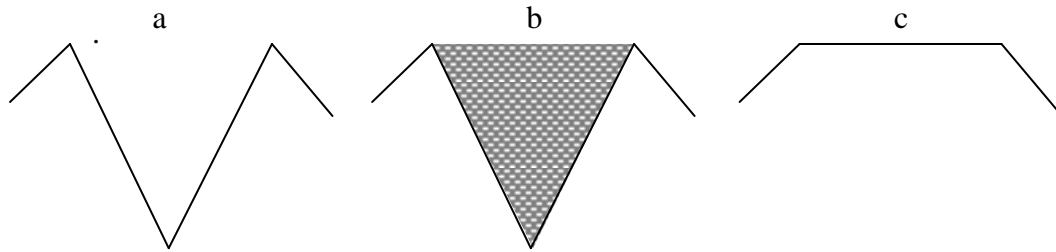


Fig.2-6: Fill depression a) Sink unfilled terrain. b) Sink filled terrain. c) Flooded terrain.

2.6.3.3 Software packages

Fig.2-7 illustrates how the three GIS used perform the DEM analysis. The algorithms used by RiverToolsV3.0 are described in some details, but the code is not available and finally it is not clear how the algorithms work in detail. The other two GIS packages (Arc hydro Tools and TNTmips) used are commercial ones and thus it is as well not truly known which algorithms are utilized for certain steps.

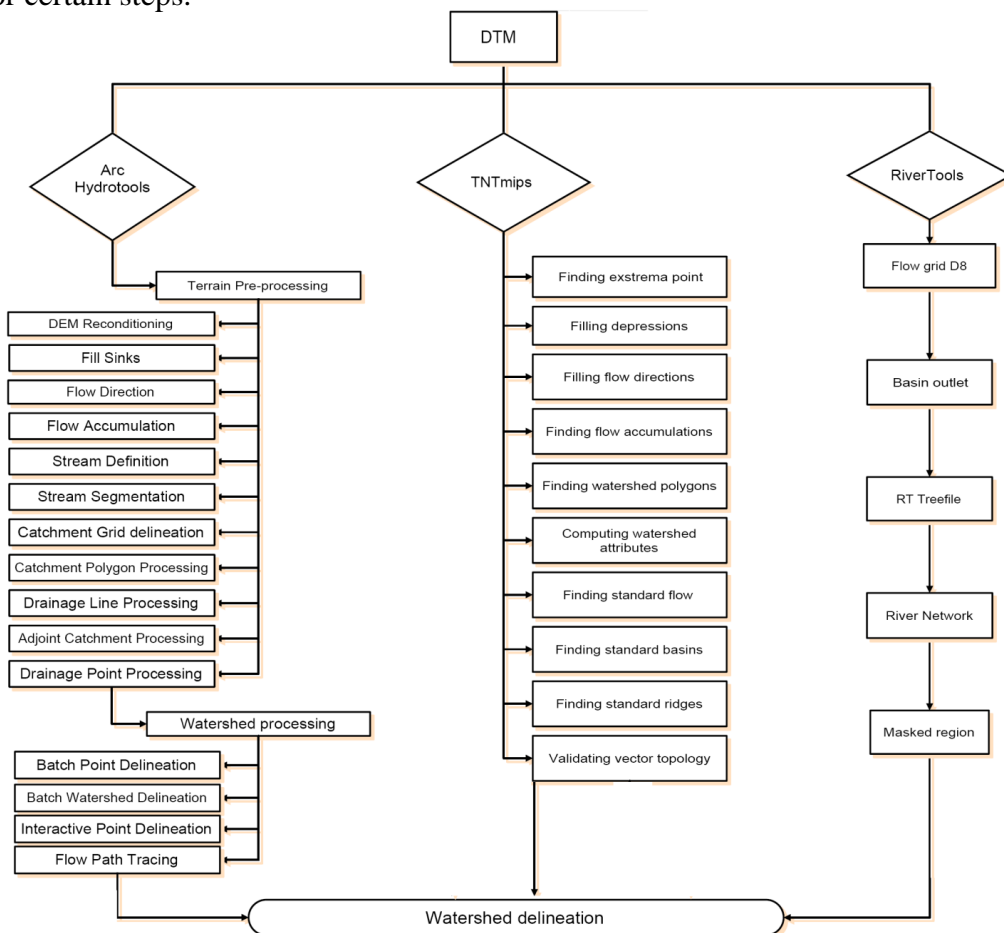


Fig.2-7: GIS software packages flowchart

a. RiverTools V.3.0

River Tools was developed by (Rivix, 2004) as add on to ESRI products for analysis and visualization of digital terrain, watersheds and river networks. River-Tools is able to import digital elevation data in a wide variety of formats and to extract geometric and hydrologic information. Several algorithms are included for DEM watershed analyzing, including D8, D_{∞} and a new mass flux algorithms which has been developed based on the D_{∞} for contributing continuous flow angles and watershed contributing areas, plus state-of-the-art methods for dealing with pits and flats. The mass flux algorithms method partitions flow between neighbor pixels by treating each pixel as a control volume. Unlike the D_{∞} method, which is superior to the D8 method but does not provide a rigorous solution to the problem of divergent flow on hill slopes, the mass flux method uses a rigorous mass balance approach by dividing each pixel into four quarter-pixels, computing a continuous flow angle using the elevations of 3 neighbor, and then computing contributing and specific area using the actual fraction of flow that would pass through each of a pixel's four edges.

As with D_{∞} method, flow from a given pixel will typically be partitioned between two neighbor pixels, except in the case of pixels that are single-pixel peaks or that lie on drainage divides. The results of the mass flux algorithms look quite similar, but the mass flux method shows significant improvements in the calculation of contributing areas. Both the D_{∞} and mass flux multiple flow direction algorithms outperform the single-direction D8, although they use a D8 flow grid to resolve ambiguous flow situations in flats and pits. (RiverTools, 2003). However, as a matter of fact, it is not clear in which manner the three techniques are implemented in the software package. E.g., it is not possible to choose between D8, D_{∞} , and the mass flux multiple flow direction algorithms. Thus one can only speculate that the mass flux multiple flow direction algorithms is used where seed points are provided by adding coordination or manual screw line concept.

b. Arc Hydrotools – GIS

Arc Hydrotools was developed since 2005 as add on to Arc GIS for building hydrologic information systems to synthesize geospatial and temporal water resources data that support hydrologic modeling and analysis. The Arc Hydro Tools have two key purposes. The first one is to manipulate key attributes in the Arc Hydro data model. These attributes form the basis for further analyses. They include the key identifiers such as HydroID and DrainI and the measure attributes such as LengthDown. The second purpose is to provide some core functionality often used in water resources applications. This includes DEM-based watershed delineation, network

generation, and attribute-based tracing. The functionality of Arc Hydro was implemented in a way allowing easy addition, either internally (by adding additional code) or externally, by providing additional functionality through the use of key Arc Hydro data structures (Table 2-4) (Hydrotools, 2009). Since Arc Hydro Tools is commercial software a description of algorithms used is not available, however, the main approach is assumed to follow (Maidment, 2002). A manual seed point option is provided.

Table 2- 4: Arc Hydro data structures

No.	Tool	Description
I	Terrain Pre-processing	Function is preprocessing a DEM. These functions are mostly used once in order to prepare spatial information for later use.
1	<i>DEM Reconditioning</i>	Enforce linear drainage pattern vector onto a DEM grid. Implements AGREE* methodology.
2	<i>Fill Sinks</i>	Fill sinks for an entire DEM grid.
3	<i>Flow Direction</i>	Create flow direction grid for a DEM grid.
4	<i>Flow Accumulation</i>	Create flow accumulation grid from a flow direction grid.
5	<i>Stream Definition</i>	Create stream grid with cells from a flow accumulation grid that exceed user-defined threshold.
6	<i>Stream Segmentation</i>	Create a stream link grid from the stream grid (every link between two stream junctions gets a unique identifier).
7	<i>Catchment Grid Delineation</i>	Create a catchment grid for segments in the stream link grid or sinks in the sink link grid. It identifies areas draining into each link.
8	<i>Catchment Polygon Processing</i>	Create catchment polygon feature class out of the catchment grid.
9	<i>Drainage Line Processing</i>	Create streamline line feature class out of the stream link grid.
10	<i>Adjoint Catchment Processing</i>	Create adjoint* catchment polygon for each catchment in the catchment polygon feature class. An adjoint catchment is the total upstream area (if any) draining into a single catchment.
11	<i>Drainage Point Process</i>	Create a drainage point at the most downstream point in the catchment (center of a grid cell with the largest value in the flow accumulation grid for that catchment).
II	Watershed Processing	Functions performing watershed and sub-watershed delineation and basin characteristic determination. These functions operate on top of the spatial data prepared in the terrain preprocessing stage.
1	<i>Batch Point Delineation</i>	Function delineates the watershed upstream of each point in an input batch point feature class.
2	<i>Batch Watershed Delineation</i>	Create a watershed for every point in the batch point feature class. Results are stored in a watershed polygon feature class. Watersheds are overlapping if points are on the same stream
3	<i>Interactive Point Delineation</i>	Interactively delineate a watershed for a user specified point based on the preprocessed DEM.
4	<i>Flow Path Tracing</i>	Trace the downstream path, based on the steepest descent, from a user specified point to the edge of the DEM by using a flow direction grid.

* *AGREE: DEM grid after reconditioning process.*

* *Adjoint: a polygon representing the whole upstream area draining to its inlet point is constructed and sorted in a feature class.*

c. TNTmips V 2007

TNTmips watershed process provide fast and efficient production of watershed boundaries, flow paths, and other derived products from very large SRTM extracted from these DEM including raster to vector conversion of the results. TNTmips can import nearly any kind of data and one may export results to these formats as well. A watershed process was part of TNTmips since the early 1990 using the (Jenson and Domingue, 1988) approach. It is not known which algorithm is used in the version V.2007, respectively the most recent version. TNTmips evaluates by default the entire DEM creating sub-catchments according to defaults or user defined criteria and the entire catchment. A seed point option can be utilized on user request.

2.6.4 PC Options

The PC that was used for the delineation process had the following characteristics: Operation system: Windows XP. 2002 professional; hardware: Intel (R) core (TM) 2 Quad CPU with 2.40 GHz; 2GB RAM.

2.6.5 Groundwater Model

Groundwater modeling in general is going through three stages, system analysis, creating a conceptual model and finally deciding the type of the model for example finite difference or finite elements. By using Visual Modflow version 4.2, the finite difference type has been chosen to conduct the model since no grid refinements will be needed for further details with such huge area. A transient model was not implemented so far due to lack of data.

Five steps mainly compose the created model: creating the input-files, running the model, checking the output, calibration by changing parameters and boundary conditions and finally performing a sensitivity analysis. The methodology for the present model (Fig.2-8) is illustrated as following:

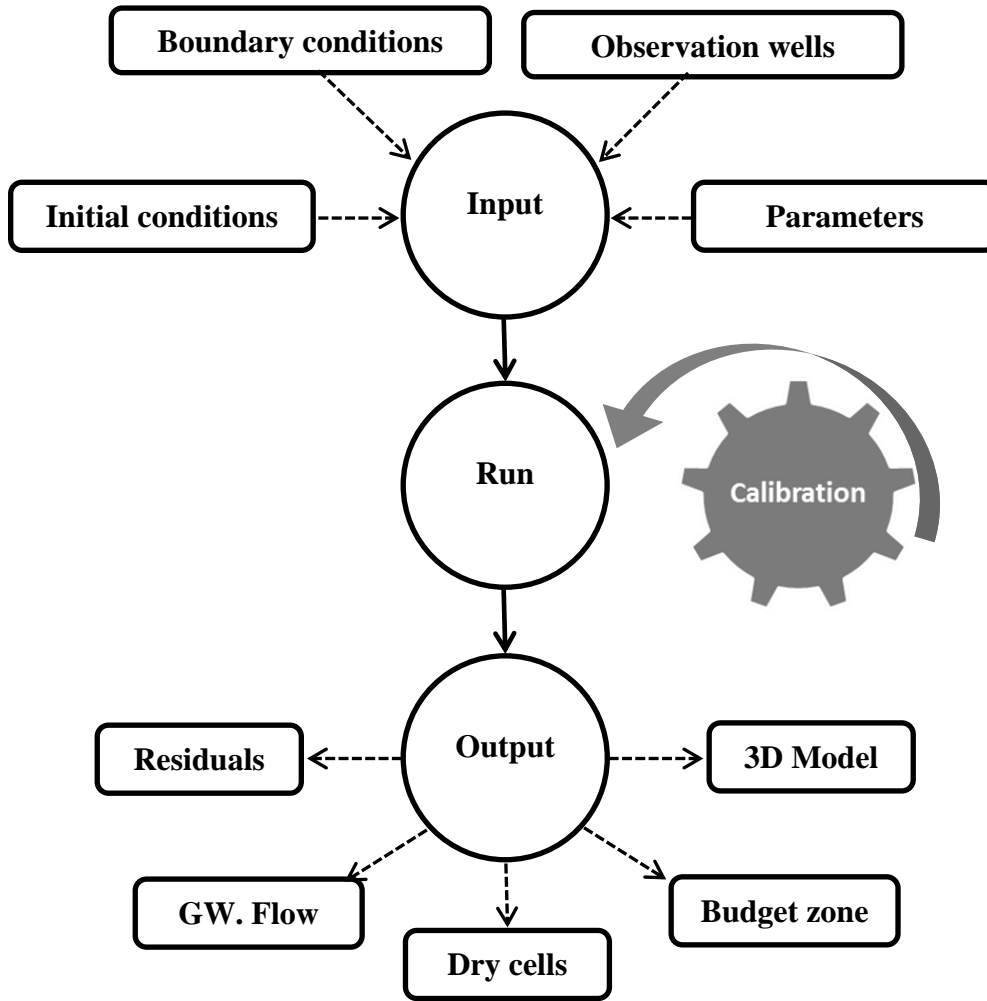


Fig.2-8: Groundwater flow Model by Visual .Modflow

2.6.5.1 Conceptual Model

The conceptual model is based on geological cross sections with 5 layers: three aquifers and two aquicludes. The surface layer was imported from the 30m SRTM data. Although the entire area is build up by hard rocks and not sediments it is assumed that a continuum approach can be applied. Thus, the Dracy equation can be used to describe and model the groundwater flow. A finite difference approach was chosen with equal grid spacing. The two main faults were implemented by using different conductivity values in comparison with the general values of the 5 layers.

2.6.5.2 Input

Any groundwater model needs data to define geometry, parameters, boundary conditions, and initial values. The geometry of the ROI was defined by using a map with UTM coordinates. The discretization chosen was 500 by 500 m. Grid refinement was not done at any part of the model. Due to a length of 155 km and a width of 80 km, each layer contained 49600 cells. The total number of cells of the model is therefore $5 \times 49600 = 248000$ cells.

5 layers representing the bottom of each aquifer were created with the Software SURFER v.8 and data from 102 boreholes (MOWR, 2010). For interpolation of the borehole data Kriging with a linear algorithm was used. The surface of the model was taken from the 30 m SRTM digital elevation model. All bottom layers and the surface layer were imported to Visual Modflow.

2.6.5.3 Properties

Conductivity (Kf) values were assigned for each layer: $1 \text{ e-}4$ m/s for the three aquifers, $1 \text{ e-}8$ m/s for the aquicludes and $2 \text{ e-}3$ m/s for the fault zone. The total and effective porosity was assumed to be 0.15% for all layers while total porosity was assumed to be 0.3%. The storage coefficient was set to $1 \text{ E-}5$ (m^{-1}) and specific yield to 0.2%.

2.6.5.4 Boundary conditions

Groundwater flows from west to the east. Therefore the flow boundary conditions have been set as following: west and east were considered as constant head boundaries while north and south as no flow boundaries because of symmetry reasons.

Constant head values were taken by observation wells close to the boundary by using the line-option of Visual Modflow. Recharge was implemented in two different options either for the entire area or only within the main Wadi drainage area (Fig. 2-9). The recharge of 17.5 mm/year is the average calculated by water balance for the period 1980-2008. Recharge was varied from 11.85 to 60 mm/year during the calibration to figure out the model sensitivity. The model failed to run with values less than 11.85 mm/year and more than 60 mm/year.

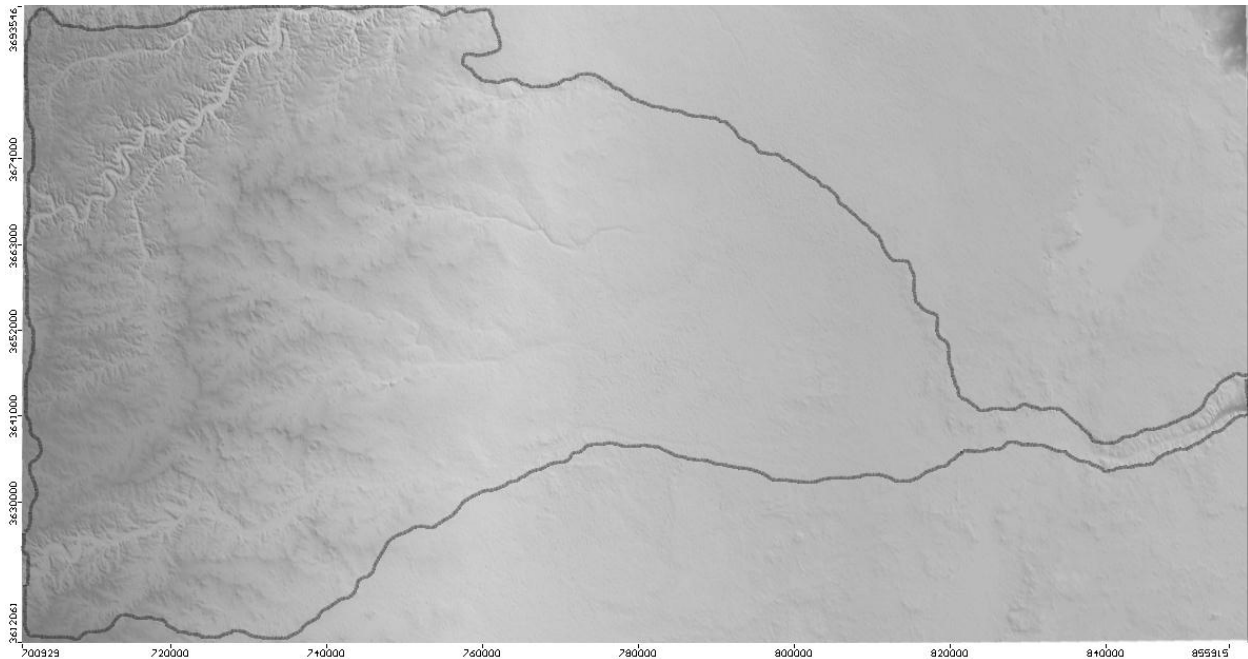


Fig. 2-9: polygon for main Wadi drainages where recharge implemented

2.6.5.5 Observation wells

102 monitoring wells were implemented in the model by importing a text file with the coordinates (well number, easting, northing and static water level - Appendix 2-3).

2.6.5.6 Solver

Visual Modflow offers six different solvers (PCG, SIP, SOR, WHS, SAMG, GMG) including implicit and explicit routines. In this study the WHS solver was used because this was the only one able to handle the model; the other solvers failed to run the model. As previously mentioned the model was run only in steady state modus with a total simulation time of 7300 days (20 years).

2.6.5.7 Calibration

During the calibration, the only parameter to change was the conductivity. Furthermore, the boundary condition recharge was changed as well. The permeability of the 3 aquifers was varied between $1 \text{ e-}4 \text{ m/s}$ and $1 \text{ e-}8 \text{ m/s}$ and for the fault zones between $2 \text{ e-}3 \text{ m/s}$ and $6 \text{ e-}4 \text{ m/s}$. The automatic calibration (inverse modeling by using PEST) was tried but probably due to the size of the model (248000 finite differences cells) PEST could not find a minimum and failed. Because not enough data were available for the region of interest, it was not possible and meaningful subdividing the entire area into sub-regions.

Furthermore, the boundary condition recharge was varied between 11.85 and 60 mm/year either for the entire region or for those areas representing the main wadis drainages. The data available did not allow calculating a spatial distribution of the recharge of the area.

The resulting pressure head were compared with measured heads in the three aquifers by means of scatter plots and statistics of the residuals.

3. Geological setting

3.1 Preface

This chapter bases mainly on (Jassim and Goff, 2006). This book is reviewing all investigations, done so far with respect to the geology of Iraq.

The region of interest is part of the western desert of Iraq and a flat terrain, sloping gently towards the Euphrates River, characterized by low rainfall, which is not sufficient to maintain a continuous plant cover. The vegetation consists of sparse desert plants and scattered shrubs. The climate is very hot and dry in summer with high diurnal changes in temperature and classified as hyper arid based on (Unep, 1992).

Iraq divided into three tectonically different areas, the Stable shelf with major buried and anti-forms but no surface anticlines, the Unstable shelf with surface anticlines and the Zagros Suture which comprises thrust sheets of radiolarian chert, igneous and metamorphic rocks (Jassim and Goff, 2006). Since the ROI belong to the stable shelf, an overview about this area is needed.

The stable shelf is a tectonically stable monocline and only little affected by late Cretaceous and Tertiary deformation. The orientations of the structures in this tectonic unit are influenced by the geometry of the underlying basement blocks and faults. Palaeozoic epirogenic events and Mesozoic arching, the depth of the Precambrian basement varies between 5 km in the centre of the shelf to 11 km. in the W and 13 km. in the E. However, the stable shelf is now divided into three major tectonic zones, from the west; the Rutba – Jazira, Salman and Mesopotamian zones (Jassim and Goff, 2006).

3.2 Tectonic and Structure

Region of interest is a part from the Rutba – Jazira zone which is an inverted Palaeozoic basin and the inversion began in the late Permian. Its basement was relatively stable during Mesozoic – Tertiary time and more active during Infracambrian and Palaeozoic times. Basement depth ranges from 5 km in the Jezira area to 11 km south of Rutba. The Jezira area was part of the Rutba uplift domain in late Permian to early Cretaceous time. After Cretaceous the Jazira area subsided while the Rutba area remained uplifted, these two areas are thus differentiated as separate subzones (Jassim and Goff, 2006).

The Rutba uplift dominates the Rutba – Jezira zone. However, the thickness and facies of its Mesozoic sequences suggests that it has often acted as a separate block sometimes affecting NW Saudi Arabia and NE Jordan but mostly affecting E Syria and W and NW Iraq (Jassim and Goff,

2006). The Rutba – Jazira zone contains thick Palaeozoic sediments; upper Permian, lower to middle Triassic and Pre Albian lower Cretaceous sediments are absent. The Jazira subzone was uplifted and eroded during mid-Devonian time, but the Rutba subzone was nearly not affected by this deformation. The Jezira subzone also subsided during late Eocene to Miocene time when the Rutba subzone was uplifted. A NW-SE cross section to the Rutba area is shown in (Fig. 3-1)

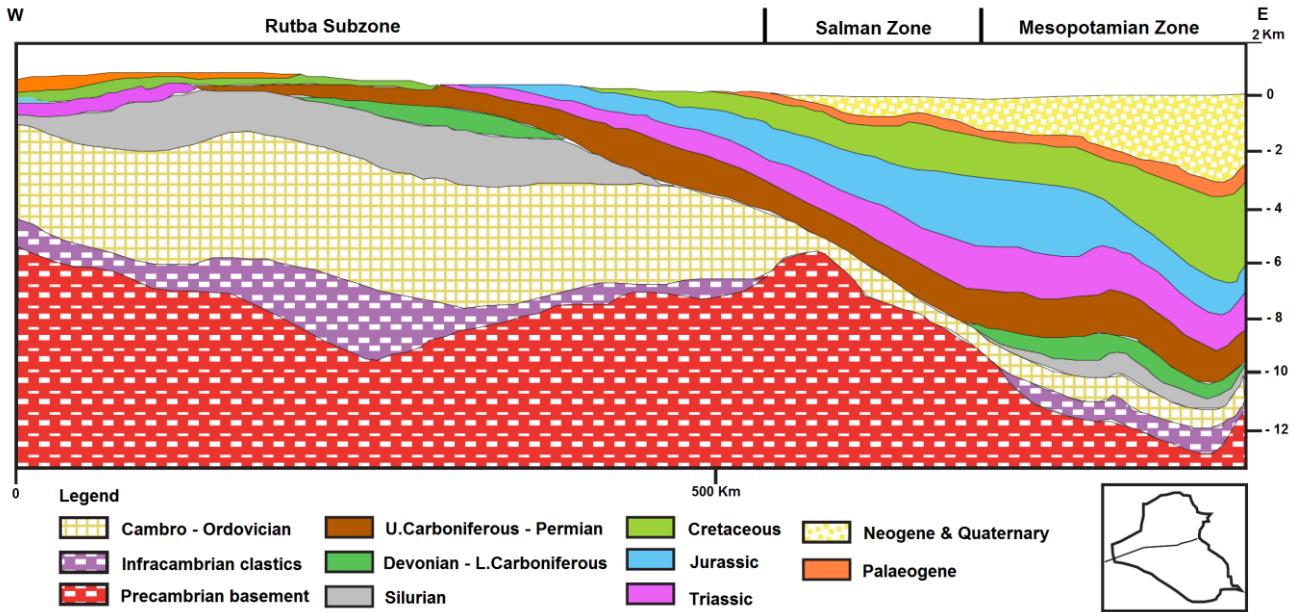


Fig.3-1: Cross section showing Rutba subzone (Jassim and Goff, 2006)

Based on (Buday, 1984) three local faults can be distinguished in the middle and eastern part of the region of interest.(Fig. 3-2) The main directions for these faults are NS & NE-SW; these directions are compatible with the main field stress of ROI which belong to the Najd – Hejaz origin movement (Precambrian – Palaeozoic) .Fault 1 has been described as a normal fault while faults 2 and 3 are classified as suspected faults.

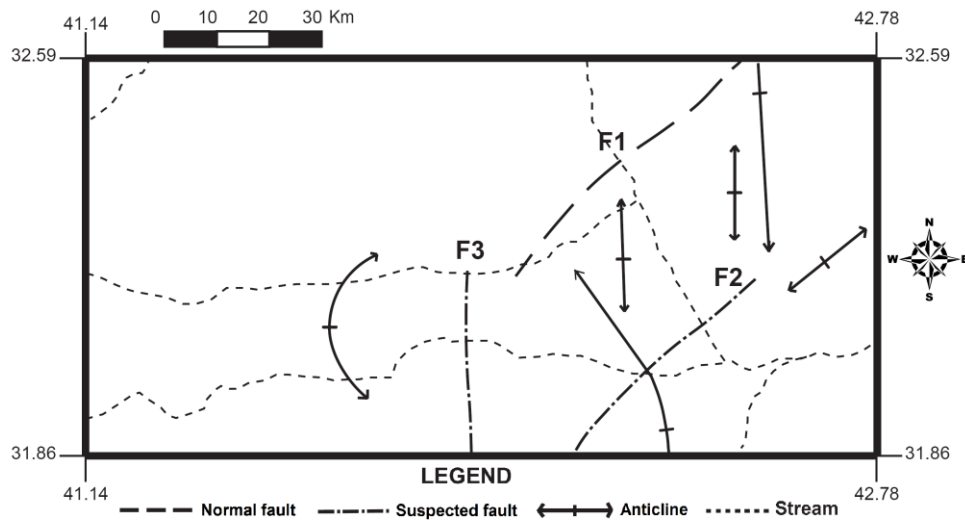


Fig. 3-2: Faults in the local ROI (Buday, 1984)

3.3 Stratigraphy

The cross section for the Western Desert shows that Limestone and dolomitic limestone are the most dominated units. (Fig. 3-3) and (Fig. 3-4) showing respectively the Stratigraphy for the western desert and the outcrops in the local ROI (Buday, 1980).

ERA	PERIOD	EPOCH	AGE	FORMATION	DESCRIPTION	THICKNESS m. - ROI.		
CENOZOIC	QUATERNARY	HOLOCENE		AEOLIAN DEPOSITS	Sand, silt, gravel, loose sand sheet curve and rock fragments.	} < 1m.		
				VALLEY FILL DEPOSITS	Moddy sand,,mainly Gypsiferous, gravel, silt and clay.			
				FLOOD PLAIN DEP.	Mainly sand with silt and clay.			
				DEPRESSION FILL DEP.	Sand and silty clay partly gypsiferous.			
		PLEISTOCENE		RESIDUAL SOIL	Silty and clayey soil.			
				SLOP DEPOSITS	Sand, silt, clay with rock fragments.			
				SABKHA	Mud with salt crust.			
				ALLUVIAL FAN	Mainly gravels with sand and silt.			
		TERrace DEP.	Gravel, sand cemented rock fragments.					
	TERTIARY	NEOGENE	PLIOCENE	Late	Dibdibba Zahra	Claystone, Siltstone, conglomerate. Sandstone, claystone, & sandy limestone, conglomerate, pebbly sandstone.	} ~ 27m. } ~ 126m. } ~ 377m. } > 90m.	
				Upper	Injana	Sandstone, claystone, siltstone, with thin limestone.		
			MIOCENE	Middle	Fatha	Red claystone, gypsum, limestone & marl.		
				Lower	Euphrates	Conglomerate & Chalky dolomitic limestone.		
		PALAEOGENE	EOCENE	Middle	Dammam	Numinulatic limestone, dolomitic limestone & marl.		
				Lower	Ratgaa	Numinulatic limestone, sandstone & dolomitic limestone.		
			PALEOCENE	Upper	Umm Er- Radhuma	Shelly chalky limestone, dolomitic limestone & marl.		
				Middle				
			MESOZOIC	CRETACEOUS	UPPER			Tayarat
						Hartha		Limestone, marl, dolomitic limestone, sandstone, fossiliferous dolostone.
	Rutba Ms'ad	Marl, fossiliferous & limestone. Marly limestone, mainly sandstone.						
LOWER		Maudud			Alternation of marl or marly limestone & recrystallized limestone.			
		Nahr Umr			Sandstone, fossiliferous marl & sandy-marly limestone.			
JURASSIC	UPPER			Najmah	Dolostone, limestone, coglomerate & sandstone.			
				Muhaiwir	Marl, dolomitic marly limestone, sandstone, siltstone, & sandy limestone.			
	LOWER			Amij	Dolomitic & marly limestone, claystone, marl & limestone.			
				Hussainiyat Ubid	Dolostone, dolomitic limestone, limestone, chert, sandstone & calystone. Dolomitic limestone, dolomite & chert.			
TERTIARY		UPPER		Zorhoraan	Marl, marly dolomitic limestone & limestone.			

Fig. 3-3: Stratigraphy for the western desert of Iraq (Buday, 1980)

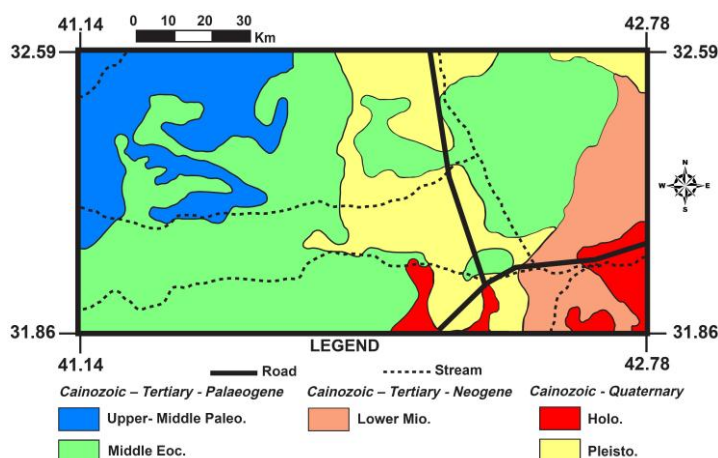


Fig. 3-4: Outcrops of the local ROI (Buday, 1980)

3.3.1 Tayarat formation (Upper Cretaceous)

The Tayarat formation was defined by Henson in 1940 (Bellen, 1959) 30 km south of Rutba town in western Iraq. It comprises 48 m of bubbly, porous, and chalky limestone, which is locally dolomitised and sandy. The phosphate containing Digma formation replaces the upper part of Tayarat formation to the west of the type section. The formation also outcrops along the west rim of Ga'ara depression where it is 25 m thick and comprises oyster-bearing limestone, Loftusia limestone, and chalky limestone. The basal unit of this section comprises limestone conglomerates, which were deposited in channels and oyster bearing limestone. The uplift and emergence of the Ga'ara anticline in Maastrichtian time strongly influenced the distribution and facies of the Tayarat formation.

The lower unit comprises conglomerate or coarse – grained calcareous sandstone, passing upwards into dolomitic limestone, dolomite, siltstone, silty marl and calcareous shale, locally containing shark teeth and thin-shelled gastropods, the clastics in the lower unit pass into carbonates to the east. The type section of the Tayarat formation includes some phosphatic beds.

The formation thickness reported to be 426 m near Anah but this thickness probably includes parts of Hartha and Shiranish formations, the formation is thinner in the Euphrates and Tigris subzones of Mesopotamian zone where it passes into Shiranish formation.

The upper contact with Umm Er Radhumma formation in south and south-west Iraq is disconformable (Bellen, 1959).

3.3.2 Umm Er Radhumma formation (Lower. – Upper Paleocene)

The Umm Er Radhumma formation was described by Steineke and Bramkamp in 1952 (Bellen, 1959) from the type locality at the Umm Er Radhumma wells in Saudi Arabia. The reference section is Wadi al Batin in Saudi Arabia. Owen and Nasr (1958) introduced a supplementary type section for Iraq (in well Zubair 3) in south Iraq. It comprises anhydrite and white to buff dolomitic microcrystalline limestone and cherts occurring in the upper part.

The Umm Er Radhumma formation in Iraq outcrops in the eastern part of Rutba subzone, south of Wadi Al Kharr along the Iraq – Saudi border and on the shoulders of the Nukhaib Graben.

Near Nukaib, the formation is 240 m thick and comprises from top to the bottom:

- 1- 30 m of recrystallized Shelly and dolomitic limestone, phosphate at the top, with red mudstone beds.
- 2- 40 m of white chalky limestone with chert beds.

- 3- 50 m of white argillaceous and chalky limestone and grey Shelly calcareous dolomite with black chert lenses.
- 4- 40 m of white chalky limestone and grey calcareous dolomite (with chert along bedding planes) containing a 5 m varicoloured calcareous sandy limestone at the base.
- 5- 40 m of grey recrystallized Shelly calcareous dolomite with chert lenses.
- 6- 40 m of white fossiliferous chalky limestone and yellow recrystallized Shelly calcareous dolomite with thin beds and lenses of chert.

3.3.3 Dammam formation (Middle Eocene)

Dammam formation was first described by Bramkamp in 1941 from the Dammam dome in east Saudi Arabia (Bellen, 1959) comprising limestone (chalky, organodetrital or dolomitic), dolomites, marls and shales. It consists mainly of neritic shoal limestone often recrystallized and/or dolomitised, nummulitic in the lower part and milliolides-bearing in the upper part.

In the outcrops, Ramsden and Andre (1953) recognized four informal units; these units comprise from bottom to top:

- 1- Chabad-Shawiya-Huweimi unit consisting of nummulitic-alveolinid limestone
- 2- Huweimi Schbicha-Sharaf unit composed of chalks and chalky limestones
- 3- Wagsa unit composed of chalky, moderately fossiliferous limestone

The thickness of the formation, in the Iraqi supplementary type area, reaches 250 m. The nummulitic limestone of western Iraq, which is up to 100 m thick NW and SW of Ga'ara, are not included within Dammam formation.

3.3.4 Euphrates formation (Lower Miocene)

The Euphrates formation is the most widespread formation of the sequence. It was originally described by De Boeckh in 1929 and later amended by Bellen in 1957. The type locality near Wadi Fuhaimi near Anah on stable shelf comprises 8 m of shelly, chalky, and well bedded recrystallized limestone; however it represents only a small part of the formation and does not include the basal conglomerate. Sands and anhydrites also occur in some subsurface sections (Bellen, 1959).

The Euphrates formation thickness based on Anah-2 well about 94 m and comprises five units from top to the bottom:

- 1- Brownish dolomite.
- 2- Olitic and chalky limestone.

- 3- Soft white limestone with macrofossils.
- 4- Dolomite.
- 5- Cream to buff dolomite with basal conglomerate.

This section is not representative of the whole formation and lacks the marly limestone and marl, which outcrop near the well.

3.4 Topography and Ubaiydh Wadi

The rather flat terrain is sloping gently towards the Euphrates River. The region of interest includes several large wadis, such as Ubaiydh, Amij, Ghadaf, Tubal, and Hauran discharging to the Euphrates River. The only map displaying drainage pattern of the area was done by the British troops during world war II (Division, 1944). The region of interest is considered to enclose some of the most important wadis in the western desert (Fig. 3-5).

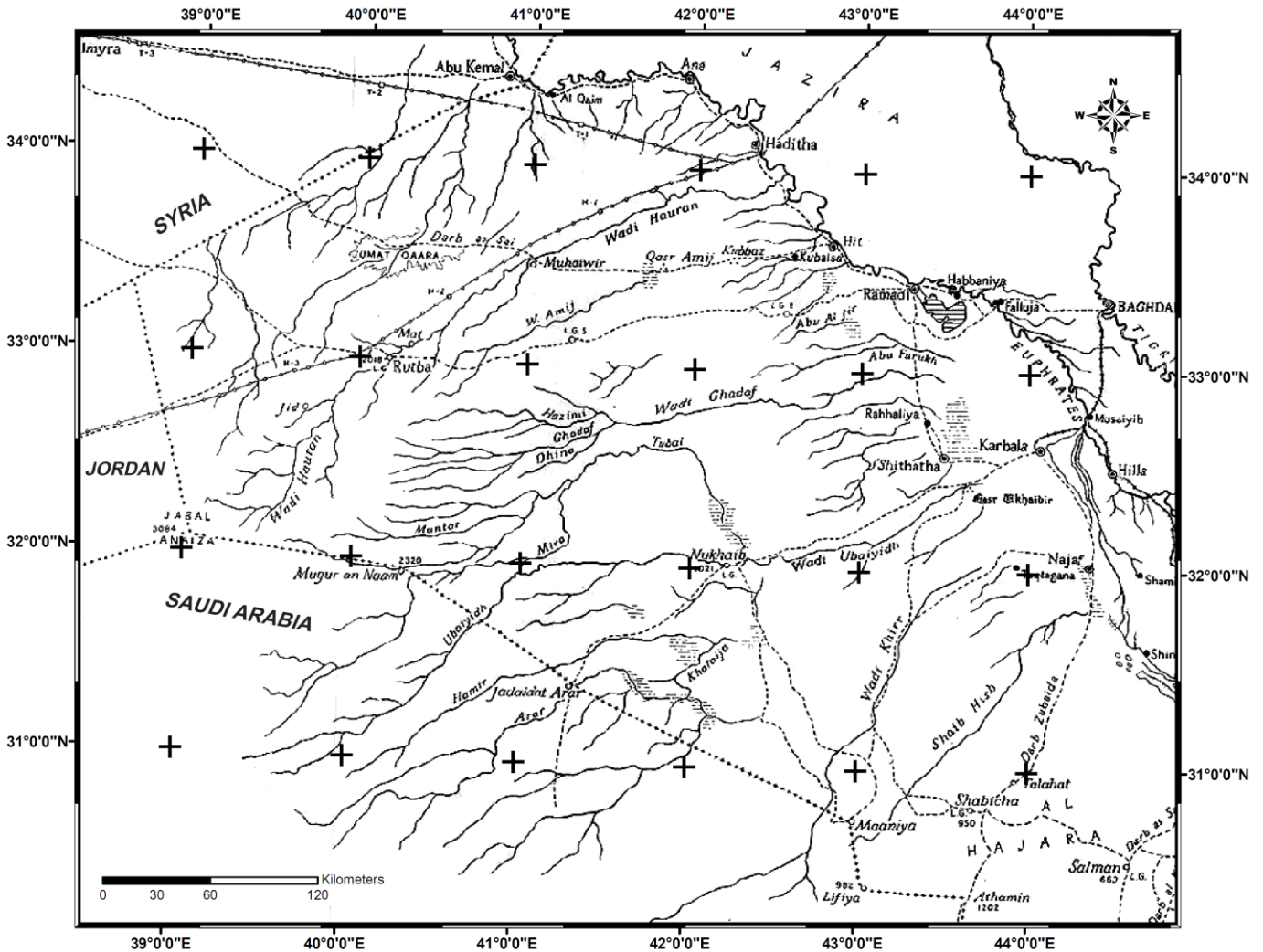


Fig. 3-5: Western desert wadis – Iraq (Division, 1944)

(Consortium-Yugoslavia, 1977) provided a hydrogeological investigation for the western desert of Iraq and part of this was a thorough catchment investigation based on a field survey. The catchment area was calculated to be 32,340 km²; however, it is not documented how this calculation was done. On contrary (Al-Mankoshy, 2008) determined for Ubaiydh wadi a total catchment of only 5912 km² (Fig. 3-6). This huge difference in catchment area calculation comparing to the above field survey can be explained only by assuming that the author has been focusing on the main single drainage line of the wadi. Therefore, this kind of biased manual delineation will not be taken in further consideration.

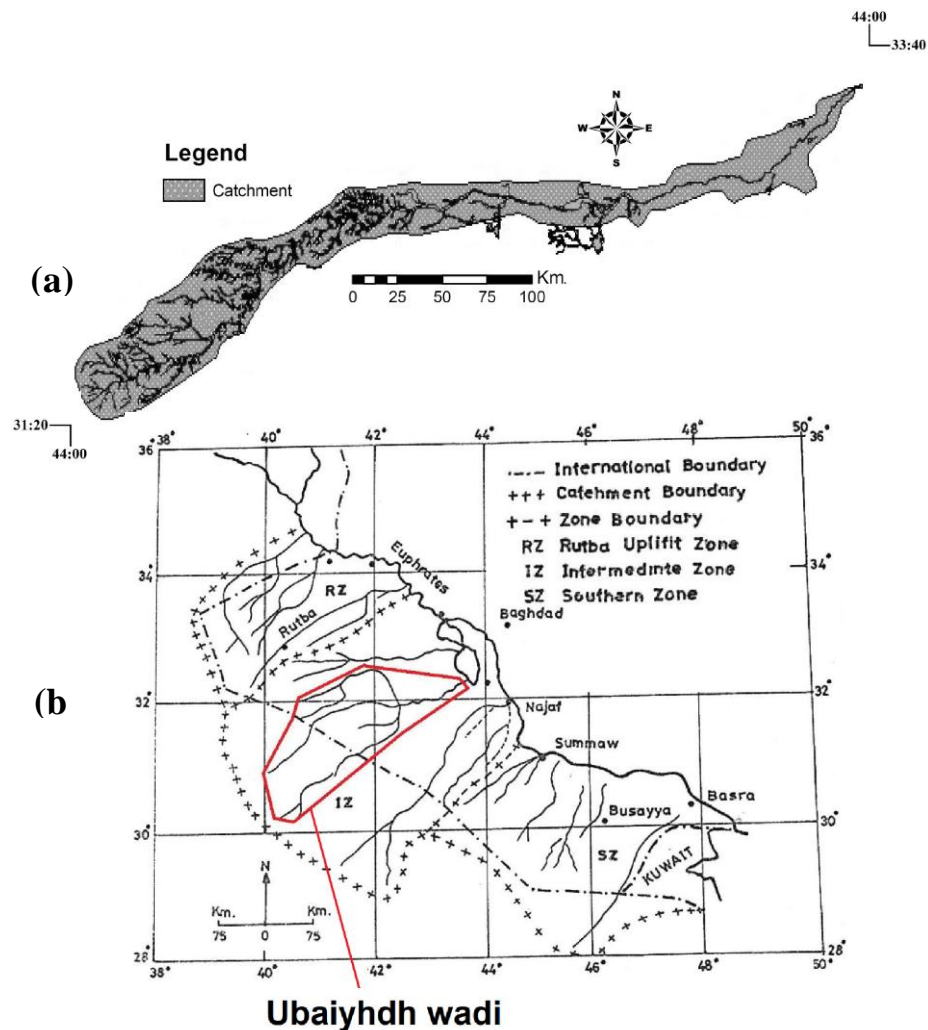


Fig. 3-6: Previous catchment area calculation for Ubaiydh Wadi
 (a) Catchment area 5912 km² (Al-Mankoshy, 2008)
 (b) Catchment area 32,340 km² (Consortium-Yugoslavia, 1977)

4. Climate and Meteorology

4.1 Preface

The meteorological data used for the present research is provided by (MOST, 2009). The data of the Nukaib meteorological station, which is the only station located in the region of interest (796510N, 3547165E) was adopted for climate analysis covering the period from 1980 to 2008 for rainfall, temperature, potential evaporation, relative humidity, wind speed, and sunshine duration. No data digitalization was conducted so far (Appendix 4-1)..

4.2 Precipitation

The season with some rain events starts from October and end at April while in summer months precipitation is almost not occurring. The average annual precipitations is 141 mm with more than 85% recorded in the colder part of the year and more than 70% of the total annual amount from November to March (Fig. 4-1). Appreciable non-uniformity of annual precipitations is another feature typical for arid zones, namely the deviations from long-term average are considerable (Consortium-Yugoslavia, 1977) The annual percipitations shown that there is at least one peacking event after each 4 years (Fig. 4-2).

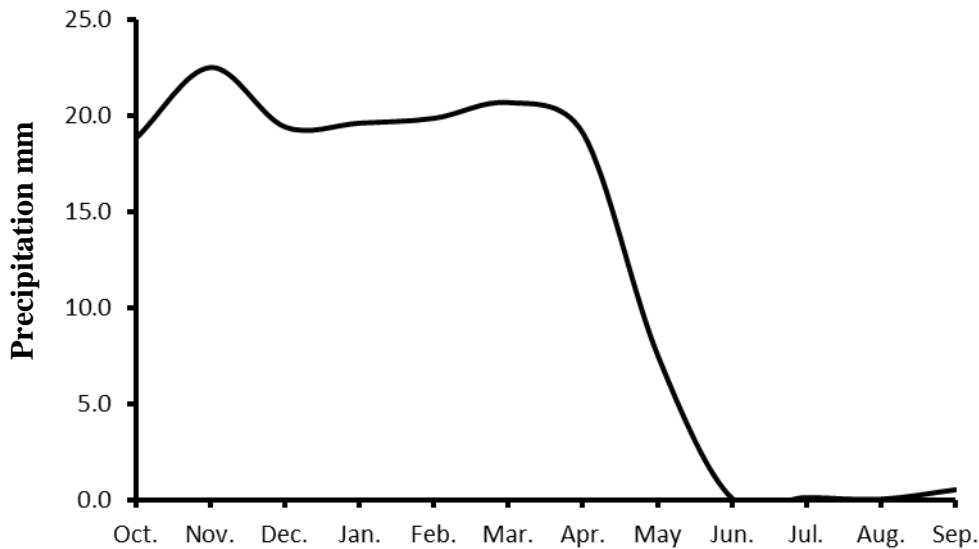


Fig. 4-1: Precipitation monthly means 1980 - 2008 Nukaib Station

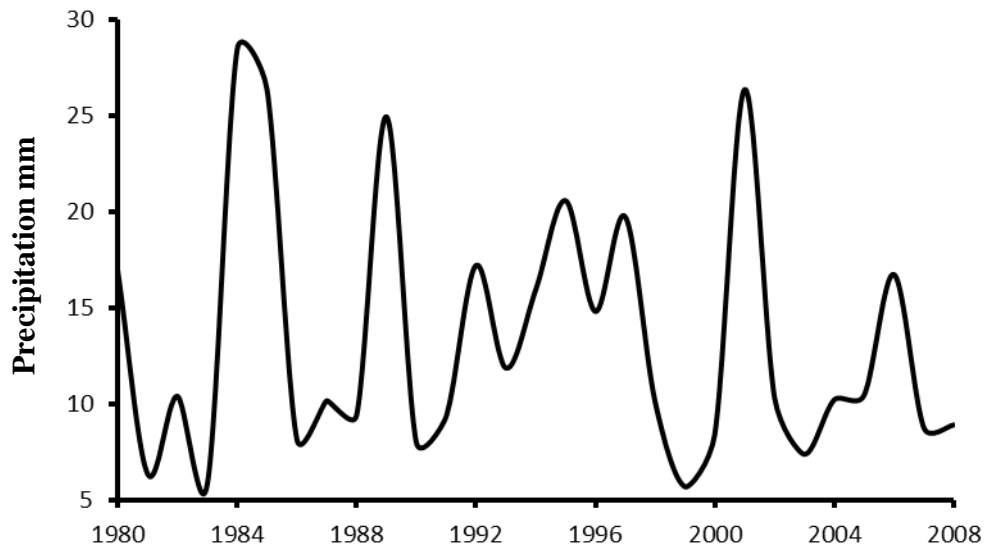


Fig. 4-2: Precipitation annual means 1980 - 2008 Nukaib Station

4.3 Temperature

The temperature follows the features of continental desert climate and they are characterized by appreciable fluctuations throughout a year. Likewise, the daily temperature fluctuations might be appreciable too (Consortium-Yugoslavia, 1977). Fig. 4-3 shows the monthly average of temperature for the ROI. Data were divided into two periods: November (13.8°C) - April (31.0°C), where the lowest value was recorded in January (7.1°C); second period is represented by May (24.7°C) - October (21.6°C), where the highest value was recorded in August (40.6°C). The annual mean of the years 1993 (22.97°C) shows the highest annual average and lowest average recorded in 1982 (18.97°C) (Fig. 4-4).

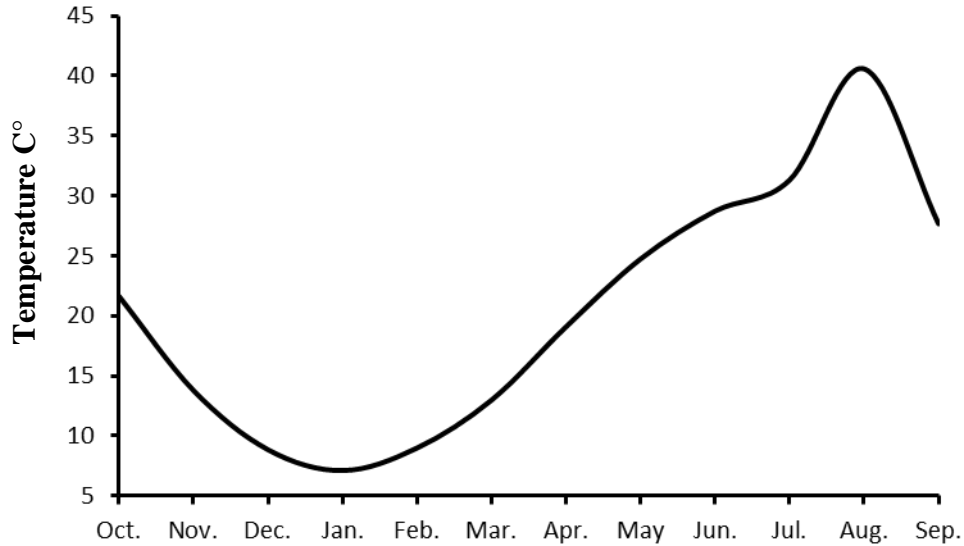


Fig. 4-3: Temperature monthly means 1980 - 2008 Nukaib Station



Fig. 4-4: Temperature annual means 1980 - 2008 Nukaib Station

4.4 Potential evaporation

Evaporation is a crucial element in the hydrological cycle. An increase in temperature would be expected to increase the rate of evaporation, but this change is also be affected by humidity, wind speed, net radiation, and water availability (Thompson and Perry, 1997).

Based on (MOST, 2009) evaporation measured by Pan class A, the evaporation has a direct relation with temperature rates and is based on the monthly averages (Fig. 4-5). Evaporation averages are divided into two periods: November (96.5 mm) - March (126.2 mm), where the lowest value was recorded in December (47.1 mm); second period represented by April (231.1 mm) - October (209.9 mm), where the highest value was recorded in July (408.2 mm). The annual mean of the years 2006 (228.2 mm) shows the highest annual average, while the lowest average was recorded in 1981 (189 mm) (Fig. 4-6)

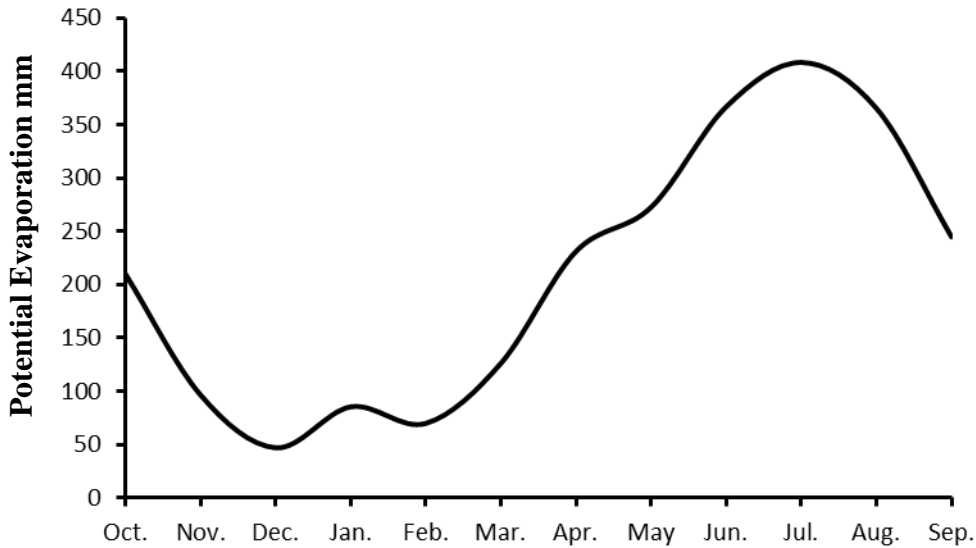


Fig. 4-5: Evaporation monthly means 1980 - 2008 Nukaib Station



Fig. 4-6: Evaporation annual means 1980 - 2008 Nukaib Station

4.5 Relative Humidity

The relative humidity (RH) is the ratio of the amount of water vapor actually in the air to the maximum amount of water vapor required for saturation at the particular temperature (and pressure). It is the ratio of the air's water vapor content to its capacity (Ahrens, 2007). Based on the monthly averages, the humidity is declined relatively within these months which the temperature increasing. The rates for the ROI are divided into two periods: November (55.4 %) - March (53.2 %), where the highest value is recorded in January (70.2 %), second period represented by April (43.9 %) - October (41.4 %), where the lowest value is recorded in July (27.1 %) (Fig. 4-7). The annual mean of the years 1997 (49.58 %) shows the highest annual average, while the lowest one was recorded in 1984 (36.17 %) (Fig. 4-8)

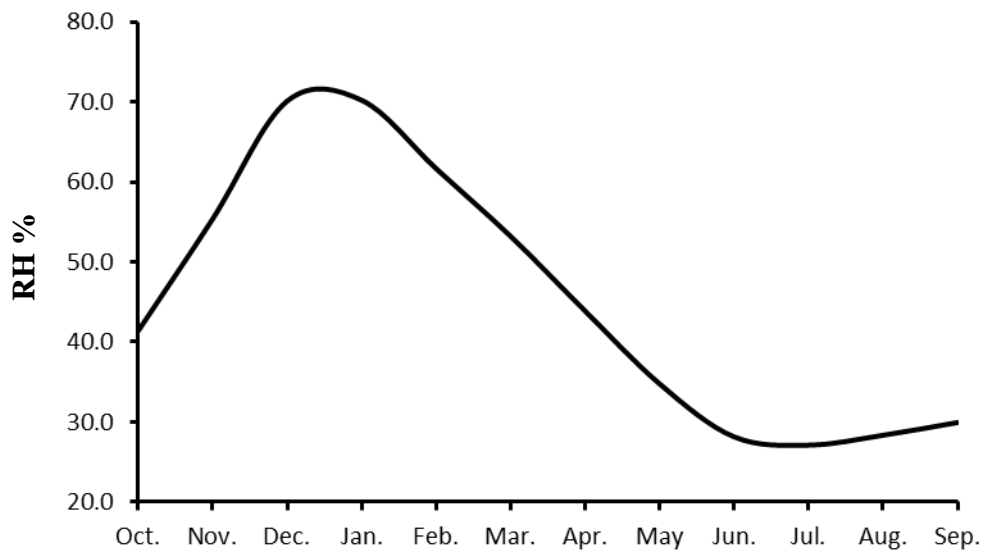


Fig. 4-7: RH monthly means 1980 - 2008 Nukaib Station

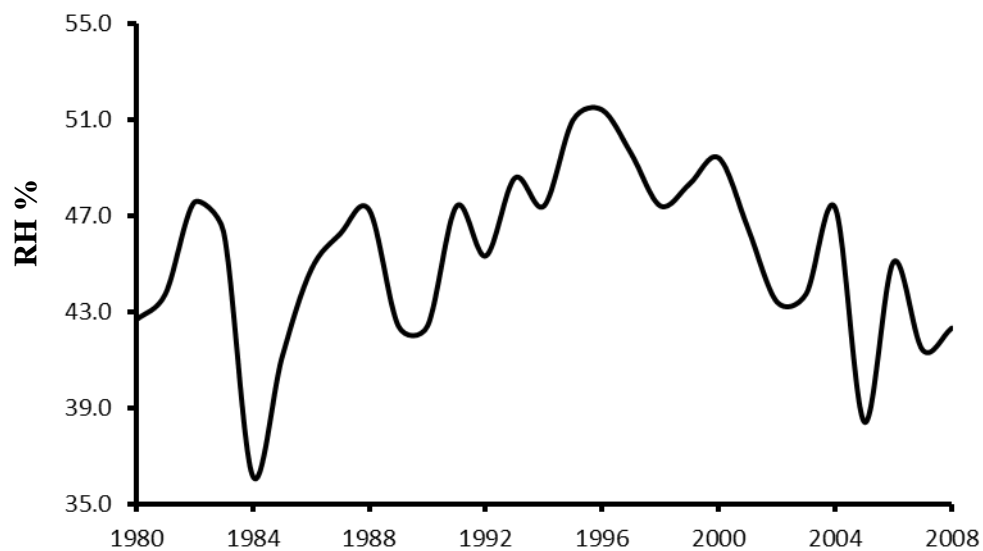


Fig. 4-8: RH annual means 1980 - 2008 Nukaib Station

4.6 Wind

It is one of the utmost and well-known important erosion factors. Wind direction is the direction from which the wind is blowing (Ahrens, 2007). The circulation of air masses is intensive for the region during the year; the winds are mostly blowing from north, north-west and west direction (Consortium-Yugoslavia, 1977).

Due to Nukaib station data, the average wind speed during the year is ~ 3.1 m/s, where the highest rate was recorded in July (3.8 m/s) and the lowest rate in November (2.2 m/sec) (Fig. 4-9).

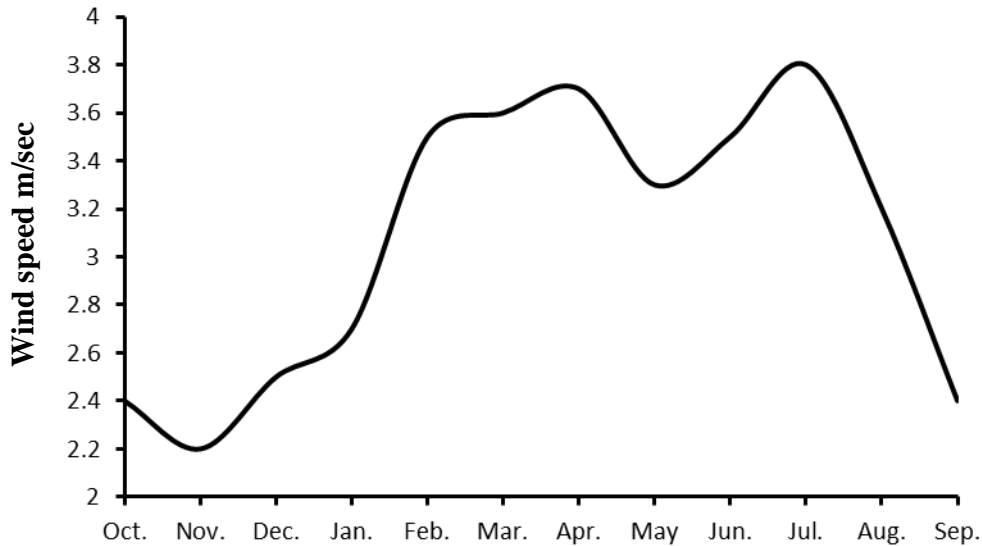


Fig. 4-9: Wind speed monthly means 1980 - 2008 Nukaib Station

4.7 Sunshine duration

Based on (Watch and Wmo, 2003) sunshine duration is the period during which direct solar irradiance exceeds a threshold value of 120 W/m^2 , solar radiation data is the best source of information for estimating the solar energy potential, which is necessary for the proper design of a solar energy conversion system (Bekele, 2009). The PSH (peak sun hour) is the equivalent number of hours per day when solar irradiance averages 1 kW/m^2 (MOST, 2006).

Fig. 4-10 shows the monthly values of solar radiation; the highest value recorded in June (13.1 h/day), while the lowest one was measured in December (6.2 h/day). Total annual average is $\sim 11.7 \text{ h/day}$.

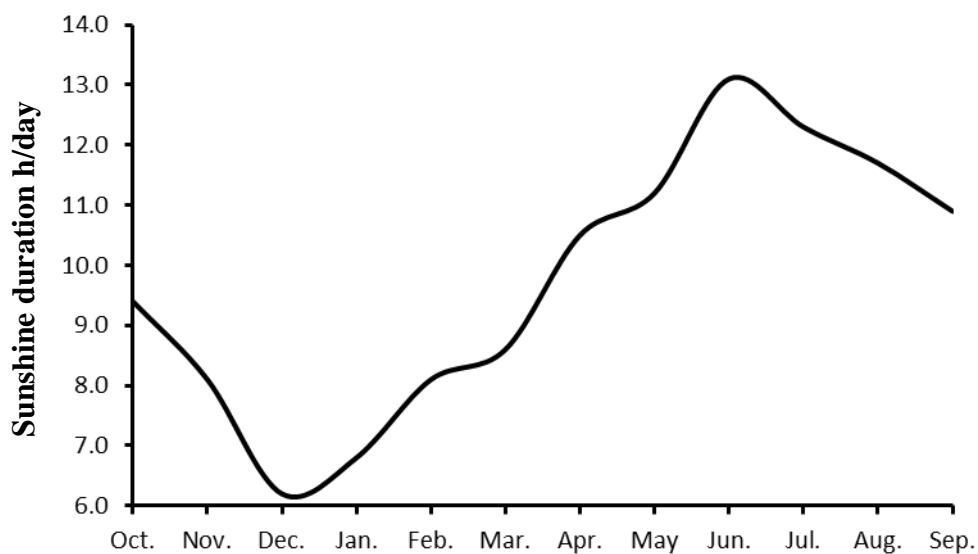


Fig. 4-10: Sunshine duration monthly means 1980 - 2008 Nukaib Station

5. Hydrogeology

5.1 Preface

The importance of any aquifer depends on few main characteristics like permeability, thickness, and extension. The region of interest comprises three main aquifers Tayarat (Upper Cretaceous), Um Er Radhumma (Upper.-Middle Paliocene), Dammam (Middle Eocene).

The Euphrates (Lower Miocene) aquifer has almost no impact upon the hydrogeological system since it is emerged only in a tiny part far east. Thus, further details with respect to the Euphrates aquifer will not be considered for this work.

The aquifers have a recharge zone located far west where the aquifers are exposed while discharge zone is located nearby Euphrates riverbank represented by numerous springs. Generally recharge occur either directly from outcrops, via cracks, and percolation through drainage patterns in Ubaiydh Wadi. Furthermore up and downward leakage by the neighboring aquifers has to be considered. Groundwater direction is following the gradient from recharge to discharge zone. Fundamental characteristics for the three main aquifers are based on (Jawad, 2001).

5.2 Tayarat Aquifer (Upper Cretaceous)

This formation is considered as the utmost scattered in the western desert, which is mostly confined and has a good water quality.

5.2.1 Pressure conditions

This formation is scattering vastly but no outcrops are shown so far, because it is located beneath the aquifers Um Er Radhumma, Dammam and Euphrates, thus the piezometric pressure is pushing the groundwater upwards into Um Er Radhumma aquifer. The average of saturated thickness is recorded with ~200 m with a total volume of around 13455.5 km³ (Jawad, 2001).

5.2.2 Hydraulic characteristics

Tayarat aquifer is a confined aquifer; it has an average Transmissivity of ~ 6851 m²/day and a storativity of ~ 1.2*10⁻⁴. The aquifer is recharged via leakage from other aquifers in particular Um Er Radhumma. However, exchange rate is still unknown.

The total average of groundwater storage is approximately 68.4*10⁹ m³, while the recharge rate within the limited outcrops depends on multi parameters like precipitation, runoff, evapotranspiration, and exposed surface area (about 15.5*10⁹ m³).

5.2.3 Water quality

Tayarat groundwater type is considered as Cl-SO₄ water based on Kurlov's classification (Kurlov, 1928). The average TDS (total dissolved solids) is 2271 ppm (Table 5-1). According to a TDS > 2000 ppm, this water has a poor quality with respect to drinking water, but may be used for artificial irrigation.

Table 5-1: Major anions and cations (epm) for Tayarat Aquifer (Jawad, 2001).

Aquifer name	Anions epm				Cations epm			TDS ppm	EC μ s/cm	SAR
	NO ₃	HCO ₃	SO ₄	Cl	Na	Mg	Ca			
Tayarat										
Average	1.35	2.41	15.96	19.019	15.41	8.495	13.06	2271	3062	4.97

*SAR: sodium adsorption ratio

5.3 Um Er Radumma Aquifer (Middle -Upper Plaiocene)

The importance of this formation is related to the following:

- Vast extending towards the western desert.
- Connections through hydraulically effective fractures up and downward with Dammam and Tayarat aquifers, so that a special groundwater system exists with multiple layers.
- Shallow depths and thus easily usable by drilling wells.
- Quality of groundwater is relatively good as potential drinking water resource and as well for agriculture purposes.

5.3.1 Pressure conditions

Generally, there are two types for this aquifer in the western desert: The confined type covering about 116559.3 km², which is available only far east close to Euphrates riverbank and the unconfined covering about 69117.6 km² within the eastern part from Rutba uplift. The outcrops nearby the uplifted area are playing a fundamental role for recharge. The maximum thickness is about 213 m.

The aquifer has almost the same piezometric pressure (~ 40 m) as the Dammam aquifer above it; this indicates that hydraulic connections exist between both aquifers.

5.3.2 Hydraulic characteristics

Since the aquifer is composed of intensively fractured limestone and dolomite, in addition to the dissolution impact, both storativity and transmissivity are varying from site to site. Transmissivity ranges from 0.88 m²/day up to 15529 m²/day and the average is about 3683.5 m²/day. Storativ-

ity for the unconfined type is reported to be between 4.3×10^{-2} and 1.2×10^{-4} for the confined state and 6.0×10^{-3} for semi-confined state. The total storage capacity is estimated to be about $386.8 \times 10^{-9} \text{ m}^3$. Only 5% out of the annual precipitation ($\sim 80 \text{ mm}$) might find a way to recharge the groundwater in particular through the outcrops, which cover an area of about $1.85 \times 10^{10} \text{ m}^2$. From this the recharge rate in this area is approximately $74 \times 10^6 \text{ m}^3/\text{year}$ (Jawad, 2001).

5.3.3 Water quality

The groundwater salinity for Um Er Radhumma aquifer is varying between 1750 ppm and 6300 ppm with an average of about 3956 ppm. This range is due to the long flow distance from recharge to discharge zone. Groundwater type is Na-SO₄-Cl based on Kurlov's classification (Kurlov, 1928), major constituents are shown in Table 5-2.

Table 5-2: Major anions and cations (epm) for Um Er Radhumma Aquifer (Jawad, 2001)

Aquifer name	Anion epm				Cations epm			TDS ppm	EC $\mu\text{s}/\text{cm}$	SAR epm
Um Er Radumma	NO ₃	HCO ₃	SO ₄	Cl	Na	Mg	Ca			
Average	0.9	2.5	34.7	27.8	27.0	16.4	20.1	3956	4816	6.2

5.4 Dammam aquifer (Middle Eocene)

Dammam aquifer is playing a significance role with respect to groundwater storage and hydraulics; it has been classified as the most important aquifers in the western desert due to the following reasons (Jawad, 2001):

- Vast extending covering most of Iraqi desert.
- Composed by fractured limestone and dolomite with a rather good permeability.
- A broad outcrop area that supports recharge by occasionally occurring floods.
- Direct connection with other aquifers forming a groundwater system with multiple layers (eg. Umm Er Radhumma aquifer located beneath Dammam aquifer).
- Shallow aquifer that might be easily reached by drilling wells.

5.4.1 Pressure conditions

Dammam is an unconfined aquifer, but in some places turned to be confined in particular far east closer to Euphrates River. Here the Dammam aquifer is covered by the Euphrates aquifer (quaternary deposits). Far west some outcrops are contributing to recharge the groundwater with very small amount. The maximum thickness for the aquifer is about 250 m in confined condition and about 90 m within unconfined state (Jawad, 2001).

5.4.2 Hydraulic characteristics

Dammam aquifer contains limestone-dolomite layers, which in some parts intensively affect the hydraulic conditions in particular transmissivity and storage coefficient. The average values for both parameters are 19110 m²/day and 3.3*10⁻¹ respectively. The total storage capacity is about 212.32*10⁹ m³. This amount compose two parts: accumulated water stored in sinkholes and fractures and recharge through the outcrops in particular in the western part from the ROI (Jawad, 2001).

5.4.3 Water quality

Dammam groundwater TDS is slightly more than 2000 ppm in the recharge zone at the border between Iraq and Saudi Arabia and is increasing towards 3000 ppm in the discharge zone close to Razaza Lake. This salinity increasing is due to the long flow distance between recharge and discharge zone and water-rock interaction during that time. The groundwater type is Ca-Cl – SO₄ based on Kurlov’s classification (Kurlov, 1928) (Table 5-3).

Table 5-3: major anions and cations in epm of Dammam Aquifer (Jawad, 2001)

Aquifer name	Anions epm				Cations epm					
	NO ₃	HCO ₃	SO ₄	Cl	Na	Mg	Ca	TDS ppm	EC μs/cm	SAR epm
Average	0.35	2.7	27.7	17.4	15.2	15.8	18.1	3018	3930	3.7

6. Result and discussion

6.1 Topographic contour map

Elevation contour maps were created by using 30 m DTM data based on SRTM. Both local and regional ROI show the highest values (609 m, 967 m) in the west while the lowest one (233 m, 22 m) are found in the east. The gradient was calculated for both regions with 0.002 (Fig. 6-1). The regional ROI is covering the entire Ubaiydh Wadi and the local ROI is of special interest because of two reasons: on the one hand it was classified by (Consortium-Yugoslavia, 1977) as a promising groundwater abstraction zone and on the other hand offering a sufficient number of wells for carrying out a thorough ground water study.

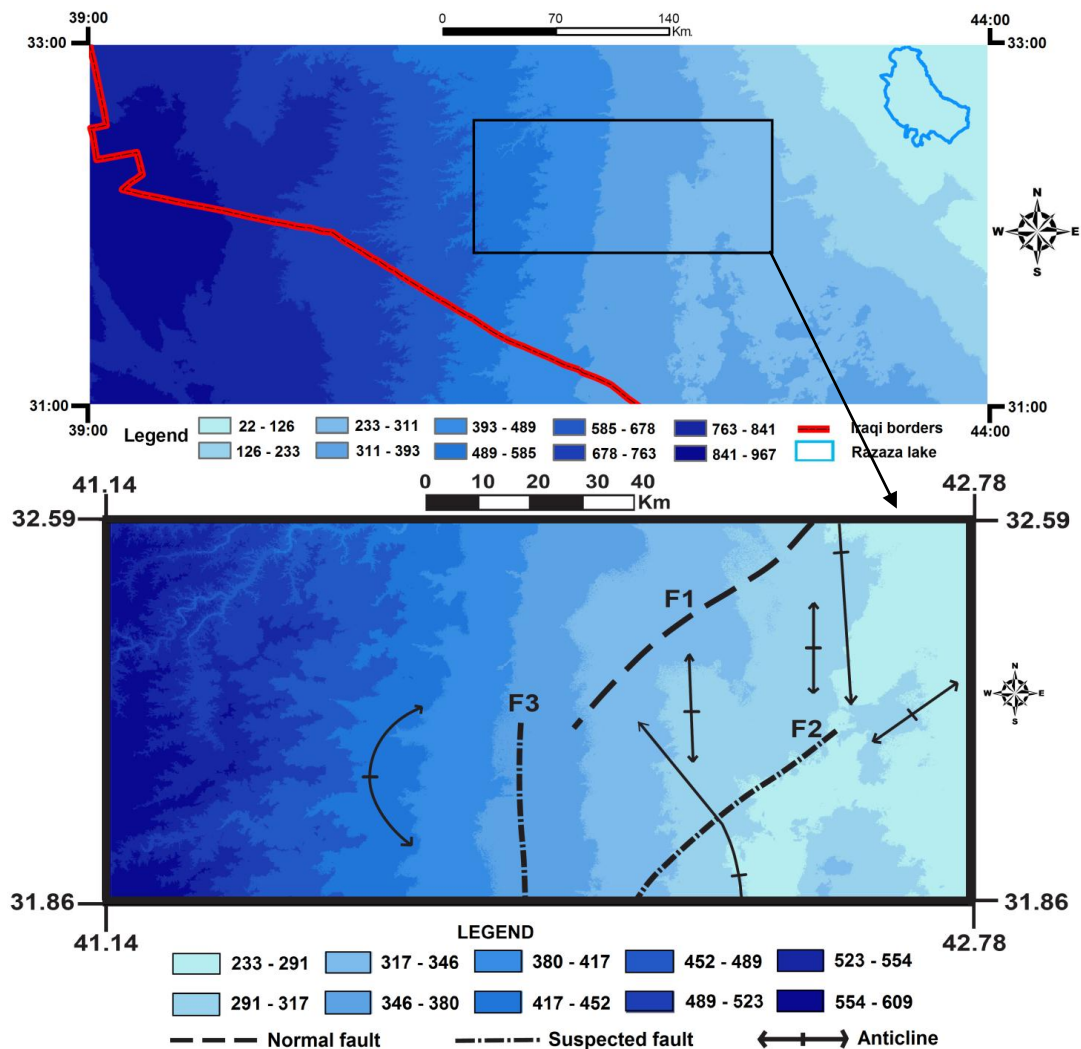


Fig. 6-1: Topographic contour map for regional and local ROI

6.2 Geological cross section

Fault 1 has been described as a normal fault while faults 2 and 3 are classified as suspected faults. The Geological cross sections (Fig. 6-2) were generated based on four boreholes (Consortium-Yugoslavia, 1977) (Fig. 6-3). The geological cross sections (Fig. 6.4) are showing the main formations, faults and thin layers from Marl (~ 20mE recedes to ~ 6m. W) Located in between the two formations Umm Er-Radhumma and Tayarat working as an aquiclude. Lenses from marl are imbedded between Dammam and Umm Er-Radhumma formations (Fig. 6-4). The general tectonic setting indicates that the maximum horizontal stress is orientated SW-NE. Groundwater flow is from W to E towards the Euphrates river with 102 pumping wells scattered in the area tapping the three main aquifers.

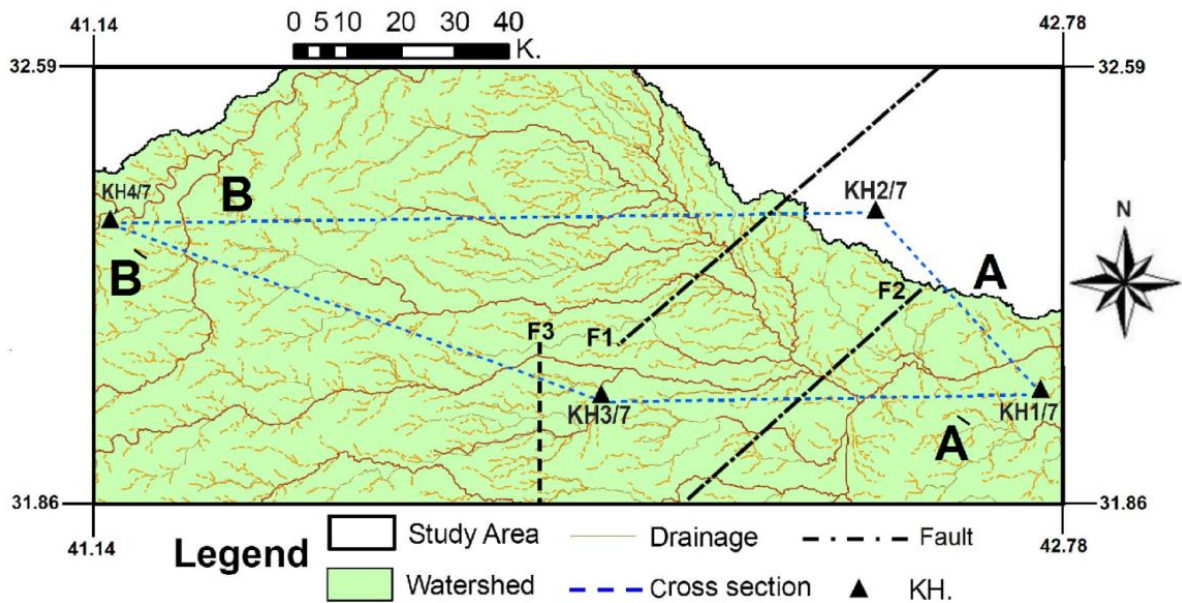


Fig. 6-2: Position of geological cross section in the local ROI

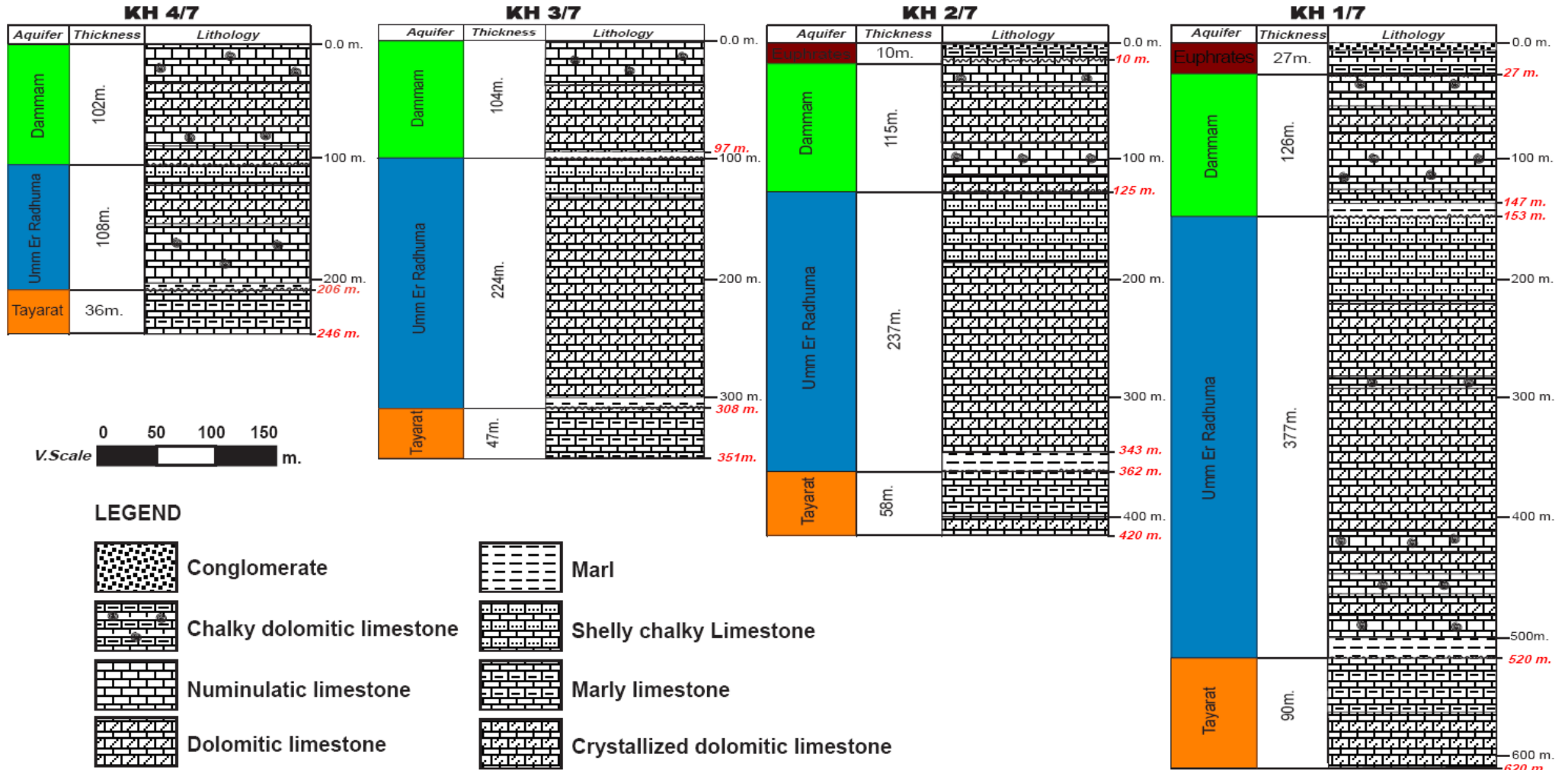


Fig. 6-3: Lithology of the 4 boreholes used to construct the cross sections (Consortium-Yugoslavia, 1977)

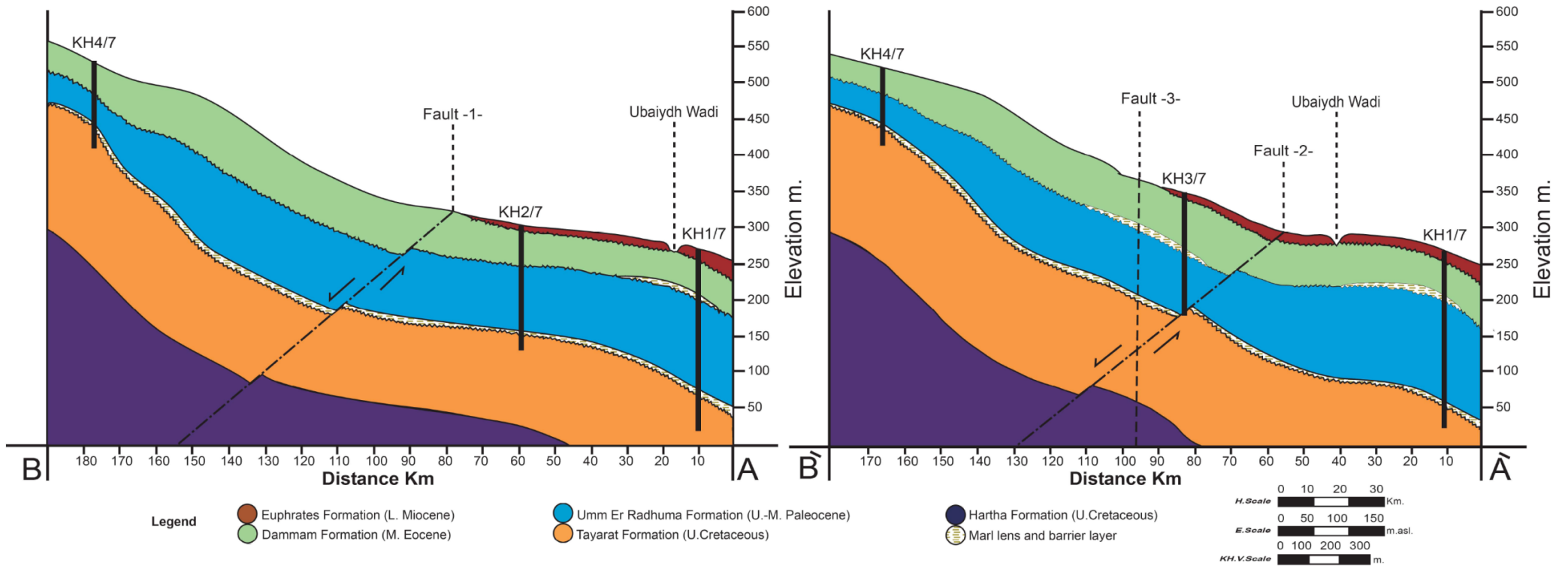


Fig. 6-4: Geological cross section's for local ROI

6.3 Lineament evaluation

A lineament is usually defined as a straight or curve linear feature to be seen on the ground surface. Lineaments can be manmade structures such as roads and canals or geological structures such as faults/fractures, folds, and unconformities, differences in vegetation and soil moisture, or drainage networks (rivers). Lineaments can be mapped during a field survey, or by using air photos and remote sensing data either manually or by means of pattern recognition algorithms (Kim *et al.*, 2004). Additionally, lineaments can be traced from digital terrain models by mathematical algorithms. Studying lineaments by means of remote sensed data is an alternative because areas in fractured aquifers with elevated groundwater yield are often associated with visible lineaments at the ground surface. An effective technique for delineation of fracture zones is based on lineament indices extracted from air-photos and from satellite imagery. In combination with structural and tectonic analysis information for understanding, groundwater flow and occurrence in hard-rock aquifers may be provided.

SRTM data with 30 m resolution and 15m Landsat ETM have been used to determine lineaments in the region of interest based on both extraction lineaments algorithm by (Geomatics, 2001) and directional filter algorithm by (Haralick *et al.*, 1987). Fig.6-5 shows that the lineaments F1 and F2 based on field survey (Buday, 1984) matching rather well with the automatically extracted lineaments with only a small difference between field data and remote sensed data. On contrary, no evidence was found by lineament interpretation for the suspected F3 element.

If lineaments are faults and deep reaching fracture, they may influence the groundwater flow either by being a zone of preferential flow or acting as barriers. Such zones can be recognized from groundwater contour lines for both unconfined and confined aquifers. Several spatial interpolation algorithms may be used for plotting groundwater contour lines.

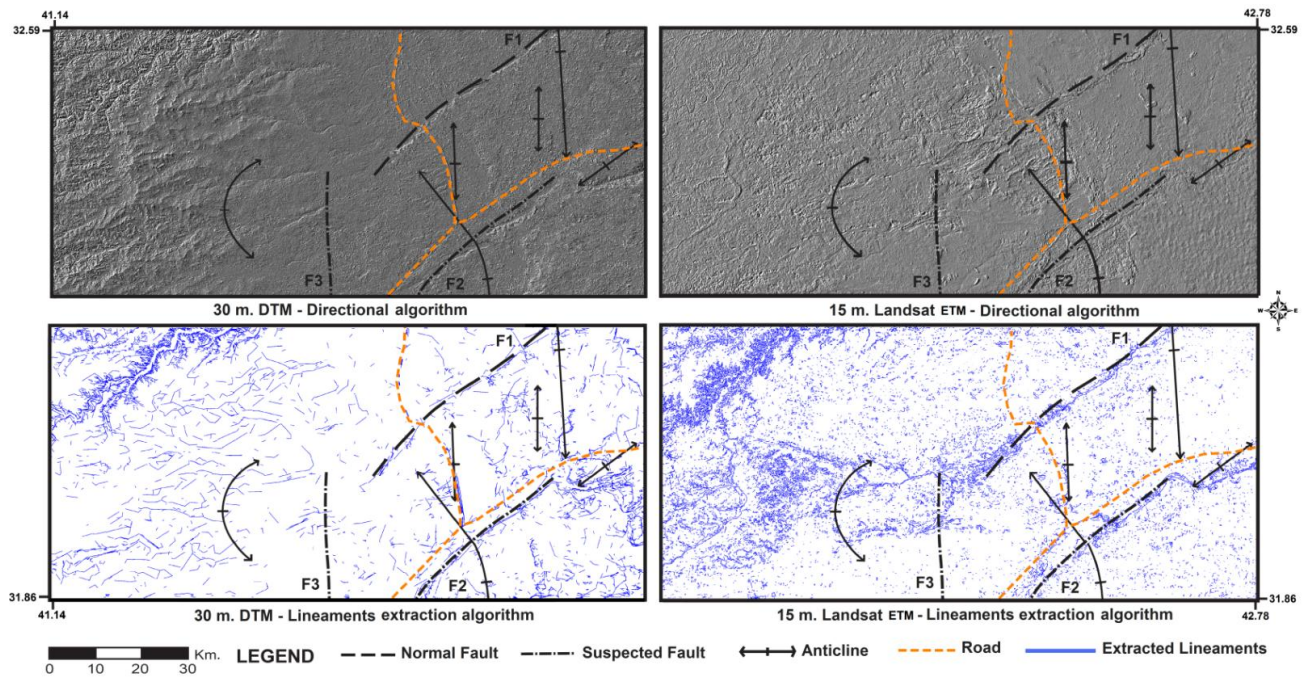


Fig.6-5: Lineament extraction into different dataset and different algorithms

6.4 Groundwater flow

The groundwater flow direction for the main aquifers has been determined by using 102 water wells (Appendix 6–1) within different spatial interpolation algorithms. However, it has to be considered that elevations of the well heads in masl is not known precisely, but only by estimation from the contour map (Figs. 6-6 , 6-7 and 6-8) showing the groundwater flow net for the three aquifers (Dammam, Umm Er Raduhmma and Tayarat). No significant difference was obtained using minimum curvature algorithm (Smith and Wessel, 1990). Kriging (Cressie, 1990) and radial basis function (Carlson and Foley, 1992). The main flow direction is W-E with the highest value in the NW (~487.5 masl. / well 5) while the lowest was in the NE (~189.8 masl. / well 31). This direction is matching well with the hydrogeological map of Iraq.

The groundwater gradient is less steep between the fault lines F1 and F2 than in the total area and the flow direction is diverted slightly from the general W-E direction to ESE. This can be explained by a better permeability in the area between F1 and F2. The main stress direction is ~ 40° and thus almost parallel to F1 and F2; perpendicular to this an anticline is assumed (Buday, 1984). Thus it can be speculated that the entire area between F1 and F2 is showing a denser fracturing than the rest of the region of interest. Evidence for any impact on groundwater hydraulics by the assumed F3 lineament was not found. Therefore, the existence of this lineament F3 has to be negated.

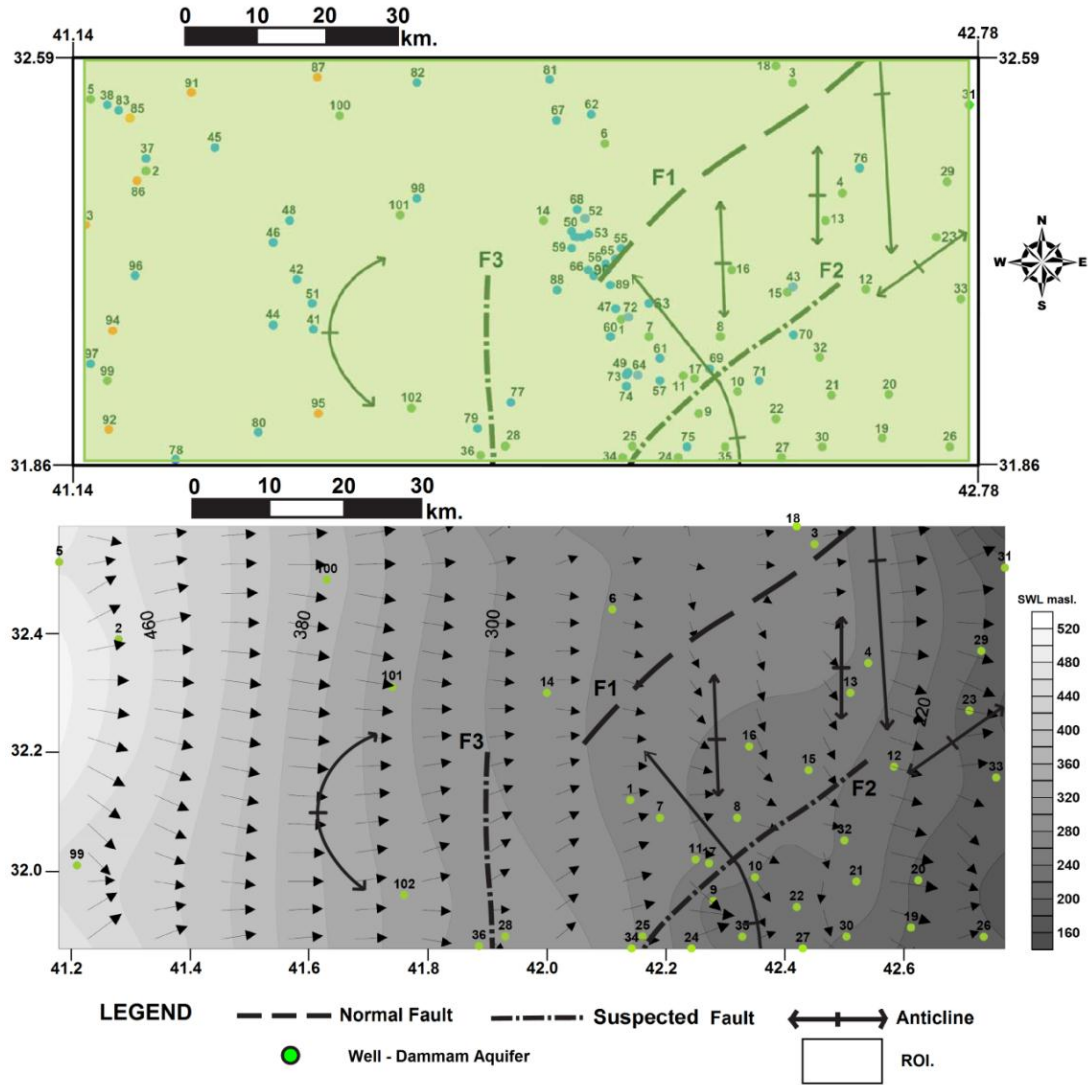


Fig. 6-6: Upper map: extension of Damman aquifer and structural elements. Lower map: groundwater contour lines and groundwater flow directions for Damman aquifer

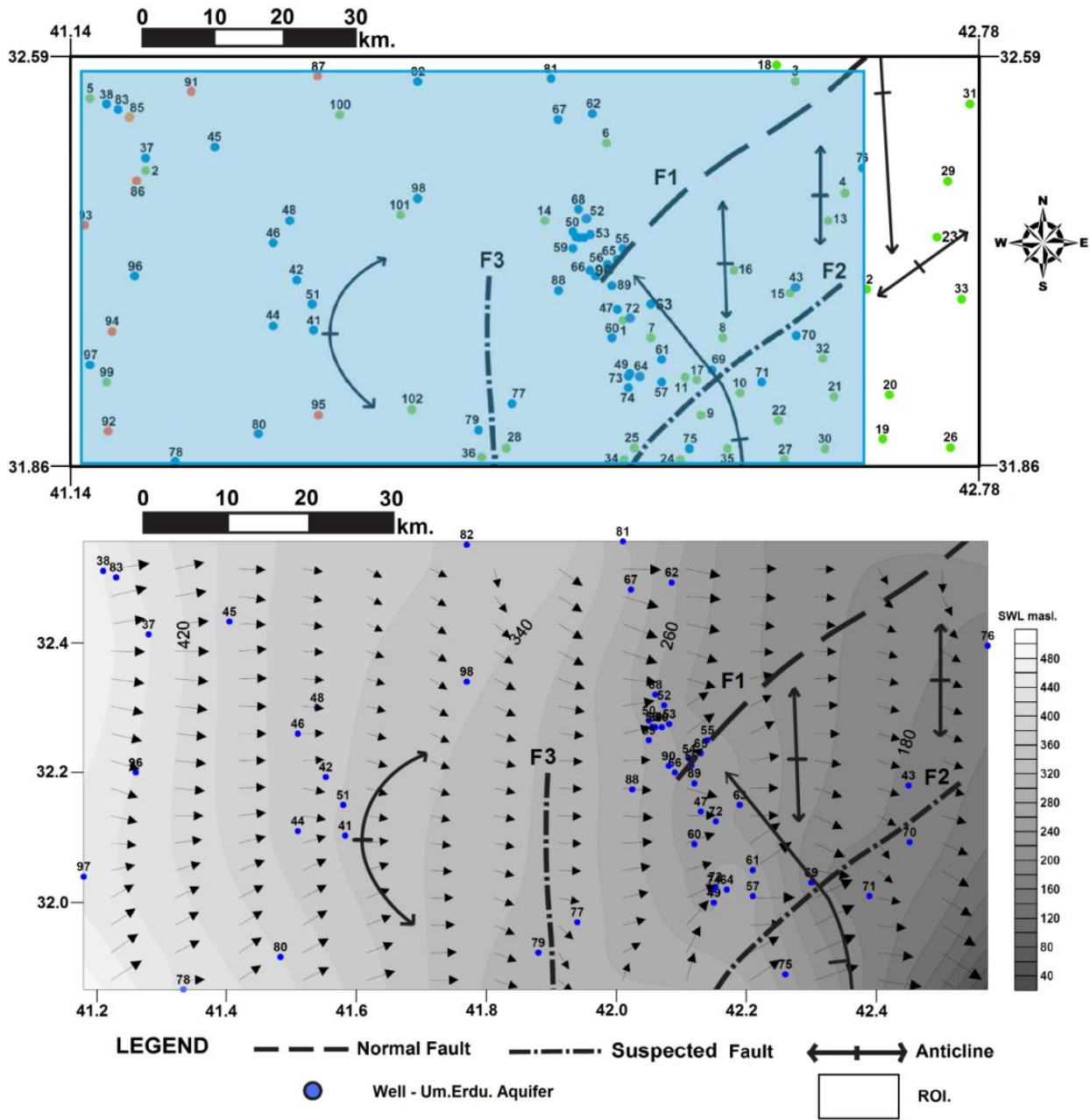


Fig. 6-7: Upper map: extension of Umm Er Radhumma aquifer and structural elements. Lower map: groundwater contour lines and groundwater flow directions for Umm Er Radhumma aquifer

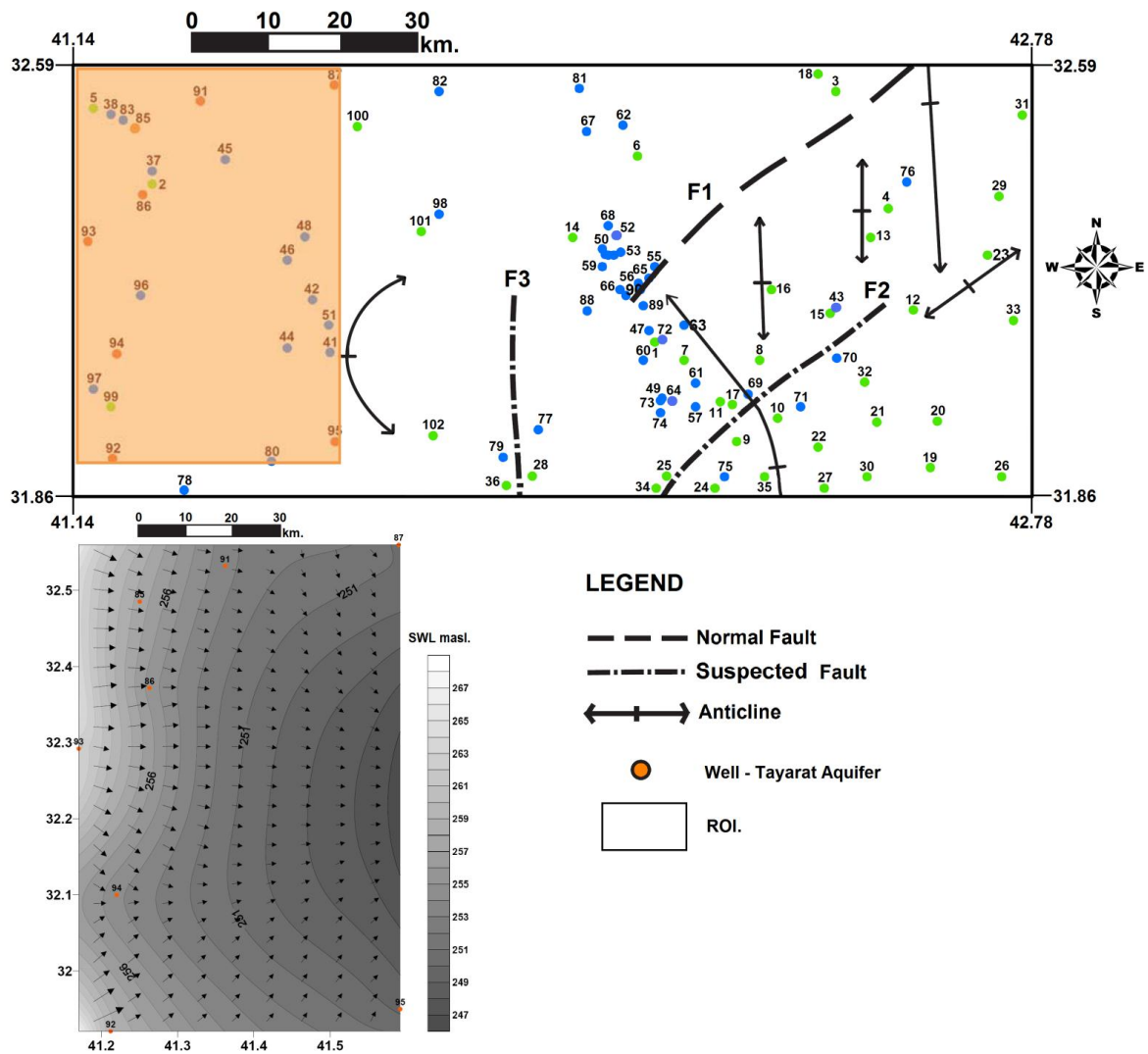


Fig. 6-8: upper map: extension of Tayarat aquifer and structural elements. Lower map: groundwater contour lines and groundwater flow directions for Tayarat aquifer

6.5 Pumping test evaluation

Two pumping test were performed close to the lineament F2 in the unconfined aquifer Damman using the wells 9 and 17. Well locations are shown in Fig.6-7. Table 6-1 shows a slight difference in depth to the groundwater between databank and field records. No adjustment of the pumping rate with respect to drawdown in the well was possible and observation wells were not available. Pumping rate was determined by means of a stopwatch filling a container with a volume of 10 liter. Drawdown was monitored with a depth sounder in the pumping well.

Pumping test in well no 9 was performed for 420 minutes to reach steady state. Then the pump was switched off to monitor recovery reaching the former static level after 72 min. Pumping test in well no 17 was performed for 360 minutes to reach steady state and then pump was switched off to monitor recovery, which was reached after 300 minutes. Results of pumping test and recovery evaluated with the analytical model MLU for Windows are presented in Figs. 6-9 and 6-10. Results shown that well 17 has a higher transitivity value ($0.1048 \text{ m}^2 / \text{min}$) in comparison with well 9 ($0.0832 \text{ m}^2 / \text{min}$). This results support the assumption of a unique elevated permeability zone occurred in between of F1 and F2.

Table 6-1: Pumping Test comparison wells

Well no.	Coordination	Elevation	Depth to GW./ Data Bank	Depth to GW. / Field	Difference	%
9	42.28 / 31.95	296.7	61.3	59.1	2.2	2
17	42.32 / 32.09	297.9	49.7	46.3	3.4	3.5
Average					2.8	2.75

Sum of squares: 1.4896E+00 m²
Conductivity = 0.00208 m/min.
Transmitivity = 0.0832 m² /min.

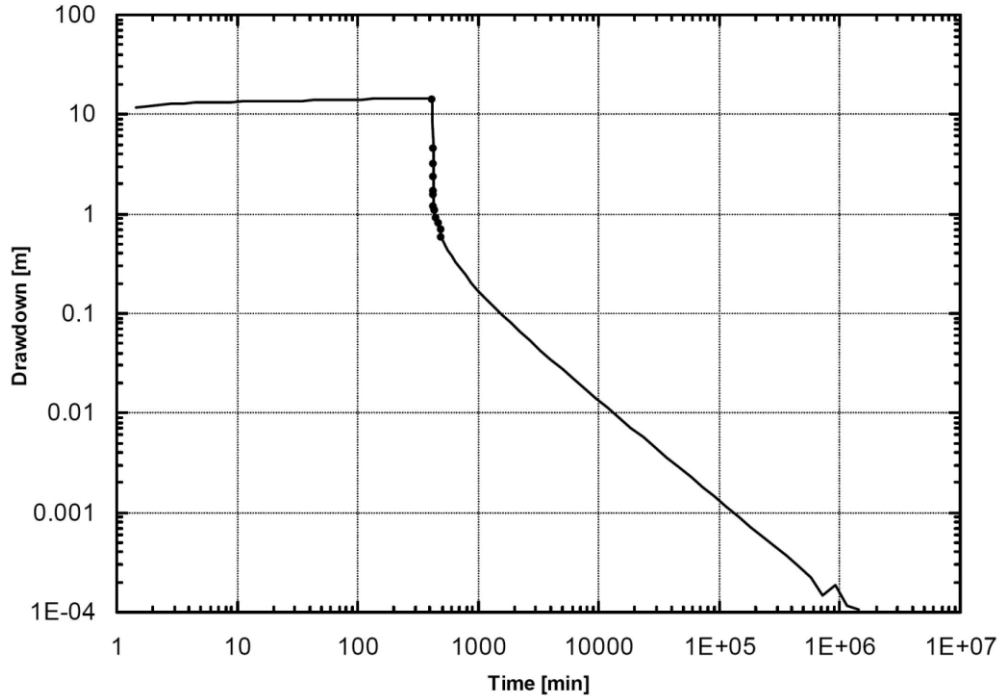


Fig.6-9: Pumping test plot for well 9

Sum of squares: 2.9944E+02 m²
Conductivity = 0.00262 m/min.
Transmitivity = 0.1048 m² /min.

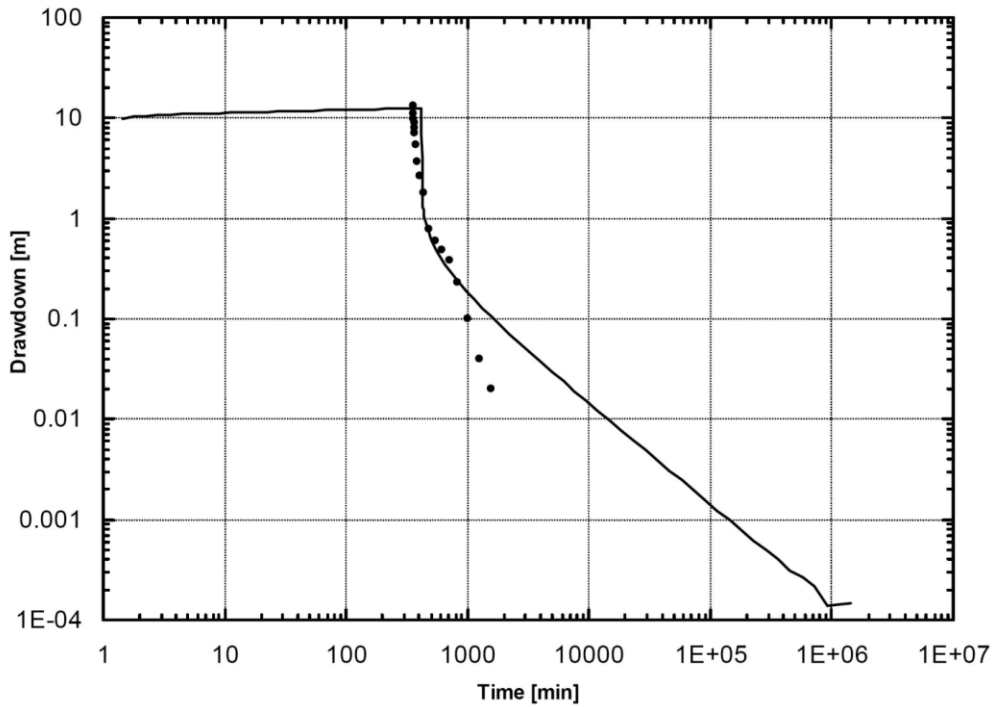


Fig.6-10: Pumping test plot for well 17

6.6 Catchment calculation

Catchment area and watershed delineation is a common task in hydrology. Accurate drainage boundaries are essential for accurate budgets and morphological characteristics are considered crucial key issues particular in flat terrains. The manual delineation of a catchment based on a topographic map with contour lines is a difficult task for flat terrains. However, in combination with a thorough field survey or evaluation of satellite images reliable catchment delineation will result. Using a digital terrain model and a computer algorithm has the advantage that the result is independent from human decisions and being less time-consuming. The accuracy of the result is depending on both quality and type of DTM and the computer algorithms used. The quality of the DTM is mainly controlled by the spatial solution and the precision of the altitude for each pixel (depending as well on vegetation cover). Thus, it is likely that a DTM with a course resolution will have difficulties to replicate hydrological patterns in particular in flats landscapes and be the reason for a false or biased watershed. The second critical factor comes with the algorithms used for delineating the watershed.

With River tools the user has to choose the outlet either by adding the coordination for the outlet or using a manual screw line window for the delineated catchment. The delineation process is rather slow and takes more than one and half day to delineate the 30m DTM; furthermore a high RAM capacity of ~4GB is recommended. A further disadvantage is that the software does not offer any restart possibility: if any kind of problem occur during the delineation analysis, the process has to be started from the very beginning.

TNTmips watershed process creates a series of temporary vector and raster objects that are saved on demand. The software offers several options to change default values with respect to flow path parameters and re-computing flow paths and basins. Additional it offers to calculate basins and flow paths from one or more seed points. Stream order can be computed according to Strahler, Horton; Shreve, and Scheidegger. TNTmips offers one more option to adjust the depression filling algorithms to prevent small depression (e.g. karst sinks) from being automatically filled. TNTmips is rather fast; it took only ~ 10:30 hours to delineate the entire 30 m DTM.

Arc Hydro Tools does not offer to analyze an entire DTM but requires a seed point for the catchment delineation. In comparison to the two other software packages Arc Hydro Tools was the fastest; it took ~8 hours for processing the 30 m DTM, which is faster than TNTmips, however, this is not directly comparable because only the upstream area from the manually set seed point was analyzed. Arc Hydro Tools is handy to use having plenty functions and automated

saving of each step separately. Table 6-2 shows the comparison of CPU times in hours and minutes for the 90 m and 30 m SRTM. Both 90 m and 30 m DTM within the three software packages using the same seed point (43° 44' 20.998" E, 32° 29' 08.085" N) and the 90 m DTM size calculated by TNTmips (46,670km²), and Arc Hydro (44,830km²) are more or less comparable. The result of River Tools (13,007 km²) has to be assumed as biased, because the comparison here is irrelevant due to the poor result with the 90 m SRTM data set.

Table 6-2: CPU comparison for watershed delineation into 3 software packages

Software	Seed point	SRTM option	Time efficiency /hour		Approach	Reference
			DTM 90m	DTM 30m		
Arc Hydro	Manual	Yes	3:30	9	Maidment 2002	ESRI
TNTmips	Manual	Yes	4	10:30	Jenson & Domingue 1988	MicrolImages
River Tools	Line Screw	No	5	38	D8,D ∞ and mass flux algorithm	RIVIX

PC. Options: Operation system: Windows XP. 2002 professional.

Hardware: Inte (R) core (TM) 2 Quad CPU, 2.4 GHz., 2GB.RAM.

With respect to the 30 m DTM Arc Hydro, TNTmips and River Tools produce rather similar shape while they show smaller catchments in comparison with 90m DTM (Fig. 6-11). However, most important is that all three 30 m based catchments show a significant difference to the 90 m based catchment in the north east (Fig. 6-12). TNTmips and Arc Hydro using the 90 m DTM included the sub wadi Tubal of the Ubaiydh wadi (Division, 1944), however, both software did not included this part of the catchment using the 30 m data. A closer evaluation of the 30 m DTM shows a local anomaly at the confluence of the two wadis. This may be a sand dune or temporarily sandbank or as well an artifact of the 30 m SRTM data set. Thus it has to be stated that the 30 m DTM needs a manually correction (e.g. river burning or manually correction) to obtain a correct catchment. Noteworthy that this error does not occur with the 90 m data set due to the fact it has a less resolution where such a sand dune could not be recognized.

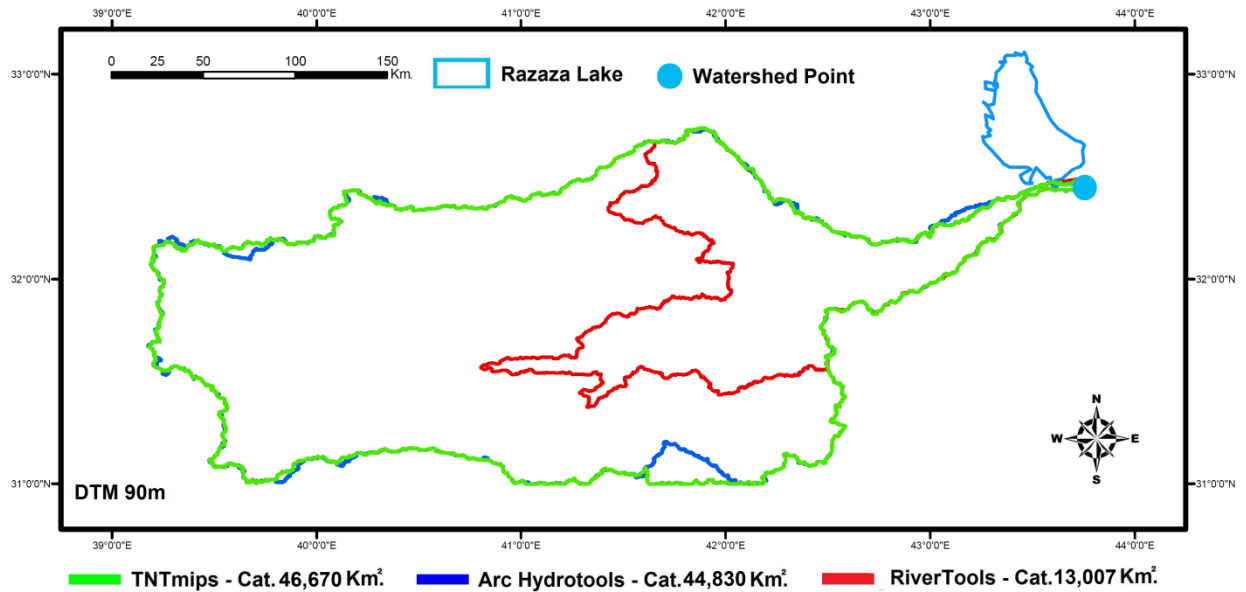


Fig. 6-11: Catchment delineation by three software packages for Ubaiydh Wadi – 90 m DTM

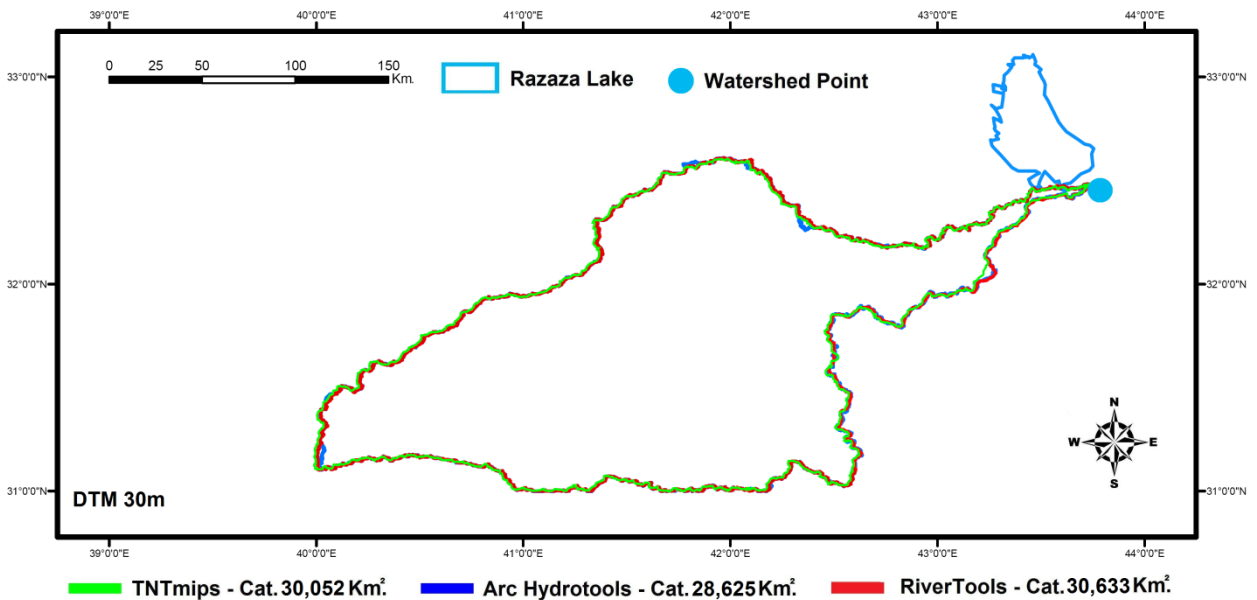


Fig. 6-12 Catchment delineation by three software packages for Ubaiydh Wadi – 30 m DTM

An additional approach is shown through TNTmips when no seeding point concept is used, the result shows that the largest catchment - due to the fact that TNTmips calculates the catchment for the entire Razaza Lake and not an arbitrary seed point where wadi Ubaiydh flows into Razaza Lake. Therefore, Razaza Lake here is considered as the outlet of the catchment (Fig. 6-13).

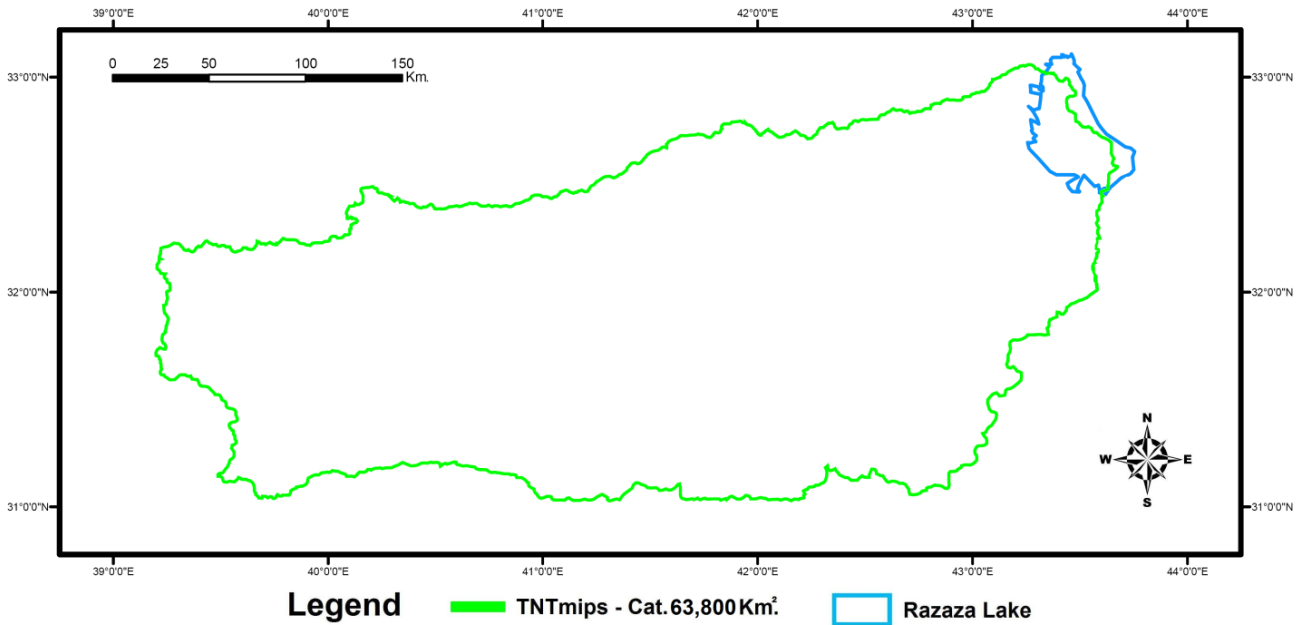


Fig. 6-13: Catchment delineation for Ubaiydh Wadi - TNT mips using no seeding point

ASTER data set with 30m resolution has been implemented to double check and Arc Hydrotools was chosen for this task, because it shows the most time efficiency although there were no significant different in results between the other software packages. The result is rather similar for both 30m DTM. An additional seeding point was added at the sand dune coordinate (41° 55' 24.832" E, 32° 37' 09.282" N) to create the sub catchments to include this part to the entire catchment (Fig. 6-14). Because the problem with the sub-catchment occurred with both 30 m DTM's a temporarily sand dune has to be assumed as the reason.

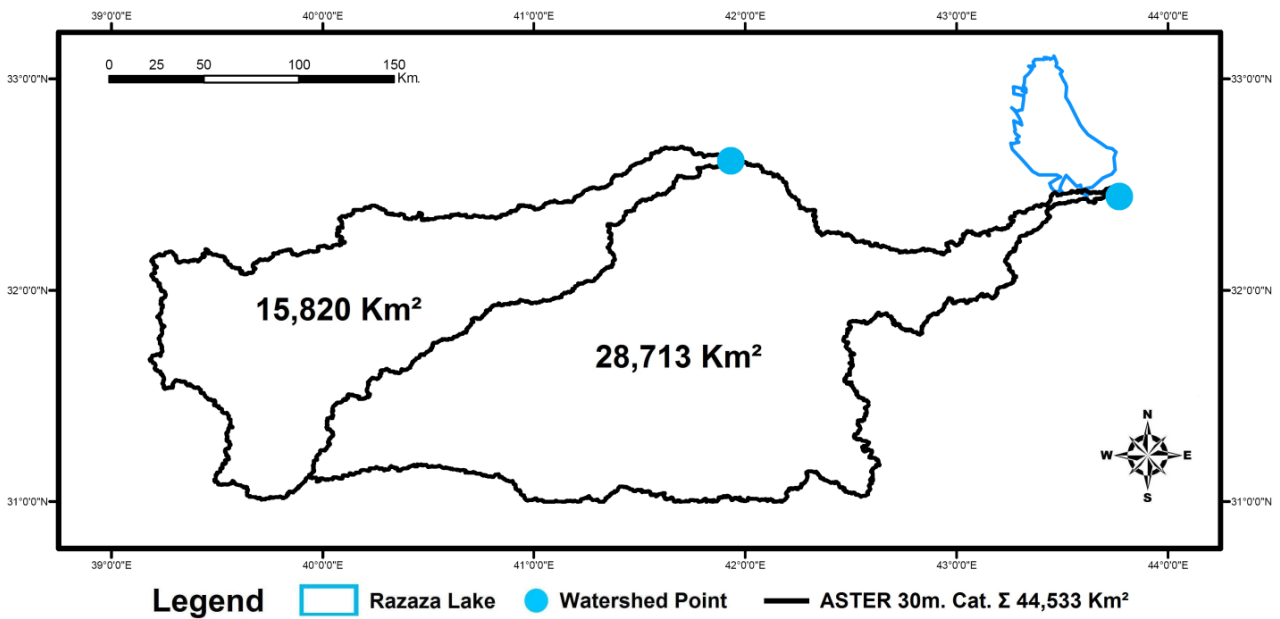


Fig. 6-14: Catchment delineation for Ubaiydh Wadi – Arc Hydro 30m ASTER

As a result, the catchment calculations are dramatically different for both RASTER 30 m and 90 m, Table 6-3 shows the RASTER and ASTER data set results using 3 software products.

Table 6-3: RASTER and ASTER dataset delineation results for three software packages

Software	30m catchment area Km ²	90m catchment area Km ²
River Tools 3.0 SRTM	30,633	13,007 (excluded - irrelevant)
TNTmips 2007 SRTM	30,052	46,670
Arc Hydro Tools 9.2 SRTM	28,625	44,830
Arc Hydro Tools 9.2 ASTER	28,713	44,533 (30m with two catchment)
Average	29,506	45,344

6.7 Water balance and Recharge

Water balance can be used to describe the flow of water in and out of a budget zone. A *budget zone* can be one of several hydrological domains, such as a column of soil or a drainage basin. The water balance assumed that the input and output are equal, where any change for one of these elements will lead to change in the storage

$$\text{Input (P)} - \text{output (ET+RO)} = \text{change in storage } (\Delta S) \dots\dots\dots (6-1)$$

Where precipitation considered the only input, conversely few outputs are available such as runoff and evapotranspiration, which is the maximum water loss. In arid regions, the precipitation to evapotranspiration ratio may be less than 0.1. For such regions, precipitation is not sufficient to meet the water demand for natural plant growing. Since we have almost no vegetation cover in the area of investigation (less than 0.1- NDVI) thus evaporation and runoff will be the only output quantity (Domenico and Schwartz, 1998).

There are three important periods with respect to the potential ET and P : when

- P = Potential ET: Water surplus is theoretically zero, because rainfall is available to satisfy the evaporation needs.
- P < Potential ET: Rainfall is available to satisfy potential evapotranspiration at least partially.
- P > Potential ET : Water surplus is existing and immediately goes into rebuilding the soil moisture component where later the recharge might happen (Domenico and Schwartz, 1998).

Water balance calculations are covering the timeframe 1980-2008; calculation details are shown in Appendix 6-2. Results for groundwater recharge show an average of ~ 17.5 mm/year. 60% from this recharge occur in December and January, while 32% occur in November, February and March. During October and April more or less no recharge occurs (Table 6-4). Furthermore, recharge fluctuation during 29 years (Fig. 6-15) gives an indication that within 10 years one can expect one or two times a higher groundwater recharge event within 30 – 50 mm/year.

Table 6-4: Groundwater recharge values for timeframe 1980-2008

Year	P mm	Month WS	GWr mm
1980	186.6	Apr	48.94
1981	63.7	-	0
1982	114.5	-	0
1983	69.8	-	0
1984	256.1	Jan, Mar	37.79
1985	263.8	Mar	8.28
1986	89.9	-	0
1987	91.5	-	0
1988	103.5	-	0
1989	249.6	Mar	27.78
1990	96.1	Feb	12.81
1991	84.1	-	0
1992	206.6	Jan,Nov,Dec	16.60
1993	130.6	Jan,Feb	3.63
1994	175.4	Nov	59.99
1995	185.3	Feb,Dec	36.46
1996	133.4	-	0
1997	236.9	Oct, Nov	5.31
1998	80.9	-	0
1999	62.6	Dec	7.07
2000	84.4	Dec	1.02
2001	263.8	Jan, Dec	55.14
2002	103.3	Jan, Feb	33.14
2003	88.6	Dec	14.97
2004	122.7	Jan, Dec	18.26
2005	125.6	Jan, Dec	32.72
2006	200.9	Jan, Feb, Nov, Dec	44.11
2007	105.2	Jan, Dec	23.23
2008	107	Jan, Dec	20.35
Average	140.8	60% Jan - Dec	17.5

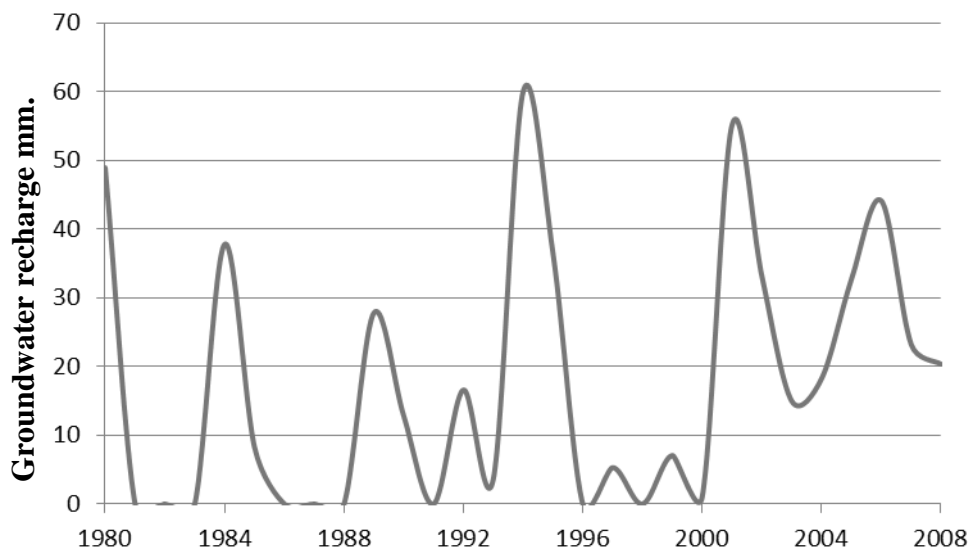


Fig. 6-15: Groundwater recharges fluctuation from 1980-2008

6.8 Groundwater Model

The groundwater model implemented in Visual Modflow was built by 5 main layers representing Dammam aquifer, first aquiclude, UmEr Duhmma aquifer, second aquiclude and the Tayarat aquifer. Averaged readings of groundwater head from 102 observation wells have been used to calibrate the model (Fig. 6-16). Dry cells occurred in the south-west part of the area on interest at least for the first aquifer. Dry cells occur in MODFLOW models when the calculated water table is below the bottom elevation of the perspective grid cell (Wen-Hsing and Kinzelbach, 2005). Because MODFLOW only simulates saturated groundwater flow in the standard mode, it does not represent a head value in the unsaturated cell, so the cell becomes dry. By means of different add-on packages to Modflow solving either the Richards equation in one dimension or using the kinematic-wave approximation (Niswonger et al., 2006) the problem of dry cells could have been circumvented. However, no data to calibrate the flow in the unsaturated zone were available.

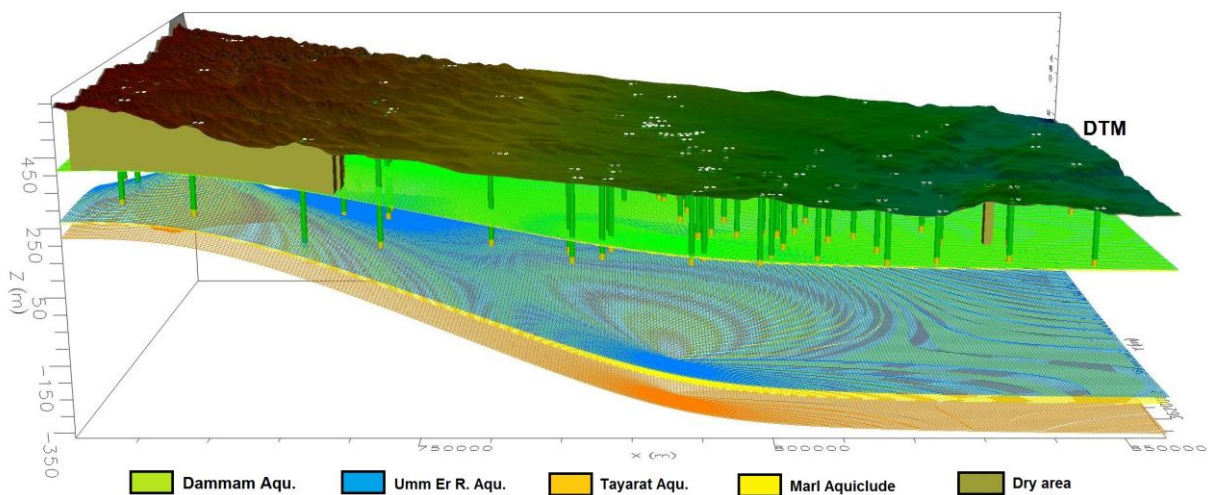


Fig. 6-16: The Model showing main layers, observation wells and dry area

A general problem is that all data about depth to the groundwater are not based on readings at the same time (date of readings are differing by 6 years). Furthermore the elevation of the wellheads are only estimates, either by GPS elevation readings or taken from a map. Finally, all wells are not observation wells rather pumping wells with unknown and not documented pumping rates. Water tables are showing the maximum values of 476 masl far west and minimum value of 124 masl far east. These values were defined by constant head boundaries, which were implemented at the western and eastern boundary of the model. No inactive cells or zone included (Fig.6-17).

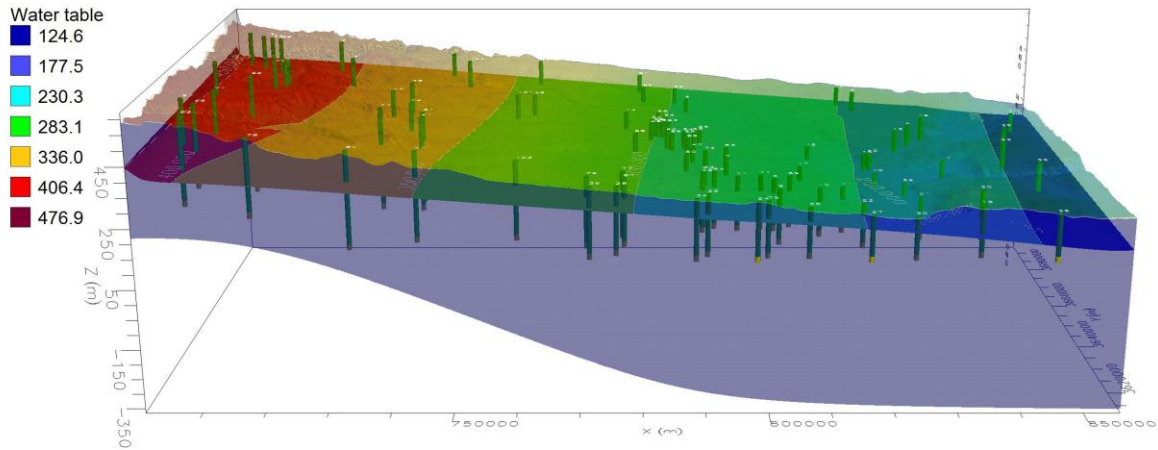


Fig.6-17: The Model showing Water table

The groundwater contour map for the upper Damman aquifer shows that groundwater flow gets a slightly other direction when reaching the fault zone. The same effect occurs with the two deeper aquifers UmEr Duhmma and Tayarat. This indicates the faults impact into groundwater flow (Fig.6-18).

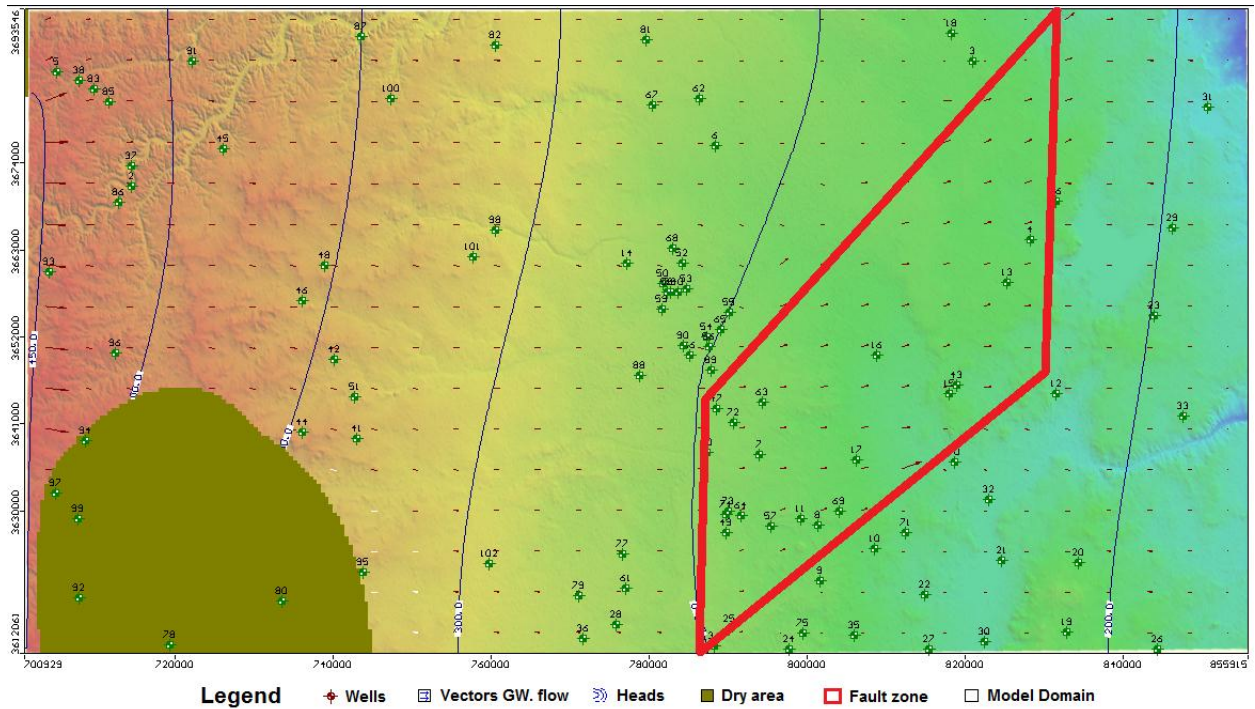


Fig. 6-18 Groundwater flow within Fault zone

6.8.1 Model sensitivity

Based on the calibration results (Table 6-5) the model seems to have a rather low sensitivity because the minimum and maximum values of the standard error of estimate were between 2.27m and 3.56 m. The model with recharge less 11.85 mm/year or more 60 mm/year did not converge and thus failed to produce a result.

Table 6-5: Results for implemented model by Visual Modflow V.4.2

Model #	Recharge mm/year		K m/sec.		Discrepancy %	Zone Budget m ³ /day			In Constant head	In Recharge	Max. Residual	Calibration m.	
	Entire region	Drinage only	Faults	Zone		In flow	Out flow	In – Out flow				Min. Residual	Standard error
1	11.85	11.85	0.002	-	0.003	4843216	4843050	166.65	4435800	407450	70.17	0.06	2.27
2	15.4	15.4	0.002	-	0.01	4861733	4861475	258.06	4332200	529510	76.31	- 0.03	2.28
3	17.5	17.5	0.002	-	-0.002	4872311	4872410	-98.72	4270600	601710	79.90	-0.02	2.30
4	20	20	0.002	-	-3.3	4885385	4885401	-15.83	4197700	687670	83.61	-0.20	2.32
5	25	25	0.002	-	-0.002	4945042	4945125	-82.62	4085500	859580	92.85	-0.87	2.42
6	30	30	0.002	-	-0.004	5042957	5043162	-204.68	4011500	1031500	101.71	0.09	2.53
7	35	35	0.002	-	0.01	5141737	5141122	615.09	3938300	1203400	110.33	0.15	2.67
8	40	40	0.002	-	0.002	5239734	5239632	102.37	3864400	1375300	118.88	1.92	2.82
9	45	45	0.002	-	- 0.001	5337160	5337233	-73.00	3789900	1547300	127.30	3.12	2.99
10	50	50	0.002	-	-0.003	5434245	5434390	-144.74	3715000	1719200	135.57	-1.25	3.18
11	55	55	0.002	-	-0.003	5534010	5534124	-144.74	3643000	1891000	143.67	-1.14	3.36
12	59.99	59.99	0.002	-	- 0.01	5636054	5636363	-309.01	3573300	2062700	151.66	2.11	3.56
13	11.85	11.85	-	0.0006	- 0.01	4843560	4843883	-322.39	4436100	407450	61.90	0.29	2.42
14	15.6	15.6	-	0.0006	- 0.01	4863359	4863808	-448.69	4327000	536380	67.75	0.10	2.36
15	21	21	-	0.0006	- 0.002	4927648	4927759	-110.75	4205600	722050	95.98	-0.15	2.31
16	25	25	-	0.0006	- 0.01	4994062	4994326	-263.90	4058600	1048700	82.01	0.07	2.30
17	30.5	30.5	-	0.0006	- 0.005	5107249	5107481	-231.70	4205600	722050	90.14	-0.42	2.30
18	35	35	-	0.0006	0.01	5200048	5199730	317.68	3996600	1203400	96.65	0.79	2.32
19	40	40	-	0.0006	- 0.01	5302387	5302656	-269.79	3996600	1203400	103.84	0.16	2.36
20	45.5	45.5	-	0.0006	0.01	5413992	5413531	460.94	3849500	1564500	111.46	1.10	2.43
21	50.5	50.5	-	0.0006	- 0.01	5516041	5516352	-310.85	3779600	1736400	118.51	2.45	2.52
22	59	59	-	0.0006	- 0.001	5713165	5713273	-108.33	3684600	2028600	130.10	-1.77	2.68
23	60	60	-	0.0006	0.005	5735738	5735467	270.66	3672800	2063000	131.42	-1.21	2.71

The roughly estimation for recharge is ~ 17.5 mm/year, thus model 3 was considered as the most reliable model. During the sensitivity analyses by using different K values for the aquifers and aquicludes (Table 6-6) the model was running stable with K values from 1e-3 to 1e-4 m/s for aquifers and from 1e-7 to 1e-8 m/s for aquicludes. The standard error shows only small difference between model 3 and 3-1 (2.3 to 2.331 m), while maximum residual difference were between 79.9 and 57.8 m.

Table 6-6: Results for implemented models for K values by Visual Modflow V.4.2

Model no.	Aquifers	Aquiclude	Model respond	Maximum Residual m.	Slandered error m.
3	1E-4	1E-8	run	79.904	2.3
3-1	1E-3	1E-7	run	57.827	2.331
3-2	1E-2	1E-6	Failed to run	-	-
3-3	1E-0	1E-4	run	85.001	3.243
3-4	1E-5	1E-9	Failed to run	-	-
3-5	1E-6	1E-10	Failed to run	-	-

Because some of the absolute residuals were rather large, it can be speculated that either readings of depth to the groundwater or determination of elevation of the wells are erroneous. By excluding wells with very high both residual and standard error were getting much better. 11 observation wells out of 102 (well numbers 43,52,70,71,76,85,87,91,92,94,96) were excluded. By this the maximum residual was reduced from 79.9 m to 43.5 m and the standard error from 2.3 m to 1.8 m. Fig.6-19 shows the plots for model 3 before and after excluding the 11 wells.

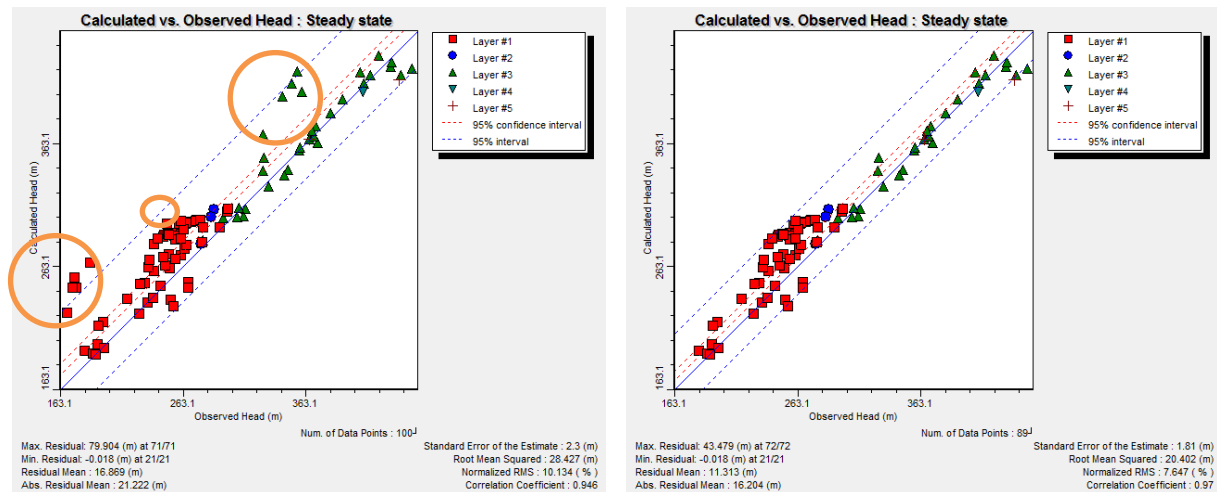


Fig. 6-19 Plots model 3 residuals before and after excluded wells

Generally water budget results shown the discrepancy for the final calibrated model was - 0.002 % with an inflow of 4872311 m³/day and outflow of 4872410 m³/day. Constant head and recharge rate were 4270600 m³/day and 601710 m³/day.

6.8.2 Groundwater Management

The average of groundwater recharge is estimated to be 17.5 mm/year (0.0175 m/year) and the total area of ROI is 12400 Km² (1.24*10¹⁰ m²). The water budget for recharge is then:

$$0.0175 * 12.4 * 10^9 \text{ m}^2 = 2.17 * 10^8 \text{ m}^3/\text{year}.$$

For irrigation purposes ~ 5000 l/ m²/year are needed for open area farming (Cummings, 2002) but only ~ 1000 l/ m²/year for greenhouses farming, because evaporation will be reduced to ~ 80% (Fernandes et al., 2003). Assuming greenhouse farming the amount of regional recharge is sufficient to utilize only 1.75% from the total area. This amount of water abstraction is very little, but it might be increases by taken in to consideration the groundwater inflow into the ROI from Saudi Arabia. However, this amount of water will be available in the long term only if an agreement or convention officially is signed between Iraq and Saudi Arabia, to avoid any sort of aquifer depleting in case groundwater abstraction conducted with absence of water resource management in both sides. (Table 6-7) showing the groundwater inflow calculation made by the model in terms of in constant head values where 50-60 % assumed to be utilized from the total amount:

Table 6-7: Groundwater inflow calculation

Recharge m³/year	Total GWi m³/year	GWi %	GWi m³/year	Total Area m²	GWi. area covered %
2.17*10 ⁸	1.54*10 ⁹	50	769*10 ⁶	1.24*10 ¹⁰	6.2
2.17*10 ⁸	1.54*10 ⁹	55	846*10 ⁶	1.24*10 ¹⁰	6.8
2.17*10 ⁸	1.54*10 ⁹	60	922*10 ⁶	1.24*10 ¹⁰	7.4

GWi = Groundwater inflow from Saudi Arabia

The result shows that ~ 8 – 9 % from the total area could be covered by greenhouse farming if both regional recharge and groundwater inflow are considered.

7. Conclusion and Recommendations

7.1 Conclusion

As a conclusion the lineaments (fault 1 and fault 2) recognized by field survey could be confirmed by automated lineament extraction from 30 m SRTM data and 15 m Landsat ETM. Interpolated groundwater heads of the uppermost Dammam aquifer display a different flow pattern between fault 1 and fault 2, which correlates with the assumption of an elevated permeability between these two lineaments due to tectonic stress and the anticline structure. Furthermore, the results of the pumping tests support the hypothesis that the area between fault 1 and fault 2 is characterized by slightly increased permeability.

With respect to the watershed delineation, the automated watershed analysis of flat areas cannot be done without manual evaluation and support. Thus, it is recommended to implement either several seeding point as shown for the data used in this study or using manual correction of the DTM (performing river burning technique). Remarkable is that the 30 meter SRTM data set was providing a poorer result in comparison to the 90 m. SRTM as long as no manual correction was done. River Tools algorithms revealed a severe weakness when using the 90 meter SRTM and show as well deficits in time efficiency.

The estimated average of groundwater recharge from 1980-2008 is 17.5 mm/year, the groundwater pressure head varies from 476 in the west to 124 masl in the east. The south-west for the first Aquifer (Dammam) is dry and seems to contain no groundwater. According to the 17.5 mm/year, a total amount of $2.17 \cdot 10^{10}$ m³/year may be pumped out from the aquifers. Because a considerable large amount of groundwater is flowing into the area of interest, at least part of the groundwater can be pumped to the surface and be used for irrigation and domestic water supply. Considering the total amount of annual precipitation (140 mm) in the region of interest artificial groundwater recharge could be a viable option to increase the groundwater recharge. The benefit of a subsurface storage is that in comparison to as surface storage (artificial dams) no evaporation occurs. The major problem is the technical implementation of injection wells with low particle (silt and clay) load.

The groundwater recharge is very little with $\sim 0.217 \cdot 10^9$ m³/year. This amount allows greenhouse irrigation farming only for 1.75 % out of the total area of ROI. Nevertheless, this average could be expanded up to 8-9 % by using 50-60% from the external groundwater inflow from Saudi Arabia.

7.2 Recommendations

- It is highly recommended to perform vast geochemistry investigation for major and minor elements, stable Isotopes and to figure out the mean residence time by C¹⁴ investigations to characterize the groundwater.
- Long term meteorological monitoring (~ 10 years) is necessary to create an empirical equation with respect to calculation of groundwater recharge. This equation could be used in particular to the western desert of Iraq being arid or hyper arid areas.
- A groundwater monitoring network has to be established by drilling piezometric wells to all relevant aquifers for daily records to document the water table and pressure head. Further meteorological stations have to be implemented including monitoring of chloride concentrations in rainfall to build a database for calculating recharge via the chloride method. A further need is to establish reliable readings of the amount of water pumped from the perspective aquifers. Finally, gauges have to be established in the major wadis to monitor flood flows after severe rain events. The latter is certainly a challenge because monitoring of wadi flows is anything but easy. All above described measures will allow after a certain time a more precise estimation of groundwater recharge and impact of climate change in the region of interest.
- Managing the water resource by means of artificial recharge as mentioned under the chapter conclusion is an important issue. In particular, the zone between the two faults has to be investigated in more detail.
- Implementation of sophisticated irrigation system such as drip irrigation, green houses and evaporation protective measures in combination with use of pre-treated wastewater for irrigation will help optimizing the utilization of water in the region of interest.
- Because the annual average of sunshine duration is ~ 11.7 h/ day solar energy harvesting could be feasible and might show a good potential for alternative energy resource.
- The recent steady state model can be upgraded towards a transient flow model and a transport model to figure out both means residence times and contamination issues.

8. References

- Ahrens, C.D., 2007. *Meteorology today: an introduction to weather, climate, and the environment*. Brooks/Cole Pub Co.
- Al-Amiri, H.M., 1978. Structural interpretation of the Landsat Satellite imagery for Western Desert-Iraq. Geosurv Iraq, Library. No.923 (Unpublished).
- Al-Azawi, T.M., 1988. The tectonic of western Euphrates by using Landsat images interpretation and geological information. Baghdad University, college of science, PhD. Thesis: 108P (Unpublished).
- Al-Mankoshy, H.J., 2008. Integration of Remote Sensing Data and GIS to Determine Potential Ground Water in Ubaiydh and Ghadaf Valleys. PhD. thesis, Baghdad University, college of science (Unpublished).
- AlFurat, C., 1989. General Scheme of water resources and Land development in Iraq. Ministry of Agriculture and Irrigation, Iraq, stage III (Unpublished).
- AlFurat, C., 1995. Groundwater recharge ,Al-Haidaria area, Karblla. Ministry of Agriculture and Irrigation, Iraq, Report 1 (Unpublished).
- Arge, L. et al., 2003. Efficient flow computation on massive grid terrain datasets. *GeoInformatica*, 7(4): 313.
- Band, L.E., 1989. A terrain-based watershed information system. *Hydrological Processes*, 3(2): 151-162.
- Bekele, G., 2009. STUDY INTO THE POTENTIAL AND FEASIBILITY OF A STANDALONE SOLAR-WIND HYBRID ELECTRIC ENERGY SUPPLY SYSTEM.
- Bellen, R.C.V., Dunnington, H. V., Wetzel, R. and Morton, D., 1959. Lexique Stratigraphique International, Asie . Iraq. Intern. Geol. Conger. Comm. Stratigr, 3,Fasc, 10a: 333 p.
- Braathen, A., 1999. Kinematics of post-Caledonian polyphase brittle faulting in the Sunnfjord region, western Norway. *Tectonophysics*, 302(1-2): 99-121.
- Buday, T., and Hak,J. , 1980. The geological survey of the Western part of the Western Desert. No.1000, Geosurv. Iraq., IRAQ (Unpublished).
- Buday, T., Saad Z. Jassim, 1984. Tectonic Map of IRAQ. Geosurv. Iraq. Baghdad (Unpublished).
- Carlson, R.E. and Foley, T.A., 1992. Interpolation of track data with radial basis methods. *Computers & Mathematics with Applications*, 24(12): 27-34.
- Cohen, Y. and Shoshany, M., 2002. A national knowledge-based crop recognition in Mediterranean environment. *International Journal of Applied Earth Observation and Geoinformation*, 4(1): 75-87.
- Consortium-Yugoslavia, 1977. Hydrogeological explorations and hydrotechnical work-Western Desert of IRAQ. Blook7, Directorate of western desert development projects. Republic of Iraq (Unpublished).
- Cressie, N., 1990. The origins of kriging. *Mathematical Geology*, 22(3): 239-252.
- Cummings, D., 2002. How much water do I need? Landcare Notes.
- Danner, A. et al., 2007. Terrastream: from elevation data to watershed hierarchies. *ACM*, pp. 28.
- Division, N.I., 1944. Western Desert of Iraq. University of Texas Libraries, Iraq.
- Domenico, P.A. and Schwartz, F.W., 1998. *Physical and chemical hydrogeology*. Wiley New York.

- Fairfield, J. and Leymarie, P., 1991. Drainage networks from grid digital elevation models. *Water Resources Research*, 27(5): 709-717.
- Fernandes, C., Corãj, J.E. and de Araãjo, J.A.C., 2003. Reference evapotranspiration estimation inside greenhouses. *Scientia Agricola*, 60(3): 591-594.
- Garbrecht, J. and Martz, L.W., 1993. NETWORK AND SUBWATERSHED PARAMETERS EXTRACTED FROM DIGITAL ELEVATION MODELS: THE BILLS CREEK EXPERIENCE1. *JAWRA Journal of the American Water Resources Association*, 29(6): 909-916.
- Geomatics, P.C.I., 2001. *Geomatica Software manual*.
- Haralick, R.M., Sternberg, S.R. and Zhuang, X., 1987. Image analysis using mathematical morphology. *IEEE PATTERN ANAL. MACH. INTELLIG.*, 9(4): 532-550.
- Hemker, C.J., 1999. Transient well flow in layered aquifer systems: the uniform well-face drawdown solution. *Journal of Hydrology*, 225(1-2): 19-44.
- Hung, L.Q., Batelaan, O. and De Smedt, F., 2005. Lineament extraction and analysis, comparison of LANDSAT ETM and ASTER imagery. Case study: Suoimuoi tropical karst catchment, Vietnam, pp. 59830T-1.
- Jassim, S.Z. and Goff, J.C., 2006. *Geology of Iraq*. Dolin.
- Jawad, S.B., Basho, D. Y., Naoom, F. H., Zamil, H. A., Said, B. M. A., 2001. Aquifer hydrogeology in the western desert, west and south Euphrates River. Ministry of Water Resource - Iraq, National program to utilize the water resource in Euphrates basin, 4: 89 p (Unpublished).
- Jenson, S.K. and Domingue, J.O., 1988. Extracting topographic structure from digital elevation data for geographic information system analysis. *Photogrammetric Engineering and remote sensing*, 54(11): 1593-1600.
- Jones, R., 2002. Algorithms for using a DEM for mapping catchment areas of stream sediment samples* 1. *Computers & geosciences*, 28(9): 1051-1060.
- Kenny, F., Matthews, B. and Todd, K., 2008. Routing overland flow through sinks and flats in interpolated raster terrain surfaces. *Computers & geosciences*, 34(11): 1417-1430.
- Kijne, J.W., 1974. Determining evapotranspiration. *Drainage Principles and Application*: 53-111.
- Kim, G.B., Lee, J.Y. and Lee, K.K., 2004. Construction of lineament maps related to groundwater occurrence with ArcView and Avenue™ scripts. *Computers and Geosciences*, 30(9-10): 1117-1126.
- Kiss, R., 2004. Determination of drainage network in Digital Elevation Models, utilities and limitations. *Journal of Hungarian Geomathematics* 2.
- Kurlov, M.G., 1928. *Classification of mineral waters of Siberia*. Tomsk, USSR.
- Laben, C.A. and Brower, B.V., 2000. Process for enhancing the spatial resolution of multi-spectral imagery using pan-sharpening. Google Patents.
- Lindsay, J.B., 2005. *The Terrain Analysis System: a tool for hydro-geomorphic applications*. Wiley InterScience.
- Maidment, D.R., 1993. *Handbook of hydrology*. New York.
- Martz, L.W. and Garbrecht, J., 1992. Numerical definition of drainage network and sub-catchment areas from digital elevation models. *Computers & Geosciences*, 18(6): 747-761.
- Martz, L.W. and Garbrecht, J., 1998. The treatment of flat areas and depressions in automated drainage analysis of raster digital elevation models. *Hydrological Processes*, 12(6): 843-855.

- Mayo, A.L. and Koontz, W., 2000. Fracture flow and groundwater compartmentalization in the Rollins Sandstone, Lower Mesaverde Group, Colorado, USA. *Hydrogeology Journal*, 8(4): 430-446.
- MOST, 2006. Solar Electric System. Ministry of Science and technology - Republic of the Union of Mayammar: 16 p (Unpublished).
- MOST, 2009. Meteorological data of Nukaib station. Ministry of science and technology - Iraq.
- MOWR, 2010. Water crisis reasons. Ministry of water resource , Al-Rafidain Magazine (Unpublished).
- NIC, 2004. Republic of Iraq National Investment Commission
- Niswonger, R.G., Prudic, D.E., Regan, R.S. and Geological Survey. Ground-water Resources, P., 2006. Documentation of the unsaturated-zone flow (UZFI) package for modeling unsaturated flow between the land surface and the water table with MODFLOW-2005. US Dept. of the Interior, US Geological Survey.
- Noaa, U.S., 2009. National Oceanic and Atmospheric Administration.
- Osma-Ruiz, V., Godino-Llorente, J.I., Sáenz-Lechón, N. and Gómez-Vilda, P., 2007. An improved watershed algorithm based on efficient computation of shortest paths. *Pattern Recognition*, 40(3): 1078-1090.
- P.Venkatchalam, B.K.M., 2001. Automatic delineation of watershed for hydrogeological applications. 22nd Asian Conference on remote sensing.
- Palacios-Velez, O.L. and Cuevas-Renaud, B., 1986. Automated river-course, ridge and basin delineation from digital elevation data. *Journal of Hydrology*, 86(3-4): 299-314.
- Parsons, R.M., 1957. Groundwater resources of Iraq. Ministry of Development Board-Baghdad, Vol. 11, Mesopotamian plain: 157P.
- Penman, H.L., 1950. The water balance of the Stour catchment area. *J. Inst. Water Eng*, 4(6): 457-469.
- Qian, J., Zhan, H., Zhao, W. and Sun, F., 2005. Experimental study of turbulent unconfined groundwater flow in a single fracture. *Journal of Hydrology*, 311(1-4): 134-142.
- Quinn, P., Beven, K., Chevallier, P. and Planchon, O., 1991. The prediction of hillslope flow paths for distributed hydrological modelling using digital terrain models. *Hydrological processes* 5(1): 59-79.
- Raghavan, V., Masumoto, S., Koike, K. and Nagano, S., 1995. Automatic lineament extraction from digital images using a segment tracing and rotation transformation approach. *Computers & Geosciences*, 21(4): 555-591.
- RiverTools, 2003. River Tools tutorial
- Rivix, L.L.C., 2004. RiverTools, Topographic and River Network Analysis. User's Guide, RiverTools Version 3. 0. Broomfield, Colorado, USA: RIVIX Limited Liability Company.
- Rojstaczer, S., 1987. The local effects of groundwater pumpage within a fault-influenced groundwater basin, Ash Meadows, Nye County, Nevada, USA. *Journal of Hydrology*, 91(3-4): 319-337.
- Saunders, W., 1999. Preparation of DEMs for use in environmental modeling analysis, pp. 1999.
- Sharma, S.P. and Baranwal, V.C., 2005. Delineation of groundwater-bearing fracture zones in a hard rock area integrating very low frequency electromagnetic and resistivity data. *Journal of Applied Geophysics*, 57(2): 155-166.
- Short, N.M., 2010. Remote sensing tutorial. National Aeronautics and Space Administration.
- Singh, V.P., 1992. Elementary hydrology. Prentice Hall.

- Smith, W.H.F. and Wessel, P., 1990. Gridding with continuous curvature splines in tension. *Geophysics*, 55: 293.
- Tarboton, D.G., 1997. A new method for the determination of flow directions and upslope areas in grid digital elevation models. *Water Resources Research*, 33(2).
- Thommeret, N., Bailly, J.S. and Puech, C., 2009. Robust Extraction of Thalwegs Networks from DTMs for Topological Characterization: A Case Study on Badlands.
- Thompson, R.D. and Perry, A.H., 1997. *Applied climatology: principles and practice*. Psychology Press.
- Thornthwaite, C.W., 1948. *Micrometeorology of the Surface Layer of the Atmosphere*. CW Thornthwaite Associates.
- Turc, L., 1954. Calcul du bilan de l'eau evaluation en fonction des prÃ©cipitations et des temperatures. *Proceedings of the General Assembly of Rome*, 101: 188-202.
- Turcotte, R., Fortin, J.P., Rousseau, A.N., Massicotte, S. and Villeneuve, J.P., 2001. Determination of the drainage structure of a watershed using a digital elevation model and a digital river and lake network. *Journal of Hydrology*, 240(3-4): 225-242.
- Unep, V., 1992. *World atlas of desertification*.
- Wanchang Zhang, C.F., 2005. *Automatic Watershed Delineation for a Complicated Terrain in the Heihe River Basin, Northwestern China*. International Institute for Earth System Science (ESSI).
- Watch, W.M.O.G.A. and Wmo, 2003. *Quality assurance in monitoring solar ultraviolet radiation: the state of the art*. WMO.
- Wen-Hsing, C. and Kinzelbach, W., 2005. *3D-Groundwater Modeling with Pmwin*. Springer. Stuttgart.

9. Appendices

Appendix 2-1 : values of corrected factor K for PE calculated by Thornthwaite (Kijne, 1974)

Lat.	Jan	Feb	Mar	Apr	May	June	July	Aug	Sep	Oct	Nov	Dec
0	1.04	.94	1.04	1.01	1.04	1.01	1.04	1.04	1.01	1.04	1.01	1.04
5	1.02	.93	1.03	1.02	1.06	1.03	1.06	1.05	1.01	1.03	.99	1.02
10	1.00	.91	1.03	1.03	1.08	1.06	1.08	1.07	1.02	1.02	.98	.99
15	.97	.91	1.03	1.04	1.11	1.08	1.12	1.08	1.02	1.01	.95	.97
20	.95	.90	1.03	1.05	1.13	1.11	1.14	1.11	1.02	1.00	.93	.94
25	.93	.89	1.03	1.06	1.15	1.14	1.17	1.12	1.02	.99	.91	.91
26	.92	.88	1.03	1.06	1.15	1.15	1.17	1.12	1.02	.99	.91	.91
27	.92	.88	1.03	1.07	1.16	1.15	1.18	1.13	1.02	.99	.90	.90
28	.91	.88	1.03	1.07	1.16	1.16	1.18	1.13	1.02	.98	.90	.90
29	.91	.87	1.03	1.07	1.17	1.16	1.19	1.13	1.03	.98	.90	.89
30	.90	.87	1.03	1.08	1.18	1.17	1.20	1.14	1.03	.98	.89	.88
31	.90	.87	1.03	1.08	1.18	1.18	1.20	1.14	1.03	.98	.89	.88
32	.89	.86	1.03	1.08	1.19	1.19	1.21	1.15	1.03	.98	.88	.87
33	.88	.86	1.03	1.09	1.19	1.20	1.22	1.15	1.03	.97	.88	.86
34	.88	.85	1.03	1.09	1.20	1.20	1.22	1.16	1.03	.97	.87	.86
35	.87	.85	1.03	1.09	1.21	1.21	1.23	1.16	1.03	.97	.86	.85
36	.87	.85	1.03	1.10	1.21	1.22	1.24	1.16	1.03	.97	.86	.84
37	.86	.84	1.03	1.10	1.22	1.23	1.25	1.17	1.03	.97	.85	.83
38	.85	.84	1.03	1.10	1.23	1.24	1.25	1.17	1.04	.96	.84	.83
39	.85	.84	1.03	1.11	1.23	1.24	1.26	1.18	1.04	.96	.84	.82
40	.84	.83	1.03	1.11	1.24	1.25	1.27	1.18	1.04	.96	.83	.81
41	.83	.83	1.03	1.11	1.25	1.26	1.27	1.19	1.04	.96	.82	.80
42	.82	.83	1.03	1.12	1.26	1.27	1.28	1.19	1.04	.95	.82	.79
43	.81	.82	1.02	1.12	1.26	1.28	1.29	1.20	1.04	.95	.81	.77
44	.81	.82	1.02	1.13	1.27	1.29	1.30	1.20	1.04	.95	.80	.76
45	.80	.81	1.02	1.13	1.28	1.29	1.31	1.21	1.04	.94	.79	.75
46	.79	.81	1.02	1.13	1.29	1.31	1.32	1.22	1.04	.94	.79	.74
47	.77	.80	1.02	1.14	1.30	1.32	1.33	1.22	1.04	.93	.78	.73
48	.76	.80	1.02	1.14	1.31	1.33	1.34	1.23	1.05	.93	.77	.72
49	.75	.79	1.02	1.14	1.32	1.34	1.35	1.24	1.05	.93	.76	.71
50	.74	.78	1.02	1.15	1.33	1.36	1.37	1.25	1.06	.92	.76	.70
5	1.06	.95	1.04	1.00	1.02	.99	1.02	1.03	1.00	1.05	1.03	1.06
10	1.08	.97	1.05	.99	1.01	.96	1.00	1.01	1.00	1.06	1.05	1.10
15	1.12	.98	1.05	.98	.98	.94	.97	1.00	1.00	1.07	1.07	1.12
20	1.14	1.00	1.05	.97	.96	.91	.95	.99	1.00	1.08	1.09	1.15
25	1.17	1.01	1.05	.96	.94	.88	.93	.98	1.00	1.10	1.11	1.18
30	1.20	1.03	1.06	.95	.92	.85	.90	.96	1.00	1.12	1.14	1.12
35	1.23	1.04	1.06	.94	.89	.82	.87	.94	1.00	1.13	1.17	1.25
40	1.27	1.06	1.07	.93	.86	.78	.84	.92	1.00	1.15	1.20	1.29
42	1.28	1.07	1.07	.92	.85	.76	.82	.92	1.00	1.16	1.22	1.31
44	1.30	1.08	1.07	.92	.83	.74	.81	.91	.99	1.17	1.23	1.33
46	1.32	1.10	1.07	.91	.82	.72	.79	.90	.99	1.17	1.25	1.35
48	1.34	1.11	1.08	.90	.80	.70	.76	.89	.99	1.18	1.27	1.37
50	1.37	1.12	1.08	.89	.77	.67	.74	.88	.99	1.19	1.29	1.41

Appendix 2-2 : Monthly Soil moisture mm.

	1980	1981	1982	1983	1984	1985	1986	1987	1988	1989	1990
Jan	11.25	33.35	39.20	67.10	21.85	33.50	33.65	29.65	50.50	33.70	33.75
Feb	14.50	44.95	48.25	94.65	23.00	21.80	40.30	27.80	28.20	34.50	42.80
Mar	24.80	55.45	47.00	94.70	29.00	11.20	48.40	32.35	30.00	39.65	54.00
Apr	27.70	54.95	58.03	87.65	29.10	14.20	50.80	32.20	35.75	36.00	47.20
May	20.95	46.00	61.90	73.35	23.20	19.50	45.80	25.00	32.20	27.30	37.80
June	15.00	34.65	47.00	55.45	17.50	26.90	34.70	19.25	23.80	19.90	28.45
July	10.70	25.12	33.85	39.95	13.00	37.00	25.20	14.40	17.15	14.30	21.15
Aug	7.65	18.00	24.45	28.85	9.50	50.15	18.10	10.30	12.35	20.30	15.35
Sep	5.60	13.05	17.75	21.40	6.90	62.50	13.10	7.60	9.10	7.40	11.35
Oct	4.30	10.05	18.85	17.20	14.70	67.40	13.05	10.00	8.80	5.80	9.30
Nov	6.50	20.02	31.83	15.35	40.70	64.00	19.75	11.00	8.80	19.00	8.10
Dec	22.30	29.10	41.15	18.90	59.00	60.00	28.60	16.75	22.25	32.80	7.60
	1991	1992	1993	1994	1995	1996	1997	1998	1999	2000	2001
Jan	12.45	24.60	15.20	12.40	27.15	10.80	19.75	43.60	8.60	10.40	19.15
Feb	20.90	33.85	17.60	25.90	32.90	14.30	24.80	49.00	12.80	10.30	26.75
Mar	35.10	39.80	16.10	33.70	36.05	19.10	25.80	52.10	14.00	9.50	31.00
Apr	36.35	36.70	19.40	27.75	32.15	22.30	23.45	47.80	11.90	8.90	28.75
May	28.40	29.25	22.60	21.65	26.05	18.40	18.40	38.40	9.40	8.00	23.50
June	21.15	21.85	18.80	16.00	19.45	13.70	13.65	28.40	6.90	6.20	17.60
July	20.90	15.85	13.40	11.60	14.15	9.80	9.90	20.30	5.00	4.40	12.60
Aug	34.95	11.45	9.60	8.40	10.15	7.00	7.25	14.50	7.20	3.20	8.95
Sep	36.35	8.35	7.00	6.70	7.60	4.90	5.40	10.50	7.50	2.40	6.60
Oct	28.40	6.55	5.60	5.90	6.00	3.80	6.50	8.10	6.70	2.30	5.60
Nov	21.20	9.45	6.90	14.50	7.00	6.20	22.45	6.70	5.90	3.50	5.70
Dec	20.30	11.25	10.30	25.60	9.10	11.40	36.65	6.10	8.40	9.30	7.40
	2002	2003	2004	2005	2006	2007	2008				
Jan	13.10	16.90	19.80	12.40	9.60	14.20	9.50				
Feb	16.70	18.50	24.30	16.20	14.12	19.30	14.90				
Mar	18.20	17.50	23.60	20.50	16.40	21.40	15.30				
Apr	19.80	17.30	23.00	20.20	20.50	22.40	13.20				
May	16.70	14.50	19.40	15.80	20.25	19.00	10.60				
June	12.20	10.60	14.20	11.50	14.90	13.80	7.50				
July	8.70	7.50	10.20	8.20	10.60	10.00	5.60				
Aug	15.30	5.30	7.20	5.90	7.50	7.00	4.00				
Sep	21.40	3.90	5.20	4.20	5.40	5.00	3.50				
Oct	16.50	3.20	3.90	3.30	7.20	3.80	4.60				
Nov	14.70	7.30	5.90	4.40	9.20	3.20	8.00				
Dec	14.60	13.80	9.10	7.00	10.50	4.80	10.50				

Appendix 2-3 : Observation wells

Well #	X	Y	SWL
2	714466	3585952	415.4
3	820554	3604270	267.3
4	828496	3581892	255
5	704763	3600171	432.7
6	788286	3592886	279.4
7	794793	3553868	265.8
8	802368	3545195	256.4
9	802899	3538124	235.4
10	809627	3542396	239.1
11	800260	3545959	261.3
12	832156	3562482	227.5
13	825543	3576413	253.1
14	777505	3577643	287.9
15	818606	3562152	244.4
16	809284	3566816	251.7
17	807067	3553556	248.2
18	817817	3607665	267.2
19	834199	3532438	197.7
20	835537	3541239	193.9
21	825704	3541249	234.2
22	816110	3536702	231.9
23	844327	3572665	193.1
24	799176	3529363	251.2
25	791456	3531827	277.3
26	845703	3530482	182.4
27	816868	3529817	227.6
28	777136	3532055	312.7
29	846429	3583748	198.7
30	823898	3530995	217.5
31	850517	3599170	189.8
32	823971	3548933	238.6
33	848297	3560113	191.9
34	789646	3529621	279.2
35	807303	3531390	234.9
36	773011	3530158	313.5
37	714413	3588447	440.8
38	707604	3599120	431.9
39	783066	3574159	269.7
40	784008	3574134	265.2

Well #	X	Y	SWL
41	743741	3554774	357.6
42	740673	3564686	365.7
43	819576	3563238	175.8
44	736833	3555387	369.8
45	726046	3590877	393.1
46	736444	3572021	370.8
47	789276	3559563	247.2
48	739166	3576523	368.1
49	790753	3543986	259.3
50	782154	3575294	274.2
51	743333	3559979	358.3
52	784449	3577851	249.7
53	785078	3574637	259.3
54	787801	3568614	256.4
55	790545	3571737	246.7
56	788109	3567430	261
57	796452	3544947	264.4
58	782615	3574227	273.3
59	782062	3571967	277.2
60	788184	3554043	250.6
61	778253	3536554	295.4
62	786112	3598728	265.4
63	794967	3560522	239.4
64	792701	3546154	278.6
65	789543	3569544	256.1
66	785682	3566319	263.1
67	780194	3597704	298.9
68	783218	3579705	261.2
69	805015	3547060	186.9
70	819517	3553586	172.7
71	813461	3544522	174.5
72	791403	3557842	242.3
73	791080	3546696	256.2
74	790812	3546204	261.4
75	800840	3531518	247.1
76	831622	3586813	168.7
77	777843	3540887	307.1
78	720738	3528034	383.5
79	772318	3535555	308.2
80	734805	3533894	365.8

Well #	X	Y	SWL
81	779258	3605922	299.3
82	760110	3604808	348.7
83	709507	3598050	449.2
85	711439	3596471	355.7
86	712909	3583900	407.2
87	743176	3605469	327.9
88	779425	3563604	286.1
89	788490	3564389	251.3
90	784845	3567473	292.5
91	721860	3601878	360.1
92	709137	3533814	343.7
93	704355	3574893	422.6
94	709486	3553688	351.4
95	745007	3537839	329.2
96	713028	3564844	439.2
97	705845	3546948	410.3
98	760715	3581496	345.3
99	708747	3543679	409.6
100	747124	3597799	372.4
101	757976	3578096	327.8
102	760855	3539329	332.9

Appendix 4-1 : Climatology elements data

Monthly Rainfall Totals(mm.)		• tr = Tiny rain											
Year	Jan.	Feb.	Mar.	Apr.	May	Jun.	Jul.	Aug.	Sep.	Oct.	Nov.	Dec.	Total
1980	7.4	10.2	16.6	123.9	7.5	0.0	0.0	0.0	0.0	tr	6.5	14.5	186.6
1981	1.0	21.6	9.6	7.2	13.1	tr	0.0	0.0	tr	4.6	1.9	4.7	63.7
1982	9.8	36.8	12.4	21.1	13.1	tr	0.0	0.0	0.0	0.0	14.5	6.8	114.5
1983	5.4	9.6	8.9	20.6	10.0	1.6	0.0	0.0	0.0	0.0	1.8	11.9	69.8
1984	32.6	17.2	89.2	59.7	5.9	tr	0.0	0.0	tr	tr	46.4	5.1	256.1
1985	37.2	13.7	35.3	60.0	tr	tr	0.0	0.0	0.0	49.8	3.0	64.8	263.8
1986	1.9	14.3	14.7	4.6	11.6	0.0	0.0	0.0	tr	7.9	22.3	12.6	89.9
1987	0.5	0.2	16.4	3.5	tr	tr	0.8	tr	0.0	59.4	0.1	10.6	91.5
1988	8.8	12.2	7.0	5.2	0.2	tr	0.0	0.0	0.0	33.1	21.6	15.4	103.5
1989	26.1	17.2	89.2	59.7	5.9	tr	0.0	0.0	0.0	tr	46.4	5.1	249.6
1990	3.0	62.5	3.5	1.2	1.5	0.0	0.0	0.0	0.0	12.3	7.6	4.5	96.1
1991	16.2	tr	30.3	tr	0.0	0.0	0.0	0.0	0.0	35.0	tr	2.6	84.1
1992	34.7	10.9	29.4	16.8	40.0	0.0	0.0	0.0	0.6	7.2	46.0	21.0	206.6
1993	17.7	22.7	12.5	32.7	23.1	0.0	0.0	0.0	tr	13.2	3.2	5.5	130.6
1994	17.9	11.1	11.5	1.7	tr	0.0	0.0	0.0	10.0	10.2	100.3	12.7	175.4
1995	5.6	67.7	22.3	28.6	6.2	0.0	tr	0.0	tr	tr	25.4	29.5	185.3
1996	15.7	22.7	37.0	1.4	3.1	tr	2.6	tr	tr	1.9	35.0	14.0	133.4
1997	17.7	2.8	19.3	6.1	2.0	0.0	0.0	0.0	0.0	101.4	57.8	29.8	236.9
1998	21.3	18.3	18.4	1.8	19.6	0.0	tr	tr	tr	0.0	tr	1.5	80.9
1999	9.9	14.3	3.8	1.8	tr	0.0	0.0	1.0	0.0	4.7	0.0	27.1	62.6
2000	8.4	3.0	0.1	0.9	11.6	tr	0.0	0.0	tr	7.9	30.0	22.5	84.4
2001	37.2	13.7	35.3	60.0	tr	tr	0.0	0.0	0.0	49.8	3.0	64.8	263.8
2002	46.4	33.6	12.0	4.1	3.3	0.0	0.0	tr	0.6	tr	2.0	1.3	103.3
2003	25.5	15.9	0	0	0	0	0	0	0	0	11.9	35.3	88.6
2004	29.3	21.3	19.5	0	0	0	0	0	0	6.2	21.3	25.1	122.7
2005	31.1	17.8	11.3	4.7	0	0	0	0	0	9.1	18.2	33.4	125.6
2006	40.7	29.7	17.8	5.2	3.8	0	0	0	0	31.2	51.2	21.3	200.9
2007	26.2	22.6	9.2	0	0	0	0	0	0	1.9	16.2	29.1	105.2
2008	33.8	12.9	7.6	2.2	0	0	0	0	0	5.1	14.5	30.9	107
Mean	19.6	19.9	20.7	19.1	7.6	0.1	0.1	0.0	0.5	18.8	22.5	19.4	140.8

Temperature Totals(C°)													
Year	Jan.	Feb.	Mar.	Apr.	May	Jun.	Jul.	Aug.	Sep.	Oct.	Nov.	Dec.	Mean
1980	6.1	8.1	13.1	18.6	24.4	29.2	32.3	38.2	26.1	20.8	14.8	9.6	20.1
1981	7.7	9.2	14.2	17.8	22.1	28.2	31.4	39.0	28.5	22.8	11.8	10.4	20.3
1982	7.5	6.4	11.4	19.7	23.5	28.0	30.0	37.5	27.5	19.8	9.7	6.6	19.0
1983	4.6	7.8	12.1	17.6	24.0	28.1	30.6	40.1	26.8	20.6	16.5	9.8	19.9
1984	8.6	11.2	14.0	18.7	23.8	28.4	31.3	41.2	26.9	20.8	13.3	6.4	20.4
1985	9.0	7.9	11.3	19.1	25.7	29.2	29.6	36.6	28.1	20.2	15.4	8.4	20.0
1986	8.1	11.0	14.1	20.1	22.3	27.5	31.5	35.8	29.8	22.3	11.7	7.6	20.2
1987	9.1	12.2	10.9	18.6	25.6	28.5	32.1	42.8	27.7	19.6	13.6	10.3	20.9
1988	7.3	9.0	12.4	17.6	24.9	28.4	32.2	41.5	27.7	21.0	12.2	9.1	20.3
1989	4.4	6.8	13.6	22.1	26.2	28.6	32.0	40.0	26.8	21.4	14.7	9.0	20.5
1990	5.4	8.2	12.7	18.9	24.6	29.0	31.8	39.7	27.7	22.2	16.4	10.7	20.6
1991	7.2	11.6	14.1	20.8	32.1	29.7	30.7	42.1	27.5	21.6	15.4	7.4	21.7
1992	4.0	6.1	10.5	18.3	22.8	28.0	29.7	41.3	26.8	22.1	13.2	6.7	19.1
1993	6.0	7.9	12.9	19.1	22.8	28.7	31.2	73.2	28.0	22.9	12.7	10.2	23.0
1994	9.7	10.1	14.4	22.0	25.8	28.9	30.4	39.0	29.2	23.6	13.3	6.3	21.1
1995	9.2	9.7	13.8	18.4	25.8	29.7	30.5	38.7	27.8	21.5	13.1	8.2	20.5
1996	8.2	10.4	12.7	18.7	27.5	29.4	34.0	36.8	28.2	20.7	14.0	11.4	21.0
1997	8.1	7.5	10.5	17.8	26.2	29.7	31.3	42.1	27.3	22.3	14.2	9.7	20.6
1998	6.8	8.5	12.0	20.2	25.4	31.0	33.4	40.2	29.0	22.2	17.6	11.6	21.5
1999	8.7	11.3	13.9	19.4	26.1	29.6	31.7	39.6	27.5	22.6	14.1	9.9	21.2
2000	7.5	8.7	12.5	21.7	25.2	29.9	35.1	39.9	27.7	20.0	13.6	10.1	21.0
2001	8.2	10.1	17.3	20.7	23.4	29.8	32.5	40.4	29.1	23.5	14.3	11.1	21.7
2002	6.7	11.3	15.6	19.3	24.8	28.8	32.9	40.8	28.6	22.7	14.2	10.7	21.4
2003	8.6	8.9	14.1	15.8	25.0	27.0	30.0	39.8	27.8	19.8	13.2	6.9	19.7
2004	5.4	5.9	12.1	19.6	22.5	28.0	29.3	40.1	27.2	23.5	13.4	5.2	19.4
2005	5.3	11.4	13.2	18.0	24.2	26.8	30.1	39.6	27.4	22.3	11.0	8.0	19.8
2006	5.5	7.4	13.0	17.6	24.4	28.9	30.5	39.2	26.0	23.6	14.7	7.9	19.9
2007	6.3	8.3	13.1	19.6	23.6	28.1	31.0	36.2	27.8	19.7	14.0	7.4	19.6
2008	7.2	7.9	11.1	17.8	22.8	28.0	28.7	35.7	26.2	21.6	13.9	10.1	19.3
Mean	7.1	9.0	13.0	19.1	24.7	28.7	31.3	40.6	27.7	21.6	13.8	8.9	20.5

Potential Evaporation Totals(mm)

Year	Jan.	Feb.	Mar.	Apr.	May	Jun.	Jul.	Aug.	Sep.	Oct.	Nov.	Dec.	Total
1980	83.4	67.5	103.2	254.3	241.1	302.6	407.2	311.4	283.8	215.7	91.3	40.1	2401.6
1981	80.7	70.5	98.4	193.2	223.3	280.7	389.4	302.1	276.3	211.2	103.2	39.5	2268.5
1982	92.6	80.5	90.2	150.7	280.3	302.5	410.2	380.1	260.6	214.9	102.1	51.2	2415.9
1983	96.2	88.3	89.5	252.6	243.1	311.2	416.3	356.7	240.3	216.2	105.1	46.8	2462.3
1984	79.2	79.1	102.3	240.1	281.3	321.5	401.5	380.4	239.1	213.5	98.5	48.1	2484.6
1985	88.5	73.2	93.5	275.3	290.1	340.1	415.1	398.2	254.3	205.7	101.0	57.6	2592.6
1986	82.4	80.5	99.8	263.2	276.4	378.2	422.6	349.7	290.1	211.9	89.7	42.4	2586.9
1987	90.2	69.7	105.2	205.7	289.6	401.1	416.2	357.8	258.7	204.0	88.2	44.0	2530.4
1988	92.1	75.8	119.3	210.4	251.6	398.4	409.1	373.1	246.3	208.4	98.5	38.6	2521.6
1989	84.9	66.2	123.4	201.3	268.7	386.2	402.9	317.0	188.5	208.9	86.3	36.6	2370.9
1990	73.1	69.3	118.2	199.6	264.5	359.5	411.8	351.2	208.4	227.5	79.9	41.0	2404.0
1991	83.2	68.8	116.1	187.8	283.1	358.3	400.4	370.6	212.0	214.0	103.1	43.2	2440.6
1992	79.6	73.6	120.8	217.9	270.5	370.0	399.5	354.9	238.9	206.1	97.6	52.6	2482.0
1993	95.5	58.2	96.7	230.1	283.2	382.3	414.2	370.1	193.6	213.7	99.2	51.0	2487.8
1994	87.4	63.4	101.2	223.5	259.7	403.1	419.0	368.7	204.3	209.1	80.8	47.2	2467.4
1995	93.9	61.1	127.5	244.1	303.4	400.7	415.6	354.3	217.0	189.5	86.5	45.4	2539.0
1996	82.7	57.9	114.3	216.3	295.3	398.6	405.0	374.2	225.3	194.3	82.7	40.0	2486.6
1997	95.1	64.2	131.2	220.8	247.9	368.2	402.3	398.1	260.4	201.7	79.3	43.1	2512.3
1998	86.4	68.7	140.6	246.6	257.8	390.1	410.7	374.2	202.6	204.1	84.2	46.7	2512.7
1999	94.3	82.6	167.6	268.4	301.4	427.7	405.6	377.5	181.4	213.9	95.5	54.6	2670.5
2000	96.1	66.6	127.2	233.3	228.3	336.6	410.2	362.1	258.2	193.8	85.9	45.8	2444.1
2001	90.7	66.9	159.3	255.6	299.0	396.2	406.8	390.2	277.4	213.7	93.3	55.7	2704.8
2002	90.6	64.9	149.5	244.8	287.4	388.0	403.1	383.3	270.5	208.6	84.7	47.7	2623.1
2003	75.3	66.2	150.2	240.0	279.0	397.1	401.0	374.0	263.9	211.0	78.9	44.9	2581.5
2004	70.0	64.3	151.1	252.1	265.2	378.9	413.0	358.3	270.0	212.2	100.5	54.2	2589.8
2005	98.3	67.9	167.4	268.4	293.5	383.0	407.1	348.0	268.8	224.7	90.2	38.1	2655.4
2006	85.8	76.8	157.2	253.1	337.1	389.7	401.2	386.8	271.2	220.9	101.5	57.3	2738.6
2007	61.1	79.6	172.2	240.8	248.3	380.2	414.8	370.2	263.0	165.5	171.7	56.6	2624.0
2008	68.0	56.1	167.8	212.5	252.7	301.0	407.3	397.3	269.4	253.5	139.4	54.5	2579.5
Mean	85.4	69.9	126.2	231.1	272.5	366.6	408.2	365.2	244.6	209.9	96.5	47.1	2523.4

RH.Totales %													
Year	Jan.	Feb.	Mar.	Apr.	May	Jun.	Jul.	Aug.	Sep.	Oct.	Nov.	Dec.	Total
1980	69.0	73.0	55.0	39.0	26.0	26.0	22.0	28.0	28.0	41.0	30.0	75.0	512.0
1981	66.0	66.0	64.0	42.0	34.0	24.0	27.0	25.0	25.0	25.0	72.0	55.0	525.0
1982	73.0	70.0	53.0	48.0	42.0	26.0	28.0	29.0	29.0	55.0	44.0	74.0	571.0
1983	70.0	66.0	55.0	47.0	35.0	27.0	25.0	28.0	27.0	33.0	75.0	68.0	556.0
1984	64.0	0.0	0.0	39.0	34.0	30.0	26.0	32.0	30.0	38.0	64.0	77.0	434.0
1985	65.0	53.0	43.0	40.0	30.0	27.0	25.0	23.0	27.0	42.0	49.0	69.0	493.0
1986	66.0	63.0	50.0	43.0	40.0	33.0	27.0	24.0	26.0	44.0	55.0	66.0	537.0
1987	59.0	55.0	63.0	44.0	36.0	33.0	29.0	29.0	31.0	54.0	50.0	72.0	555.0
1988	78.0	64.0	56.0	56.0	30.0	26.0	22.0	27.0	26.0	50.0	63.0	69.0	567.0
1989	69.0	56.0	57.0	31.0	29.0	24.0	24.0	30.0	32.0	41.0	51.0	65.0	509.0
1990	59.0	73.0	49.0	38.0	28.0	24.0	26.0	29.0	28.0	40.0	53.0	62.0	509.0
1991	77.0	61.0	61.0	33.0	38.0	28.0	28.0	33.0	33.0	56.0	58.0	63.0	569.0
1992	66.0	71.0	52.0	39.0	40.0	30.0	26.0	27.0	28.0	34.0	56.0	75.0	544.0
1993	67.0	62.0	46.0	50.0	45.0	36.0	30.0	30.0	29.0	42.0	76.0	70.0	583.0
1994	71.0	55.0	55.0	34.0	35.0	35.0	36.0	30.0	35.0	53.0	52.0	78.0	569.0
1995	82.0	79.0	62.0	49.0	31.0	31.0	32.0	31.0	31.0	41.0	68.0	75.0	612.0
1996	75.0	68.0	65.0	49.0	33.0	30.0	29.0	29.0	35.0	50.0	78.0	76.0	617.0
1997	84.0	60.0	57.0	45.0	36.0	32.0	30.0	33.0	33.0	52.0	49.0	84.0	595.0
1998	67.0	72.0	67.0	44.0	36.0	28.0	30.0	27.0	36.0	44.0	58.0	60.0	569.0
1999	72.0	64.0	48.0	43.0	31.0	35.0	34.0	33.0	37.0	45.0	63.0	75.0	580.0
2000	84.0	60.0	50.0	40.0	39.0	32.0	27.0	33.0	41.0	60.0	45.0	82.0	593.0
2001	70.0	73.0	61.0	55.0	41.0	30.0	26.0	28.0	32.0	34.0	43.0	65.0	558.0
2002	65.0	51.0	47.0	50.0	37.0	29.0	31.0	30.0	29.0	31.0	47.0	74.0	521.0
2003	61.0	61.0	42.0	56.0	33.0	25.0	27.0	27.0	27.0	35.0	60.0	71.0	525.0
2004	79.0	65.0	61.0	51.0	43.0	26.0	26.0	25.0	26.0	32.0	64.0	70.0	568.0
2005	61.0	54.0	45.0	42.0	31.0	24.0	20.0	20.0	24.0	31.0	47.0	62.0	461.0
2006	77.0	73.0	72.0	41.0	27.0	21.0	22.0	27.0	27.0	28.0	55.0	71.0	541.0
2007	75.0	65.0	45.0	37.0	31.0	22.0	23.0	29.0	28.0	33.0	44.0	65.0	497.0
2008	65.0	55.0	62.0	47.0	37.0	22.0	28.0	26.0	28.0	36.0	37.0	65.0	508.0
Mean	70.2	61.7	53.2	43.9	34.8	28.1	27.1	28.3	29.9	41.4	55.4	70.1	544.1

Wind speed (m/sec.)	Jan.	Feb.	Mar.	Apr.	May	Jun.	Jul.	Aug.	Sep.	Oct.	Nov.	Dec.
Mean 1980-2008	2.7	3.5	3.6	3.7	3.3	3.5	3.8	3.2	2.4	2.4	2.2	2.5

Sun shine duration (h/day)	Jan.	Feb.	Mar.	Apr.	May	Jun.	Jul.	Aug.	Sep.	Oct.	Nov.	Dec.
Mean 1980-2008	6.8	8.1	8.6	10.5	11.2	13.1	12.3	11.7	10.9	9.4	8.1	6.2

Appendix 6-2: Water Balance and Groundwater recharge calculation

1980 : I = 107.82 / a =2.20													WS / WD	GWr
Month	TC°	p(mm)	(T/5)	(T/5) ^{1.514}	(T*10)/I	[(T*10)/I] ^a	PE	K	PEc	AE	SM	p - (AE +SM)	WS - RO	
Jan	6.1	7.4	1.22	1.35	0.57	0.29	4.57	0.98	4.48	4.48	11.25	-8.33	0.0	
Feb	8.1	10.2	1.62	2.08	0.75	0.53	8.53	0.88	7.50	7.50	14.50	-11.80	0.0	
Mar	13.1	16.6	2.62	4.30	1.21	1.53	24.56	0.87	21.36	16.60	24.80	-24.80	0.0	
Apr	18.6	123.9	3.72	7.31	1.73	3.32	53.10	0.89	47.26	47.26	27.70	48.94	48.94	
May	24.4	7.5	4.88	11.02	2.26	6.03	96.48	0.86	82.97	7.50	20.95	-20.95	0.0	
June	29.2	0	5.84	14.47	2.71	8.95	155.40	1.03	160.06	0.00	15.00	-15.00	0.0	
July	32.3	0	6.46	16.85	3.00	11.18	175.30	1.08	189.32	0.00	10.70	-10.70	0.0	
Aug	38.2	0	7.64	21.73	3.54	16.17	185.00	1.19	220.15	0.00	7.65	-7.65	0.0	
Sep	26.1	0	5.22	12.21	2.42	6.99	111.89	1.19	133.15	0.00	5.60	-5.60	0.0	
Oct	20.8	0	4.16	8.66	1.93	4.24	67.91	1.21	82.17	0.00	4.30	-4.30	0.0	
Nov	14.8	6.5	2.96	5.17	1.37	2.01	32.12	1.15	36.94	6.50	6.50	-6.50	0.0	
Dec	9.6	14.5	1.92	2.68	0.89	0.77	12.39	1.03	12.76	12.76	22.30	-20.56	0.0	
SUM		186.6		107.8									48.94	
1981 : I = 108.5 / a =2.20													WS / WD	GWr
Month	TC°	p(mm)	(T/5)	(T/5) ^{1.514}	(T*10)/I	[(T*10)/I] ^a	PE	K	PEc	AE	SM	p - (AE +SM)	WS - RO	
Jan	7.7	1.0	1.54	1.92	0.71	0.47	7.52	0.98	7.37	1.0	33.35	-33.35	0	
Feb	9.2	21.6	1.84	2.52	0.85	0.70	11.13	0.88	9.79	9.8	44.95	-33.14	0	
Mar	14.2	9.6	2.84	4.86	1.31	1.81	28.92	0.87	25.16	9.6	55.45	-55.45	0	
Apr	17.8	7.2	3.56	6.84	1.64	2.97	47.54	0.89	42.31	7.2	54.95	-54.95	0	
May	22.1	13.1	4.42	9.49	2.04	4.78	76.53	0.86	65.82	13.1	46.00	-46.00	0	
June	28.2	0	5.64	13.72	2.60	8.18	147.80	1.03	152.23	0.0	34.65	-34.65	0	
July	31.4	0	6.28	16.15	2.89	10.36	170.70	1.08	184.36	0.0	25.12	-25.12	0	
Aug	39.0	0	7.8	22.42	3.59	16.69	185.00	1.19	220.15	0.0	18.00	-18.00	0	
Sep	28.5	0	5.7	13.94	2.63	8.37	151.70	1.19	180.52	0.0	13.05	-13.05	0	
Oct	22.8	4.6	4.56	9.95	2.10	5.12	81.97	1.21	99.18	4.6	10.05	-10.05	0	
Nov	11.8	1.9	2.36	3.67	1.09	1.20	19.24	1.15	22.13	1.9	20.02	-20.02	0	
Dec	10.4	4.7	2.08	3.03	0.96	0.91	14.58	1.03	15.01	4.7	29.10	-29.10	0	
SUM		63.7		108.50									0	

1982 : I = 100.4/ a =2.11												WS / WD	GWr
Month	TC°	p(mm)	(T/5)	(T/5)^1.514	(T*10)/I	[(T*10)/I]^a	PE	K	PEc	AE	SM	p - (AE +SM)	WS - RO
Jan	7.5	9.8	1.5	1.85	0.75	0.54	8.65	0.98	8.47	8.47	39.20	-37.87	0
Feb	6.4	36.8	1.28	1.45	0.64	0.39	6.19	0.88	5.44	5.44	48.25	-16.89	0
Mar	11.4	12.4	2.28	3.48	1.14	1.31	20.92	0.87	18.20	12.40	47.00	-47.00	0
Apr	19.7	21.1	3.94	7.97	1.96	4.15	66.34	0.89	59.04	21.10	58.03	-58.03	0
May	23.5	13.1	4.7	10.41	2.34	6.02	96.25	0.86	82.78	13.10	61.90	-61.90	0
June	28.0	0	5.6	13.58	2.79	8.71	147.80	1.03	152.23	0.00	47.00	-47.00	0
July	30.0	0	6	15.07	2.99	10.07	162.10	1.08	175.07	0.00	33.85	-33.85	0
Aug	37.5	0	7.5	21.13	3.74	16.13	185.00	1.19	220.15	0.00	24.45	-24.45	0
Sep	27.5	0	5.5	13.21	2.74	8.38	143.70	1.19	171.00	0.00	17.75	-17.75	0
Oct	19.8	0	3.96	8.03	1.97	4.19	67.05	1.21	81.14	0.00	18.85	-18.85	0
Nov	9.7	14.5	1.94	2.73	0.97	0.93	14.88	1.15	17.11	14.50	31.83	-31.83	0
Dec	6.6	6.8	1.32	1.52	0.66	0.41	6.60	1.03	6.80	6.80	41.15	-41.15	0
SUM		114.5		100.43									0
1983 : I = 106.8/ a =2.21												WS / WD	GWr
Month	TC°	p(mm)	(T/5)	(T/5)^1.514	(T*10)/I	[(T*10)/I]^a	PE	K	PEc	AE	SM	p - (AE +SM)	WS - RO
Jan	4.6	5.4	0.92	0.88	0.43	0.16	2.49	0.98	2.44	2.44	67.10	-64.1	0
Feb	7.8	9.6	1.56	1.96	0.73	0.50	7.99	0.88	7.03	7.03	94.65	-92.1	0
Mar	12.1	8.9	2.42	3.81	1.13	1.32	21.08	0.87	18.34	8.9	94.70	-94.7	0
Apr	17.6	20.6	3.52	6.72	1.65	3.02	48.26	0.89	42.95	20.6	87.65	-87.7	0
May	24.0	10.0	4.8	10.75	2.25	5.99	95.77	0.86	82.37	10	73.35	-73.4	0
June	28.1	1.6	5.62	13.65	2.63	8.48	147.80	1.03	152.23	1.6	55.45	-55.5	0
July	30.6	0	6.12	15.53	2.87	10.24	165.20	1.08	178.42	0	39.95	-40.0	0
Aug	40.1	0	8.02	23.38	3.75	18.61	185.00	1.19	220.15	0	28.85	-28.9	0
Sep	26.8	0	5.36	12.70	2.51	7.64	139.50	1.19	166.01	0	21.40	-21.4	0
Oct	20.6	0	4.12	8.53	1.93	4.27	68.33	1.21	82.68	0	17.20	-17.2	0
Nov	16.5	1.8	3.3	6.10	1.54	2.62	41.84	1.15	48.12	1.8	15.35	-15.4	0
Dec	9.8	11.9	1.96	2.77	0.92	0.83	13.23	1.03	13.63	11.9	18.90	-18.9	0
SUM		69.8		106.79									0

1984 : I = 109.98/ a =2.30												WS / WD	GWr
Month	TC°	p(mm)	(T/5)	(T/5)^1.514	(T*10)/I	[(T*10)/I]^a	PE	K	PEc	AE	SM	p - (AE +SM)	WS - RO
Jan	8.6	32.6	1.72	2.27	0.78	0.57	9.09	0.98	8.91	8.91	21.85	1.84	1.84
Feb	11.2	17.2	2.24	3.39	1.02	1.04	16.68	0.88	14.68	14.68	23.00	-20.48	0.0
Mar	14.0	89.2	2.8	4.75	1.27	1.74	27.87	0.87	24.25	24.25	29.00	35.95	35.95
Apr	18.7	59.7	3.74	7.37	1.70	3.39	54.24	0.89	48.28	48.28	29.10	-17.68	0.0
May	23.8	5.9	4.76	10.61	2.16	5.90	94.46	0.86	81.23	5.90	23.20	-23.20	0.0
June	28.4	0	5.68	13.87	2.58	8.86	151.70	1.03	156.25	0.00	17.50	-17.50	0.0
July	31.3	0	6.26	16.07	2.85	11.08	170.70	1.08	184.36	0.00	13.00	-13.00	0.0
Aug	41.2	0	8.24	24.36	3.75	20.86	185.00	1.19	220.15	0.00	9.50	-9.50	0.0
Sep	26.9	0	5.38	12.78	2.45	7.82	139.50	1.19	166.01	0.00	6.90	-6.90	0.0
Oct	20.8	0	4.16	8.66	1.89	4.33	69.29	1.21	83.84	0.00	14.70	-14.70	0.0
Nov	13.3	46.4	2.66	4.40	1.21	1.55	24.77	1.15	28.49	28.49	40.70	-22.79	0.0
Dec	6.4	5.1	1.28	1.45	0.58	0.29	4.61	1.03	4.74	4.74	59.00	-58.64	0.0
SUM		256.1		109.98									37.79
1985 : I = 106.6 / a =2.20												WS / WD	GWr
Month	TC°	p(mm)	(T/5)	(T/5)^1.514	(T*10)/I	[(T*10)/I]^a	PE	K	PEc	AE	SM	p - (AE +SM)	WS - RO
Jan	9.0	37.2	1.8	2.43	0.84	0.69	11.02	0.98	10.80	10.80	33.50	-7.10	0
Feb	7.9	13.7	1.58	2.00	0.74	0.52	8.27	0.88	7.28	7.28	21.80	-15.38	0
Mar	11.3	35.3	2.26	3.44	1.06	1.14	18.19	0.87	15.82	15.82	11.20	8.28	8.28
Apr	19.1	60.0	3.82	7.61	1.79	3.61	57.71	0.89	51.36	51.36	14.20	-5.56	0
May	25.7	0.0	5.14	11.92	2.41	6.93	110.87	0.86	95.35	0.00	19.50	-19.50	0
June	29.2	0	5.84	14.47	2.74	9.18	155.40	1.03	160.06	0.00	26.90	-26.90	0
July	29.6	0	5.92	14.77	2.78	9.46	158.90	1.08	171.61	0.00	37.00	-37.00	0
Aug	36.6	0	7.32	20.36	3.43	15.08	184.70	1.19	219.79	0.00	50.15	-50.15	0
Sep	28.1	0	5.62	13.65	2.64	8.43	147.80	1.19	175.88	0.00	62.50	-62.50	0
Oct	20.2	49.8	4.04	8.28	1.89	4.08	65.27	1.21	78.98	49.80	67.40	-67.40	0
Nov	15.4	3.0	3.08	5.49	1.44	2.25	35.93	1.15	41.32	3.00	64.00	-64.00	0
Dec	8.4	64.8	1.68	2.19	0.79	0.59	9.47	1.03	9.75	9.75	60.00	-4.95	0
SUM		263.8		106.61									8.28

1986 : I = 107.2 / a =2.22													
Month	TC°	p(mm)	(T/5)	(T/5) ^{1.514}	(T*10)/I	[(T*10)/I] ^a	PE	K	PEc	AE	SM	WS / WD p - (AE +SM)	GWr WS - RO
Jan	8.1	1.9	1.62	2.08	0.76	0.54	8.59	0.98	8.42	1.9	33.65	-33.65	0
Feb	11.0	14.3	2.2	3.30	1.03	1.06	16.94	0.88	14.91	14.3	40.30	-40.30	0
Mar	14.1	14.7	2.82	4.80	1.32	1.84	29.40	0.87	25.58	14.7	48.40	-48.40	0
Apr	20.1	4.6	4.02	8.22	1.88	4.04	64.59	0.89	57.49	4.6	50.80	-50.80	0
May	22.3	11.6	4.46	9.62	2.08	5.08	81.34	0.86	69.96	11.6	45.80	-45.80	0
June	27.5	0	5.5	13.21	2.57	8.10	143.70	1.03	148.01	0	34.70	-34.70	0
July	31.5	0	6.3	16.23	2.94	10.95	170.70	1.08	184.36	0	25.20	-25.20	0
Aug	35.8	0	7.16	19.69	3.34	14.54	184.30	1.19	219.32	0	18.10	-18.10	0
Sep	29.8	0	5.96	14.92	2.78	9.68	185.00	1.19	220.15	0	13.10	-13.10	0
Oct	22.3	7.9	4.46	9.62	2.08	5.08	81.34	1.21	98.43	7.9	13.05	-13.05	0
Nov	11.7	22.3	2.34	3.62	1.09	1.21	19.43	1.15	22.34	22.3	19.75	-19.75	0
Dec	7.6	12.6	1.52	1.88	0.71	0.47	7.46	1.03	7.68	7.68	28.60	-23.68	0
SUM		89.9		107.19									0
1987 : I = 114.0 / a =2.32													
Month	TC°	p(mm)	(T/5)	(T/5) ^{1.514}	(T*10)/I	[(T*10)/I] ^a	PE	K	PEc	AE	SM	WS / WD p - (AE +SM)	GWr WS - RO
Jan	9.1	0.5	1.82	2.48	0.80	0.59	9.49	0.98	9.30	0.5	29.65	-29.65	0
Feb	12.2	0.2	2.44	3.86	1.07	1.17	18.73	0.88	16.48	0.2	27.80	-27.80	0
Mar	10.9	16.4	2.18	3.25	0.96	0.90	14.42	0.87	12.54	12.5	32.35	-28.49	0
Apr	18.6	3.5	3.72	7.31	1.63	3.11	49.82	0.89	44.34	3.5	32.20	-32.20	0
May	25.6	0	5.12	11.85	2.25	6.53	104.52	0.86	89.89	0	25.00	-25.00	0
June	28.5	0	5.7	13.94	2.50	8.38	151.70	1.03	156.25	0	19.25	-19.25	0
July	32.1	0.8	6.42	16.70	2.82	11.04	173.10	1.08	186.95	0.8	14.40	-14.40	0
Aug	42.8	0.0	8.56	25.81	3.75	21.52	185.00	1.19	220.15	0	10.30	-10.30	0
Sep	27.7	0.0	5.54	13.36	2.43	7.84	147.80	1.19	175.88	0	7.60	-7.60	0
Oct	19.6	59.4	3.92	7.91	1.72	3.52	56.25	1.21	68.06	59.4	10.00	-10.00	0
Nov	13.6	0.1	2.72	4.55	1.19	1.51	24.09	1.15	27.71	0.1	11.00	-11.00	0
Dec	10.3	10.6	2.06	2.99	0.90	0.79	12.64	1.03	13.02	10.6	16.75	-16.75	0
SUM		91.5		114.00									0

1988 : I = 110.0 / a =2.26												WS / WD	GWr
Month	TC°	p(mm)	(T/5)	(T/5) ^{1.514}	(T*10)/I	[(T*10)/I] ^a	PE	K	PEc	AE	SM	p - (AE +SM)	WS - RO
Jan	7.3	8.8	1.46	1.77	0.66	0.40	6.33	0.98	6.21	6.21	50.50	-47.91	0
Feb	9.0	12.2	1.8	2.43	0.82	0.64	10.17	0.88	8.95	8.95	28.20	-24.95	0
Mar	12.4	7.0	2.48	3.96	1.13	1.31	20.98	0.87	18.25	7	30.00	-30.00	0
Apr	17.6	5.2	3.52	6.72	1.60	2.89	46.28	0.89	41.19	5.2	35.75	-35.75	0
May	24.9	0.2	4.98	11.37	2.26	6.34	101.39	0.86	87.19	0.2	32.20	-32.20	0
June	28.4	0	5.68	13.87	2.58	8.53	151.70	1.03	156.25	0	23.80	-23.80	0
July	32.2	0	6.44	16.77	2.93	11.33	173.10	1.08	186.95	0	17.15	-17.15	0
Aug	41.5	0	8.3	24.63	3.77	20.10	185.00	1.19	220.15	0	12.35	-12.35	0
Sep	27.7	0	5.54	13.36	2.52	8.06	139.50	1.19	166.01	0	9.10	-9.10	0
Oct	21.0	33.1	4.2	8.78	1.91	4.31	68.99	1.21	83.48	33.1	8.80	-8.80	0
Nov	12.2	21.6	2.44	3.86	1.11	1.26	20.22	1.15	23.25	21.6	8.80	-8.80	0
Dec	9.1	15.4	1.82	2.48	0.83	0.65	10.42	1.03	10.74	1.82	22.25	-8.67	0
SUM		103.5		110.00									0
1989 : I = 111.96/ a =2.30												WS / WD	GWr
Month	TC°	p(mm)	(T/5)	(T/5) ^{1.514}	(T*10)/I	[(T*10)/I] ^a	PE	K	PEc	AE	SM	p - (AE +SM)	WS - RO
Jan	4.4	26.1	0.88	0.82	0.39	0.12	1.87	0.98	1.83	1.83	33.70	-9.43	0
Feb	6.8	17.2	1.36	1.59	0.61	0.32	5.08	0.88	4.47	4.47	34.50	-21.77	0
Mar	13.6	89.2	2.72	4.55	1.21	1.56	25.03	0.87	21.77	21.77	39.65	27.78	27.78
Apr	22.1	59.7	4.42	9.49	1.97	4.78	76.45	0.89	68.04	59.70	36.00	-36.00	0
May	26.2	5.9	5.24	12.28	2.34	7.07	113.08	0.86	97.24	5.90	27.30	-27.30	0
June	28.6	0	5.72	14.02	2.55	8.65	151.70	1.03	156.25	0.00	19.90	-19.90	0
July	32.0	0	6.4	16.62	2.86	11.19	173.10	1.08	186.95	0.00	14.30	-14.30	0
Aug	40.0	0	8	23.30	3.57	18.70	185.00	1.19	220.15	0.00	20.30	-20.30	0
Sep	26.8	0	5.36	12.70	2.39	7.45	139.50	1.19	166.01	0.00	7.40	-7.40	0
Oct	21.4	0	4.28	9.04	1.91	4.44	70.99	1.21	85.90	0.00	5.80	-5.80	0
Nov	14.7	46.4	2.94	5.12	1.31	1.87	29.93	1.15	34.42	34.42	19.00	-7.02	0
Dec	9.0	5.1	1.8	2.43	0.80	0.61	9.68	1.03	9.97	5.10	32.80	-32.80	0
SUM		249.6		111.96	21.94	66.74	981.41		1051.18	133.19	290.65		27.78

1990 : I = 111.91/ a =2.30												WS / WD	GWr
Month	TC°	p(mm)	(T/5)	(T/5)^1.514	(T*10)/I	[(T*10)/I]^a	PE	K	PEc	AE	SM	p - (AE +SM)	WS - RO
Jan	5.4	3.0	1.08	1.12	0.48	0.19	2.99	0.98	2.93	2.93	33.75	-33.68	0
Feb	8.2	62.5	1.64	2.11	0.73	0.49	7.83	0.88	6.89	6.89	42.80	12.81	12.81
Mar	12.7	3.5	2.54	4.10	1.13	1.34	21.41	0.87	18.62	3.5	54.00	-54.00	0
Apr	18.9	1.2	3.78	7.49	1.69	3.34	53.42	0.89	47.54	1.2	47.20	-47.20	0
May	24.6	1.5	4.92	11.16	2.20	6.12	97.94	0.86	84.23	1.5	37.80	-37.80	0
June	29.0	0	5.8	14.32	2.59	8.94	155.40	1.03	160.06	0	28.45	-28.45	0
July	31.8	0	6.36	16.46	2.84	11.05	173.10	1.08	186.95	0	21.15	-21.15	0
Aug	39.7	0	7.94	23.03	3.55	18.40	185.00	1.19	220.15	0	15.35	-15.35	0
Sep	27.7	0	5.54	13.36	2.48	8.04	147.80	1.19	175.88	0	11.35	-11.35	0
Oct	22.2	12.3	4.44	9.55	1.98	4.83	77.34	1.21	93.59	12.3	9.30	-9.30	0
Nov	16.4	7.6	3.28	6.04	1.47	2.41	38.54	1.15	44.33	7.6	8.10	-8.10	0
Dec	10.7	4.5	2.14	3.16	0.96	0.90	14.43	1.03	14.87	4.5	7.60	-7.60	0
SUM		96.1		111.91									12.81
1991 : I = 120.77/ a =2.40												WS / WD	GWr
Month	TC°	p(mm)	(T/5)	(T/5)^1.514	(T*10)/I	[(T*10)/I]^a	PE	K	PEc	AE	SM	p - (AE +SM)	WS - RO
Jan	7.2	16.2	1.44	1.74	0.60	0.29	4.62	0.98	4.53	4.53	12.45	-0.78	0
Feb	11.6	0	2.32	3.58	0.96	0.91	14.52	0.88	12.77	0	20.90	-20.90	0
Mar	14.1	30.3	2.82	4.80	1.17	1.45	23.19	0.87	20.17	20.2	35.10	-24.97	0
Apr	20.8	0	4.16	8.66	1.72	3.68	58.95	0.89	52.47	0	36.35	-36.35	0
May	32.1	0	6.42	16.70	2.66	10.44	167.02	0.86	143.64	0	28.40	-28.40	0
June	29.7	0	5.94	14.84	2.46	8.66	138.60	1.03	142.76	0	21.15	-21.15	0
July	30.7	0	6.14	15.61	2.54	9.38	150.07	1.08	162.07	0	20.90	-20.90	0
Aug	42.1	0	8.42	25.17	3.49	20.01	320.21	1.19	381.05	0	34.95	-34.95	0
Sep	27.5	0	5.5	13.21	2.28	7.20	115.23	1.19	137.12	0	36.35	-36.35	0
Oct	21.6	35.0	4.32	9.16	1.79	4.03	64.54	1.21	78.10	35	28.40	-28.40	0
Nov	15.4	0	3.08	5.49	1.27	1.79	28.66	1.15	32.95	0	21.20	-21.20	0
Dec	7.4	2.6	1.48	1.81	0.61	0.31	4.94	1.03	5.08	2.6	20.30	-20.30	0
SUM		84.1		120.77									0

1992 : I = 107.82 / a =2.20												WS / WD	GWr
Month	TC°	p(mm)	(T/5)	(T/5)^1.514	(T*10)/I	[(T*10)/I]^a	PE	K	PEc	AE	SM	p - (AE +SM)	WS - RO
Jan	4.0	34.7	0.8	0.71	0.39	0.13	2.09	0.98	2.04	2.04	24.60	8.06	8.06
Feb	6.1	10.9	1.22	1.35	0.59	0.32	5.17	0.88	4.55	4.55	33.85	-27.50	0.0
Mar	10.5	29.4	2.1	3.07	1.02	1.04	16.61	0.87	14.45	14.45	39.80	-24.85	0.0
Apr	18.3	16.8	3.66	7.13	1.77	3.43	54.85	0.89	48.81	16.80	36.70	-36.70	0.0
May	22.8	40.0	4.56	9.95	2.21	5.50	87.99	0.86	75.67	40.00	29.25	-29.25	0.0
June	28.0	0	5.6	13.58	2.71	8.55	147.80	1.03	152.23	0.00	21.85	-21.85	0.0
July	29.7	0	5.94	14.84	2.88	9.71	158.90	1.08	171.61	0.00	15.85	-15.85	0.0
Aug	41.3	0	8.26	24.45	4.00	19.73	185.00	1.19	220.15	0.00	11.45	-11.45	0.0
Sep	26.8	0.6	5.36	12.70	2.60	7.79	139.50	1.19	166.01	0.60	8.35	-8.35	0.0
Oct	22.1	7.2	4.42	9.49	2.14	5.14	82.29	1.21	99.57	7.20	6.55	-6.55	0.0
Nov	13.2	46.0	2.64	4.35	1.28	1.70	27.17	1.15	31.25	31.25	9.45	5.30	5.30
Dec	6.7	21.0	1.34	1.56	0.65	0.40	6.32	1.03	6.51	6.51	11.25	3.24	3.24
SUM		206.6		103.2									16.60
1993 : I = 143.95/ a =2.80												WS / WD	GWr
Month	TC°	p(mm)	(T/5)	(T/5)^1.514	(T*10)/I	[(T*10)/I]^a	PE	K	PEc	AE	SM	p - (AE +SM)	WS - RO
Jan	6.0	17.7	1.2	1.32	0.42	0.09	1.38	0.98	1.35	1.35	15.20	1.15	1.15
Feb	7.9	22.7	1.58	2.00	0.55	0.19	2.98	0.88	2.62	2.62	17.60	2.48	2.48
Mar	12.9	12.5	2.58	4.20	0.90	0.73	11.76	0.87	10.23	10.2	16.10	-13.83	0
Apr	19.1	32.7	3.82	7.61	1.33	2.21	35.29	0.89	31.40	31.4	19.40	-18.10	0
May	22.8	23.1	4.56	9.95	1.58	3.62	57.93	0.86	49.82	23.1	22.60	-22.60	0
June	28.7	0	5.74	14.09	1.99	6.90	155.40	1.03	160.06	0	18.80	-18.80	0
July	31.2	0	6.24	15.99	2.17	8.71	168.00	1.08	181.44	0	13.40	-13.40	0
Aug	73.2	0	14.64	58.16	5.08	94.89	185.00	1.19	220.15	0	9.60	-9.60	0
Sep	28.0	0	5.6	13.58	1.94	6.44	147.80	1.19	175.88	0	7.00	-7.00	0
Oct	22.9	13.2	4.58	10.01	1.59	3.67	58.65	1.21	70.96	13.2	5.60	-5.60	0
Nov	12.7	3.2	2.54	4.10	0.88	0.70	11.26	1.15	12.94	3.2	6.90	-6.90	0
Dec	10.2	5.5	2.04	2.94	0.71	0.38	6.09	1.03	6.28	5.5	10.30	-10.30	0
SUM		130.6		143.95									3.63

1994 : I = 114.80/ a =2.30												WS / WD	GWr
Month	TC°	p(mm)	(T/5)	(T/5)^1.514	(T*10)/I	[(T*10)/I]^a	PE	K	PEc	AE	SM	p - (AE +SM)	WS - RO
Jan	9.7	17.9	1.94	2.73	0.84	0.68	10.86	0.98	10.64	10.6	12.40	-5.14	0
Feb	10.1	11.1	2.02	2.90	0.88	0.74	11.92	0.88	10.49	10.5	25.90	-25.29	0
Mar	14.4	11.5	2.88	4.96	1.25	1.68	26.95	0.87	23.44	11.5	33.70	-33.70	0
Apr	22.0	1.7	4.4	9.42	1.92	4.46	71.42	0.89	63.56	1.7	27.75	-27.75	0
May	25.8	0	5.16	11.99	2.25	6.44	103.03	0.86	88.61	0	21.65	-21.65	0
June	28.9	0	5.78	14.24	2.52	8.36	155.40	1.03	160.06	0	16.00	-16.00	0
July	30.4	0	6.08	15.38	2.65	9.39	165.20	1.08	178.42	0	11.60	-11.60	0
Aug	39.0	0	7.8	22.42	3.40	16.66	185.00	1.19	220.15	0	8.40	-8.40	0
Sep	29.2	10.0	5.84	14.47	2.54	8.56	155.40	1.19	184.93	10	6.70	-6.70	0
Oct	23.6	10.2	4.72	10.48	2.06	5.25	83.94	1.21	101.56	10.2	5.90	-5.90	0
Nov	13.3	100.3	2.66	4.40	1.16	1.40	22.44	1.15	25.81	25.8	14.50	59.99	59.99
Dec	6.3	12.7	1.26	1.42	0.55	0.25	4.02	1.03	4.15	12.7	25.60	-25.60	0
SUM		175.4		114.80									59.99
1995 : I = 110.5 / a =2.30												WS / WD	GWr
Month	TC°	p(mm)	(T/5)	(T/5)^1.514	(T*10)/I	[(T*10)/I]^a	PE	K	PEc	AE	SM	p - (AE +SM)	WS - RO
Jan	9.2	5.6	1.84	2.52	0.83	0.66	10.50	0.98	10.29	5.60	27.15	-27.15	0
Feb	9.7	67.7	1.94	2.73	0.88	0.74	11.86	0.88	10.44	10.44	32.90	24.36	24.36
Mar	13.8	22.3	2.76	4.65	1.25	1.67	26.69	0.87	23.22	22.30	36.05	-36.05	0
Apr	18.4	28.6	3.68	7.19	1.67	3.23	51.72	0.89	46.03	28.60	32.15	-32.15	0
May	25.8	6.2	5.16	11.99	2.34	7.03	112.54	0.86	96.78	6.20	26.05	-26.05	0
June	29.7	0	5.94	14.84	2.69	9.72	158.90	1.03	163.67	0.00	19.45	-19.45	0
July	30.5	0	6.1	15.45	2.76	10.34	165.20	1.08	178.42	0.00	14.15	-14.15	0
Aug	38.7	0	7.74	22.16	3.50	17.87	185.00	1.19	220.15	0.00	10.15	-10.15	0
Sep	27.8	0.0	5.56	13.43	2.52	8.35	147.80	1.19	175.88	0.00	7.60	-7.60	0
Oct	21.5	0.0	4.3	9.10	1.95	4.62	73.99	1.21	89.53	0.00	6.00	-6.00	0
Nov	13.1	25.4	2.62	4.30	1.19	1.48	23.68	1.15	27.23	25.40	7.00	-7.00	0
Dec	8.2	29.5	1.64	2.11	0.74	0.50	8.06	1.03	8.30	8.30	9.10	12.10	12.10
SUM		185.3		110.5									36.46

1996 : I = 113.74/ a =2.30												WS / WD	GWr
Month	TC°	p(mm)	(T/5)	(T/5)^1.514	(T*10)/I	[(T*10)/I]^a	PE	K	PEc	AE	SM	p - (AE +SM)	WS - RO
Jan	8.2	15.7	1.64	2.11	0.72	0.47	7.54	0.98	7.39	7.39	10.80	-2.49	0
Feb	10.4	22.7	2.08	3.03	0.91	0.81	13.03	0.88	11.47	11.5	14.30	-3.07	0
Mar	12.7	37.0	2.54	4.10	1.12	1.29	20.64	0.87	17.95	18	19.10	-0.05	0
Apr	18.7	1.4	3.74	7.37	1.64	3.14	50.25	0.89	44.72	1.4	22.30	-22.30	0
May	27.5	3.1	5.5	13.21	2.42	7.62	143.70	0.86	123.58	3.1	18.40	-18.40	0
June	29.4	0	5.88	14.62	2.59	8.89	158.90	1.03	163.67	0	13.70	-13.70	0
July	34.0	2.6	6.8	18.21	2.99	12.42	180.50	1.08	194.94	2.6	9.80	-9.80	0
Aug	36.8	0	7.36	20.53	3.24	14.90	184.00	1.19	218.96	0	7.00	-7.00	0
Sep	28.2	0	5.64	13.72	2.48	8.08	147.80	1.19	175.88	0	4.90	-4.90	0
Oct	20.7	1.9	4.14	8.59	1.82	3.97	63.47	1.21	76.80	1.9	3.80	-3.80	0
Nov	14.0	35.0	2.8	4.75	1.23	1.61	25.82	1.15	29.69	29.7	6.20	-0.89	0
Dec	11.4	14.0	2.28	3.48	1.00	1.01	16.10	1.03	16.58	14	11.40	-11.40	0
SUM		133.4		113.74									0
1997 : I = 112.5/ a =2.30												WS / WD	GWr
Month	TC°	p(mm)	(T/5)	(T/5)^1.514	(T*10)/I	[(T*10)/I]^a	PE	K	PEc	AE	SM	p - (AE +SM)	WS - RO
Jan	8.1	17.7	1.62	2.08	0.72	0.47	7.52	0.98	7.37	7.37	19.75	-9.42	0
Feb	7.5	2.8	1.5	1.85	0.67	0.39	6.30	0.88	5.55	2.80	24.80	-24.80	0
Mar	10.5	19.3	2.1	3.07	0.93	0.85	13.66	0.87	11.89	11.89	25.80	-18.39	0
Apr	17.8	6.1	3.56	6.84	1.58	2.88	46.00	0.89	40.94	6.10	23.45	-23.45	0
May	26.2	2.0	5.24	12.28	2.33	7.00	111.92	0.86	96.25	2.00	18.40	-18.40	0
June	29.7	0	5.94	14.84	2.64	9.33	158.90	1.03	163.67	0.00	13.65	-13.65	0
July	31.3	0	6.26	16.07	2.78	10.53	170.70	1.08	184.36	0.00	9.90	-9.90	0
Aug	42.1	0	8.42	25.17	3.74	20.82	185.00	1.19	220.15	0.00	7.25	-7.25	0
Sep	27.3	0.0	5.46	13.07	2.43	7.69	143.70	1.19	171.00	0.00	5.40	-5.40	0
Oct	22.3	101.4	4.46	9.62	1.98	4.83	77.25	1.21	93.48	93.48	6.50	1.42	1.42
Nov	14.2	57.8	2.84	4.86	1.26	1.71	27.36	1.15	31.46	31.46	22.45	3.89	3.89
Dec	9.7	29.8	1.94	2.73	0.86	0.71	11.39	1.03	11.73	11.73	36.65	-18.58	0
SUM		236.9		112.5									5.31

1998 : I = 118.79/ a =2.40												WS / WD	GW_r
Month	TC°	p(mm)	(T/5)	(T/5)^{1.514}	(T*10)/I	[(T*10)/I]^a	PE	K	PEc	AE	SM	p - (AE +SM)	WS - RO
Jan	6.8	21.3	1.36	1.59	0.57	0.26	4.19	0.98	4.11	4.11	43.60	-26.41	0
Feb	8.5	18.3	1.7	2.23	0.72	0.45	7.16	0.88	6.30	6.3	49.00	-37.00	0
Mar	12.0	18.4	2.4	3.76	1.01	1.02	16.39	0.87	14.26	14.3	52.10	-47.96	0
Apr	20.2	1.8	4.04	8.28	1.70	3.58	57.20	0.89	50.91	1.8	47.80	-47.80	0
May	25.4	19.6	5.08	11.71	2.14	6.20	99.12	0.86	85.24	19.6	38.40	-38.40	0
June	31.0	0	6.2	15.84	2.61	9.99	168.00	1.03	173.04	0	28.40	-28.40	0
July	33.4	0	6.68	17.73	2.81	11.95	179.00	1.08	193.32	0	20.30	-20.30	0
Aug	40.2	0	8.04	23.47	3.38	18.65	185.00	1.19	220.15	0	14.50	-14.50	0
Sep	29.0	0	5.8	14.32	2.44	8.52	155.40	1.19	184.93	0	10.50	-10.50	0
Oct	22.2	0	4.44	9.55	1.87	4.48	71.75	1.21	86.81	0	8.10	-8.10	0
Nov	17.6	0	3.52	6.72	1.48	2.57	41.10	1.15	47.26	0	6.70	-6.70	0
Dec	11.6	1.5	2.32	3.58	0.98	0.94	15.11	1.03	15.56	1.5	6.10	-6.10	0
SUM		80.9		118.79									0
1999 : I = 115.18/ a =2.30												WS / WD	GW_r
Month	TC°	p(mm)	(T/5)	(T/5)^{1.514}	(T*10)/I	[(T*10)/I]^a	PE	K	PEc	AE	SM	p - (AE +SM)	WS - RO
Jan	8.7	9.9	1.74	2.31	0.76	0.52	8.39	0.98	8.22	8.22	8.60	-6.92	0
Feb	11.3	14.3	2.26	3.44	0.98	0.96	15.31	0.88	13.47	13.5	12.80	-11.97	0
Mar	13.9	3.8	2.78	4.70	1.21	1.54	24.64	0.87	21.44	3.8	14.00	-14.00	0
Apr	19.4	1.8	3.88	7.79	1.68	3.32	53.05	0.89	47.22	1.8	11.90	-11.90	0
May	26.1	0	5.22	12.21	2.27	6.56	104.97	0.86	90.27	0	9.40	-9.40	0
June	29.6	0	5.92	14.77	2.57	8.76	135.00	1.03	139.05	0	6.90	-6.90	0
July	31.7	0	6.34	16.38	2.75	10.26	173.10	1.08	186.95	0	5.00	-5.00	0
Aug	39.6	1.0	7.92	22.94	3.44	17.11	185.00	1.19	220.15	1	7.20	-7.20	0
Sep	27.5	0	5.5	13.21	2.39	7.40	143.70	1.19	171.00	0	7.50	-7.50	0
Oct	22.6	4.7	4.52	9.81	1.96	4.71	75.38	1.21	91.20	4.7	6.70	-6.70	0
Nov	14.1	0	2.82	4.80	1.22	1.59	25.47	1.15	29.29	0	5.90	-5.90	0
Dec	9.9	27.1	1.98	2.81	0.86	0.71	11.29	1.03	11.63	11.6	8.40	7.07	7.07
SUM		62.6		115.18									7.07

2000 : I = 115.24/ a =2.30												WS / WD	GW_r
Month	TC°	p(mm)	(T/5)	(T/5)^{1.514}	(T*10)/I	[(T*10)/I]^a	PE	K	PE_c	AE	SM	p - (AE +SM)	WS - RO
Jan	7.5	8.4	1.5	1.85	0.65	0.37	5.96	0.98	5.84	5.84	10.40	-7.84	0
Feb	8.7	3.0	1.74	2.31	0.76	0.52	8.39	0.88	7.38	3	10.30	-10.30	0
Mar	12.5	0.1	2.5	4.00	1.09	1.21	19.31	0.87	16.80	0.1	9.50	-9.50	0
Apr	21.7	0.9	4.34	9.23	1.88	4.29	68.65	0.89	61.10	0.9	8.90	-8.90	0
May	25.2	11.6	5.04	11.57	2.19	6.05	96.83	0.86	83.27	11.6	8.00	-8.00	0
June	29.9	0	5.98	14.99	2.60	8.97	162.10	1.03	166.96	0	6.20	-6.20	0
July	35.1	0	7.02	19.11	3.05	12.97	182.90	1.08	197.53	0	4.40	-4.40	0
Aug	39.9	0	7.98	23.21	3.46	17.41	185.00	1.19	220.15	0	3.20	-3.20	0
Sep	27.7	0	5.54	13.36	2.40	7.52	147.80	1.19	175.88	0	2.40	-2.40	0
Oct	20.0	7.9	4	8.16	1.74	3.56	56.90	1.21	68.85	7.9	2.30	-2.30	0
Nov	13.6	30.0	2.72	4.55	1.18	1.46	23.44	1.15	26.95	27	3.50	-0.45	0
Dec	10.1	22.5	2.02	2.90	0.88	0.74	11.82	1.03	12.18	12.2	9.30	1.02	1.02
SUM		84.4		115.24									1.02
2001 : I = 119.1/ a =2.40												WS / WD	GW_r
Month	TC°	p(mm)	(T/5)	(T/5)^{1.514}	(T*10)/I	[(T*10)/I]^a	PE	K	PE_c	AE	SM	p - (AE +SM)	WS - RO
Jan	8.2	37.2	1.64	2.11	0.69	0.41	6.53	0.98	6.40	6.40	19.15	11.65	11.65
Feb	10.1	13.7	2.02	2.90	0.85	0.67	10.76	0.88	9.47	9.47	26.75	-22.52	0.0
Mar	17.3	35.3	3.46	6.55	1.45	2.45	39.16	0.87	34.07	34.07	31.00	-29.77	0.0
Apr	20.7	60.0	4.14	8.59	1.74	3.77	60.24	0.89	53.62	53.62	28.75	-22.37	0.0
May	23.4	0.0	4.68	10.35	1.96	5.05	80.85	0.86	69.53	0.00	23.50	-23.50	0.0
June	29.8	0	5.96	14.92	2.50	9.03	162.10	1.03	166.96	0.00	17.60	-17.60	0.0
July	32.5	0	6.5	17.01	2.73	11.12	175.30	1.08	189.32	0.00	12.60	-12.60	0.0
Aug	40.4	0	8.08	23.65	3.39	18.74	185.00	1.19	220.15	0.00	8.95	-8.95	0.0
Sep	29.1	0.0	5.82	14.39	2.44	8.53	155.40	1.19	184.93	0.00	6.60	-6.60	0.0
Oct	23.5	49.8	4.7	10.41	1.97	5.11	81.69	1.21	98.84	49.80	5.60	-5.60	0.0
Nov	14.3	3.0	2.86	4.91	1.20	1.55	24.80	1.15	28.52	3.00	5.70	-5.70	0.0
Dec	11.1	64.8	2.22	3.34	0.93	0.84	13.50	1.03	13.91	13.91	7.40	43.49	43.49
SUM		263.8		119.1									55.14

2002 : I = 117.04/ a =2.40												WS / WD	GWr
Month	TC°	p(mm)	(T/5)	(T/5) ^{1.514}	(T*10)/I	[(T*10)/I] ^a	PE	K	PEc	AE	SM	p - (AE +SM)	WS - RO
Jan	6.7	46.4	1.34	1.56	0.57	0.26	4.20	0.98	4.11	4.11	13.10	29.19	29.19
Feb	11.3	33.6	2.26	3.44	0.97	0.92	14.72	0.88	12.95	13	16.70	3.95	3.95
Mar	15.6	12.0	3.12	5.60	1.33	1.99	31.91	0.87	27.76	12	18.20	-18.20	0
Apr	19.3	4.1	3.86	7.73	1.65	3.32	53.19	0.89	47.34	4.1	19.80	-19.80	0
May	24.8	3.3	4.96	11.30	2.12	6.07	97.09	0.86	83.49	3.3	16.70	-16.70	0
June	28.8	0	5.76	14.17	2.46	8.69	155.40	1.03	160.06	0	12.20	-12.20	0
July	32.9	0	6.58	17.33	2.81	11.96	173.10	1.08	186.95	0	8.70	-8.70	0
Aug	40.8	0	8.16	24.00	3.49	20.04	185.00	1.19	220.15	0	15.30	-15.30	0
Sep	28.6	0.6	5.72	14.02	2.44	8.54	155.40	1.19	184.93	0.6	21.40	-21.40	0
Oct	22.7	0	4.54	9.88	1.94	4.91	78.51	1.21	95.00	0	16.50	-16.50	0
Nov	14.2	2.0	2.84	4.86	1.21	1.59	25.47	1.15	29.29	2	14.70	-14.70	0
Dec	10.7	1.3	2.14	3.16	0.91	0.81	12.91	1.03	13.30	1.3	14.60	-14.60	0
SUM		103.3		117.04									33.14
2003 : I = 105.09/ a =2.20												WS / WD	GWr
Month	TC°	p(mm)	(T/5)	(T/5) ^{1.514}	(T*10)/I	[(T*10)/I] ^a	PE	K	PEc	AE	SM	p - (AE +SM)	WS - RO
Jan	8.6	25.5	1.72	2.27	0.82	0.64	10.29	0.98	10.09	10.1	16.90	-1.49	0
Feb	8.9	15.9	1.78	2.39	0.85	0.69	11.10	0.88	9.77	9.77	18.50	-12.37	0
Mar	14.1	0	2.82	4.80	1.34	1.91	30.54	0.87	26.57	0	17.50	-17.50	0
Apr	15.8	0	3.16	5.71	1.50	2.45	39.23	0.89	34.92	0	17.30	-17.30	0
May	25.0	0	5	11.44	2.38	6.73	107.66	0.86	92.59	0	14.50	-14.50	0
June	27.0	0	5.4	12.85	2.57	7.97	139.50	1.03	143.69	0	10.60	-10.60	0
July	30.0	0	6	15.07	2.85	10.05	162.10	1.08	175.07	0	7.50	-7.50	0
Aug	39.8	0	7.96	23.12	3.79	18.72	185.00	1.19	220.15	0	5.30	-5.30	0
Sep	27.8	0	5.56	13.43	2.65	8.50	155.40	1.19	184.93	0	3.90	-3.90	0
Oct	19.8	0	3.96	8.03	1.88	4.03	64.46	1.21	77.99	0	3.20	-3.20	0
Nov	13.2	11.9	2.64	4.35	1.26	1.65	26.42	1.15	30.38	11.9	7.30	-7.30	0
Dec	6.9	35.3	1.38	1.63	0.66	0.40	6.34	1.03	6.53	6.53	13.80	14.97	14.97
SUM		88.6		105.09									14.97

2004 : I = 104.30/ a =2.20												WS / WD	GWr
Month	TC°	p(mm)	(T/5)	(T/5)^1.514	(T*10)/I	[(T*10)/I]^a	PE	K	PEc	AE	SM	p - (AE +SM)	WS - RO
Jan	5.4	29.3	1.08	1.12	0.52	0.23	3.76	0.98	3.68	3.68	19.80	5.82	5.82
Feb	5.9	21.3	1.18	1.28	0.57	0.29	4.57	0.88	4.02	4.02	24.30	-7.02	0
Mar	12.1	19.5	2.42	3.81	1.16	1.39	22.18	0.87	19.30	19.3	23.60	-23.40	0
Apr	19.6	0	3.92	7.91	1.88	4.01	64.10	0.89	57.05	0	23.00	-23.00	0
May	22.5	0	4.5	9.75	2.16	5.43	86.84	0.86	74.68	0	19.40	-19.40	0
June	28.0	0	5.6	13.58	2.68	8.78	147.80	1.03	152.23	0	14.20	-14.20	0
July	29.3	0	5.86	14.54	2.81	9.70	158.90	1.08	171.61	0	10.20	-10.20	0
Aug	40.1	0	8.02	23.38	3.84	19.35	185.00	1.19	220.15	0	7.20	-7.20	0
Sep	27.2	0	5.44	12.99	2.61	8.24	139.50	1.19	166.01	0	5.20	-5.20	0
Oct	23.5	6.2	4.7	10.41	2.25	5.97	95.55	1.21	115.62	6.2	3.90	-3.90	0
Nov	13.4	21.3	2.68	4.45	1.28	1.74	27.77	1.15	31.93	21.3	5.90	-5.90	0
Dec	5.2	25.1	1.04	1.06	0.50	0.22	3.46	1.03	3.56	3.56	9.10	12.44	12.44
SUM		122.7		104.30									18.26
2005 : I = 105.65/ a =2.20												WS / WD	GWr
Month	TC°	p(mm)	(T/5)	(T/5)^1.514	(T*10)/I	[(T*10)/I]^a	PE	K	PEc	AE	SM	p - (AE +SM)	WS - RO
Jan	5.3	31.1	1.06	1.09	0.50	0.22	3.51	0.98	3.44	3.44	12.40	15.26	15.26
Feb	11.4	17.8	2.28	3.48	1.08	1.18	18.91	0.88	16.64	16.6	16.20	-15.04	0
Mar	13.2	11.3	2.64	4.35	1.25	1.63	26.11	0.87	22.72	11.3	20.50	-20.50	0
Apr	18.0	4.7	3.6	6.95	1.70	3.23	51.67	0.89	45.98	4.7	20.20	-20.20	0
May	24.2	0	4.84	10.89	2.29	6.19	99.08	0.86	85.21	0	15.80	-15.80	0
June	26.8	0	5.36	12.70	2.54	7.75	139.50	1.03	143.69	0	11.50	-11.50	0
July	30.1	0	6.02	15.15	2.85	10.01	162.10	1.08	175.07	0	8.20	-8.20	0
Aug	39.6	0	7.92	22.94	3.75	18.30	185.00	1.19	220.15	0	5.90	-5.90	0
Sep	27.4	0	5.48	13.14	2.59	8.14	143.70	1.19	171.00	0	4.20	-4.20	0
Oct	22.3	9.1	4.46	9.62	2.11	5.17	82.77	1.21	100.15	9.1	3.30	-3.30	0
Nov	11.0	18.2	2.2	3.30	1.04	1.09	17.49	1.15	20.11	18.2	4.40	-4.40	0
Dec	8.0	33.4	1.6	2.04	0.76	0.54	8.68	1.03	8.94	8.94	7.00	17.46	17.46
SUM		125.6		105.65									32.72

2006 : I = 108.5 / a =2.20												WS / WD	GWr
Month	TC°	p(mm)	(T/5)	(T/5)^1.514	(T*10)/I	[(T*10)/I]^a	PE	K	PEc	AE	SM	p - (AE +SM)	WS - RO
Jan	5.5	40.7	1.1	1.16	0.51	0.23	3.70	0.98	3.63	3.63	9.60	27.47	27.47
Feb	7.4	29.7	1.48	1.81	0.69	0.44	7.11	0.88	6.26	6.26	14.12	9.32	9.32
Mar	13.0	17.8	2.6	4.25	1.22	1.54	24.57	0.87	21.37	17.80	16.40	-16.40	0
Apr	17.6	5.2	3.52	6.72	1.65	2.99	47.84	0.89	42.58	5.20	20.50	-20.50	0
May	24.4	3.8	4.88	11.02	2.28	6.13	98.15	0.86	84.41	3.80	20.25	-20.25	0
June	28.9	0	5.78	14.24	2.70	8.90	155.40	1.03	160.06	0.00	14.90	-14.90	0
July	30.5	0	6.1	15.45	2.85	10.02	160.37	1.08	173.20	0.00	10.60	-10.60	0
Aug	39.2	0	7.84	22.59	3.66	17.41	278.54	1.19	331.46	0.00	7.50	-7.50	0
Sep	26.0	0.0	5.2	12.13	2.43	7.05	112.87	1.19	134.32	0.00	5.40	-5.40	0
Oct	23.6	31.2	4.72	10.48	2.21	5.70	91.21	1.21	110.37	31.20	7.20	-7.20	0
Nov	14.7	51.2	2.94	5.12	1.37	2.01	32.19	1.15	37.02	37.02	9.20	4.98	4.98
Dec	7.9	21.3	1.58	2.00	0.74	0.51	8.21	1.03	8.46	8.46	10.50	2.34	2.34
SUM		200.9		107.0									44.11
2007 : I = 103.74/ a =2.20												WS / WD	GWr
Month	TC°	p(mm)	(T/5)	(T/5)^1.514	(T*10)/I	[(T*10)/I]^a	PE	K	PEc	AE	SM	p - (AE +SM)	WS - RO
Jan	6.3	26.2	1.26	1.42	0.61	0.33	5.34	0.98	5.23	5.23	14.20	6.77	6.77
Feb	8.3	22.6	1.66	2.15	0.80	0.61	9.80	0.88	8.62	8.62	19.30	-5.32	0
Mar	13.1	9.2	2.62	4.30	1.26	1.67	26.73	0.87	23.26	9.2	21.40	-21.40	0
Apr	19.6	0	3.92	7.91	1.89	4.05	64.86	0.89	57.73	0	22.40	-22.40	0
May	23.6	0	4.72	10.48	2.27	6.10	97.60	0.86	83.94	0	19.00	-19.00	0
June	28.1	0	5.62	13.65	2.71	8.96	147.80	1.03	152.23	0	13.80	-13.80	0
July	31.0	0	6.2	15.84	2.99	11.12	168.00	1.08	181.44	0	10.00	-10.00	0
Aug	36.2	0	7.24	20.03	3.49	15.63	184.30	1.19	219.32	0	7.00	-7.00	0
Sep	27.8	0	5.56	13.43	2.68	8.75	147.80	1.19	175.88	0	5.00	-5.00	0
Oct	19.7	1.9	3.94	7.97	1.90	4.10	65.59	1.21	79.37	1.9	3.80	-3.80	0
Nov	14.0	16.2	2.8	4.75	1.35	1.93	30.94	1.15	35.58	16.2	3.20	-3.20	0
Dec	7.4	29.1	1.48	1.81	0.71	0.48	7.61	1.03	7.84	7.84	4.80	16.46	16.46
SUM		105.2		103.74									23.23

2008 : I = 100.19/ a =2.10												WS / WD	GWr
Month	TC°	p(mm)	(T/5)	(T/5)^1.514	(T*10)/I	[(T*10)/I]^a	PE	K	PEc	AE	SM	p - (AE +SM)	WS - RO
Jan	7.2	33.8	1.44	1.74	0.72	0.48	7.73	0.98	7.58	7.58	9.50	16.72	16.72
Feb	7.9	12.9	1.58	2.00	0.79	0.59	9.48	0.88	8.35	8.35	14.90	-10.35	0
Mar	11.1	7.6	2.22	3.34	1.11	1.25	20.04	0.87	17.44	7.6	15.30	-15.30	0
Apr	17.8	2.2	3.56	6.84	1.78	3.54	56.64	0.89	50.41	2.2	13.20	-13.20	0
May	22.8	0	4.56	9.95	2.28	6.10	97.65	0.86	83.98	0	10.60	-10.60	0
June	28.0	0	5.6	13.58	2.79	9.59	147.80	1.03	152.23	0	7.50	-7.50	0
July	28.7	0	5.74	14.09	2.86	10.13	155.40	1.08	167.83	0	5.60	-5.60	0
Aug	35.7	0	7.14	19.61	3.56	16.37	184.30	1.19	219.32	0	4.00	-4.00	0
Sep	26.2	0	5.24	12.28	2.61	8.29	132.58	1.19	157.77	0	3.50	-3.50	0
Oct	21.6	5.1	4.32	9.16	2.16	5.42	86.70	1.21	104.90	5.1	4.60	-4.60	0
Nov	13.9	14.5	2.78	4.70	1.39	2.05	32.87	1.15	37.80	14.5	8.00	-8.00	0
Dec	10.1	30.9	2.02	2.90	1.01	1.02	16.28	1.03	16.77	16.8	10.50	3.63	3.63
SUM		107		100.19									20.35



Field work Mar.2009 – Western desert of Iraq



Curriculum Vitae



Sameh Wisam Al-Muqdadi

Borne: Baghdad – Iraq

Date of Birth: Dec.01.1976



Academic Education

- BSC. Geology – Petroleum & Geochemistry, Baghdad University 2000.
- MSC. Geology – Hydrogeology, Baghdad University 2003.
- PhD. Geology – Hydrogeology, TU.Bergakademie Freiberg 2012.

Special Education

- Operation risk and Human resource management, Jordan Feb.2007.
- Confirmed scientific diver - TUBAF / CMAS *** – Germany Sep.2009.

Profession Experience

Dec.2002 – Mar.2004

Field Geologist

(JC.) Al-Jawf Company - General trading & constructions

- Monitoring drilling process.
- Field investigations and water sampling.

April 2004 – July 2007

**Chief of Auditing unite & Director Consultant
CHF International – ACSI Program (US.NGO)**

- Conduct the annual plan and risk assessment report.
- Supervising the operation staff.

Aug.2009 – Dec.2011

**Project coordinator
TU.Freiberg / Hydrogeology Institute**

GRI. (Geoscience Ressources Iraq) funded by German government via DAAD to reconstruction the higher education sector in Iraq ,supervised by Prof.Dr.Broder J.Merkel:

- Organizing scientific courses and workshops.
- Establish scientific diving center in Basrah - southern Iraq.

Thesis publications

- Sameh W. Al-Muqdadi and Broder J. Merkel, "**Automated Watershed Evaluation of Flat Terrain**" *Journal of Water Resource and Protection*, Vol. 3 No. 12, 2011.
- Sameh W. Al-Muqdadi and Broder J. Merkel, "**Interpretation of Groundwater Flow into Fractured Aquifer**" *International Journal of Geosciences*, Vol. 3 No. 2, 2012.

Languages

- **Arabic** (Native)
- **English** (Fluent)
- **German** (Very good)